universität wien

MASTERARBEIT/MASTER'S THESIS

Titel der Masterarbeit / Title of the Master's Thesis

Unique metal-microbe interactions of the extreme thermoacidophile *Metallosphaera sedula* and the extreme radioresistant *Deinococcus radiodurans*

verfasst von / submitted by

Denise Kölbl BSc

angestrebter akademischer Grad / in partial fulfilment of the requirements for the degree of

Master of Science (MSc)

Wien, 2019 / Vienna 2019

Studienkennzahl lt. Studienblatt / degree programme code as it appears on the student record sheet:	A 066 877
Studienrichtung lt. Studienblatt / degree programme as it appears on the student record sheet:	Masterstudium Genetik und Entwicklungsbiologie
Betreut von / Supervisor:	Univ.-Prof. Dr. Annette Rompel
Mitbetreut von / Co-Supervisor:	Dr. Tetyana Milojevic

ACKNOWLEDGEMENTS

First and foremost, I'd like to thank my supervisor Dr. Tetyana Milojevic for giving me the opportunity to rediscover my interest for the subject of minerals and metals interacting with their (microbial) environment. Thank you for bringing me along to conferences, meetings and giving me the opportunity to go to Paris to learn new skills.

I want to spread the gratitude to the other members of our Space Biochemistry group, Emanuel Ott and Natalie Özgen, thanks for all your skills, help and input throughout this time during my thesis work.

Many thanks to all the members and former members of the Department of Biophysical chemistry for helping me out when I got lost in the lab. Thanks to the department head Dr. Annette Rompel, for giving me the opportunity to conduct my thesis in her lab and having access to everything I needed for the work.

Special thanks to Daniela Gruber and Norbert Cyran of the CIUS lab, Marc Pignitter from the Department of Nutritional Chemistry, Stephan Puchegger from the Department of Physics and Adrienne Kish from the Natural History Museum in Paris, who helped making this work possible.

A special shout out to my friends for their emotional support and always listening and giving me advice, support and lots of their time.

Last but not least I want to thank my family for their patience and understanding for the many things they never got to experience themselves. Thank you for listening and supporting me for all those years.

This thesis is dedicated to my father whose pride would be impossible to beat.

ABSTRACT

The metal-mobilizing archaeon *Metallosphaera sedula* thrives under the extreme conditions (73°C, pH 2) while transforming its metal bearing substrates, e.g., minerals. Physiological versatility allows this microorganism to grow in a chemolithotrophic mode where cells propagate supplemented with either terrestrial or extraterrestrial materials. For this work we investigated the growth capacity, metal extraction abilities as well as ultrastructural and spectroscopic fingerprints left upon *M. sedulas* cultivation on Martian Regolith Simulants (MRSs) and the ordinary chondrite meteorite NWA 1172. *M. sedula* cells actively colonized both mineral materials while solubilizing metals out of the MRSs into the medium. Scanning electron microscopy revealed surface alterations of the solid MRSs after cultivation along with distinct mineralogical fingerprints uncovered by spectroscopy. Additionally, a technique to produce ultrathin sections of microbes grown on genuine extraterrestrial mineral material was developed to promote our future examinations of mineral-microbial interactions. The obtained results provide a deeper knowledge about the detection of biosignatures and microbial fingerprints on extraterrestrial material and the future implementation of bioleaching on other celestial bodies in our solar system.

Deinococcus radiodurans is a polyextremophilic gram-positive bacterium, resistant to high doses of ionizing radiation, desiccation and other oxidizing agents. Due to these characteristics this microorganism is a prime candidate to further investigate its remarkable defense and protection mechanisms during interplanetary transfer. *D. radiodurans* poses an interesting model organism to investigate the possibility of the panspermia theory which proposes the interplanetary transfer of microbes through space. Before *Deinococci* cells are exposed to real outer space conditions at the Japanese module on the International Space Station (ISS) in frames of the Tanpopo mission, a variety of simulation experiments (e.g., UVC and vacuum) have been performed. A look on the morphology and cellular integrity of the exposed cells via electron microscopy showed that multi-layers of cells are well protected despite being exposed to space simulating conditions. Along with an integrative proteometabolomic approach, these results present that stress response in *D. radiodurans* is a multi-layered process and it requires high amounts of energy to preserve cellular integrity and morphology in a simulated outer space environment.

ZUSAMMENFASSUNG

Das Metalle mobilisierende Archaeon *Metallosphaera sedula* wächst und vermehrt sich unter extremen Bedingungen (73°C, pH 2) während es dabei u.a. metallhaltige Substrate wie Mineralien transformiert. Eine erstaunliche physiologische Vielseitigkeit erlaubt es diesem Mikroorganismus auf unterschiedlichsten terrestrischen oder extraterrestrischen Materialien chemolithotroph zu leben und sich zu vermehren. Die wissenschaftlichen Gegenstände der folgenden Arbeit befassten sich mit der Untersuchung der Fähigkeit des Wachstums von *M. sedula* auf synthetischem Mars Regolith, sowie der Gewinnung von Metallen aus diesen. Weiters wurden Aspekte von ultrastrukturellen und spektroskopischen Fingerabdrücken nach der Kultivierung mit *M. sedula* auf synthetischem Mars Regolith und dem gewöhnlichen chondrititschen Meteoriten NWA 1172 untersucht. *M. sedula* Zellen waren in der Lage erfolgreich die synthetischen Mars Regolith Mineralien zu besiedeln und gleichzeitig wertvolle Metalle daraus löslich zu machen („Bioleaching“). Rasterelektronenmikroskopische und spektroskopische Untersuchungen zeigten uns eine deutliche Veränderung der soliden mineralischen Oberfläche nach der Kultivierung. Zusätzlich wurde eine Technik entwickelt um Ultradünnschnitte von auf extraterrestrischem Material kultivierte Mikroben zu erhalten welche in Zukunft zur tiefergehenden Aufklärung vom Zusammenspiel zwischen Mineralien und Mikroorganismen dienen. Die Ergebnisse dieser Arbeit liefern uns weitere Anhaltspunkte für die zukünftige Detektion von Biosignaturen und Fingerabdrücken, die von Mikroben auf extraterrestrischem Material hinterlassen wurden. Ebenfalls könnte die Fähigkeit unlösliche Metalle aus Mineralien zu extrahieren in Zukunft auch auf anderen Himmelskörpern in unserem Sonnensystem angewandt werden.

Deinococcus radiodurans ist ein polyextremophiles Gram-positives Bakterium welches gegen immense ionisierende Strahlungsdosen, Austrocknung, sowie andere oxidierende Agentien resistent ist. Diese Eigenschaften machen *D. radiodurans* zu einem hervorragenden Kandidaten um tiefere Erkenntnisse über dessen Abwehr- und Schutzmechanismen während des interplanetaren Transfers zu gewinnen (Panspermie). *D. radiodurans* stellt einen vielversprechenden Modellorganismus zur Erforschung der Hypothese der Panspermie dar, welche besagt, dass sich Mikroorganismen über große Distanzen durch das Weltall bewegen. Bevor Mikroorganismen den realen Bedingungen des Weltalls am Japanischen Modul der Internationalen Weltraumstation (ISS) im Rahmen der Tanpopo Mission ausgesetzt werden, müssen Simulationsexperimente (z.B., UVC und Vakuum Exposition) durchgeführt werden. Ein Blick mittels Rasterelektronenmikroskop auf Weltraum-exponierte *Deinococci* zeigt eine unveränderte Morphologie der mehrschichtig gelagerten Zellen, sowie den Erhalt von zellulärer Integrität trotz simulierten Weltraumbedingungen. Zusammen mit einer integrativen Proteomics und Metabolomics Methode verweisen unsere Resultate auf eine komplexe und vielschichtige Stressantwort, welche eine große Menge Energie benötigt um die Zellen in einem morphologisch unveränderten Zustand zu erhalten, auch unter Weltraumbedingungen.

Publications

As first author:
Kolbl, D., Pignitter, M., Somoza, V., Schimak, M. P., Strbak, O., Blazevic, A., Milojevic, T. (2017). Exploring Fingerprints of the Extreme Thermoacidophile *Metallosphaera sedula* Grown on Synthetic Martian Regolith Materials as the Sole Energy Sources. Published in Frontiers in Microbiology 8:1918.

As co-author:
Ott, E., Kawaguchi, Y., **Kolbl, D**., Chaturvedi, P., Nakagawa, K., Yamagishi, A., Weckwerth, W., Milojevic, T. (2017). Proteometabolomic response of *Deinococcus radiodurans* exposed to UVC and vacuum conditions: Initial studies prior to the Tanpopo space mission. Published in PLoS One 12(12): e0189381.

CONTENTS

1. Goals and Objectives 1
2. Introduction 2
2.1. Metal-Microbe Interactions 2
2.1.1. *Metallosphaera sedula* 6
2.1.2. *Deinococcus radiodurans* 8
2.2. Astrobiological implications of Metal-Microbe-Interactions 10
2.2.1. Biominerals & Chemolithotrophy 10
2.2.2. Interplanetary Transfer of Life & Tanpopo Orbital Mission 11
3. Results Synopsis - Publication 1 (as main author) 12
3.1. Growth and Identification of *M. sedula* grown on Martian Regolith simulants 12
3.2. Metal Release into the Medium by *M. sedula* 12
3.3. Alterations of the Solid Mineral Phase upon *M. sedulas* Growth 13
3.4. Spectroscopic inspection of the Solid Mineral Phase upon *M. sedulas* Growth 13
4. Results Synopsis – Publication 2 (as co-author) 13
4.1. Effects of UVC/vacuum on cellular integrity of *D. radiodurans* 13
5. Publication 1 as main author 14
5.1. Contribution of the Author 14
6. Publication 2 - as co-author 34
6.1. Contribution of co-author 34
7. *Metallosphaera sedula* - interactions with a stony meteorite 58
7.1. Introduction 58
7.2. Materials & Methods 60
7.2.1. Strain and Media Composition 60
7.2.2. Cultivation Setup 60
7.2.3. EPR Analysis 61
7.2.4. SEM Sample Preparation and Analysis 61
7.2.5. TEM Sample Preparation and Analysis 61
7.3. Results 63

7.3.3. Chemolithotrophic Growth on Meteorite NWA 1172 63

7.3.4. EPR of M. sedula after cultivation 63

7.3.5. TEM Observations of M. sedula cells 65

7.4. Conclusion 66

References 67

List of Figures 74

1. GOALS AND OBJECTIVES

During the experimental period of this master thesis, specific metal-microbe interactions were elucidated on different levels implying various techniques. Assessment of certain biological aspects of the metal mobilizing archaeon *Metallosphaera sedula* and the extremely radiation-resistant bacterium *Deinococcus radiodurans* are reported therein.

The utilization of metal-transforming extremophiles such as *Metallosphaera sedula* have the potential to grow in a chemolithoautrotrophic mode when supplemented with energy providing mineral materials. Ancient archaeal organisms and their metabolisms can help us to gain a deeper look into the biogeochemistry of bygone and recent terrestrial and extraterrestrial life. Objectives of this thesis include the assessment of growth potential and subsequent metal mobilization and solubilization of synthetic and real extraterrestrial material. By applying spectroscopic and ultrastructural techniques we can observe putative alterations of the solid mineral phase induced by *M. sedula* which can serve as potential fingerprints of microbial metabolism in the search for life forms on other planetary bodies in our solar system.

Deinococcus radiodurans as an extreme radiation and desiccation resistant bacterium was chosen to study the possibility of interplanetary transfer of life (Panspermia theory) in frames of the Tanpopo orbital mission. Before real space-exposure experiments are conducted, *D. radiodurans* was subjected to simulated UVC/vacuum conditions for preliminary studies. General objectives included the deciphering of molecular survival mechanisms on a proteometabolomic and transcriptomic level and space-related stress response. Specific to this thesis electron microscopy investigations were applied to check on the morphology and cellular integrity after a long-term exposure to simulated space conditions.

This work is presented as a cumulative master's thesis giving a short introduction about metal-microbial interactions, the two presented organisms and their astrobiological implications followed by two published articles in scientific journals and a separate discussion. Unpublished results will be presented succeeding the articles.

2. INTRODUCTION

2.1. Metal-Microbe Interactions

In multicellular and unicellular biological entities, metal ions and their complexes take over many essential tasks. Microorganisms commonly utilize elements (Na, K, Mg, Ca, V, Mn, Fe, Co, Ni, Cu, Zn, Mo and W) for mechanisms such as enzyme catalysis, hydrolysis, transport and storage of small molecules, structure stabilisation, to keep up intracellular osmotic pressure and many more [1]. On the other hand, metals and especially heavy metals are well known for their potential toxicity in living organisms because of their avidity to replace naturally occurring metals in specific enzymes and prosthetic groups, thereby destroying their vital function. The toxicity of (heavy) metals is not consistent and cannot be generalised for different bacterial or archaeal species, they tend to response individually even though some similarities between species are evident [2]. *Bacillus subtilis* is a gram-positive bacterium that can bind substantial amounts of cations of the surrounding aqueous, metal-laden environment due to its functional groups in the cell wall [3]. Metal biosorption and accumulation investigations with *Bacillus* species reveal that they are able to tolerate high levels of Cu, Cd, Zn, Ni, Mn and Co in liquid media as a response of the polluted habitat they were isolated from [4]. The potential of absorption, precipitation or solubilization of pollutants in form of (heavy) metals is being exploited in microbe-mediated bioremediation of contaminated environments. Mixed bacterial cultures of gram-positive and gram-negative bacteria demonstrated that synergism is more effective in bioremediation compared to individual cultures which have a lower capacity in growth and therefore also in removal of pollutants [5]. Archaeal species such as *Methanobacterium bryantii*, *Sulfolobus acidocaldarius* and *Halobacterium* sp. are also able to chelate copper, uranium or manganese at high concentrations onto their cell surface and can therefore also be deployed for bioremediation purposes [6]. *Metallosphaera sedula* is able to grow and mobilize 100% of zinc, copper and uranium in 2-3 weeks of cultivation on ore mixtures [7]. *M. prunae*, which most likely appeared as a spontaneous mutation of *M. sedula,* dodges cytotoxic effects caused by high concentrations of uranium (VI) in the environment by shutting down its cellular metabolism through rRNA degradation [8].

Metals are not only hazardous components in our environment but also ubiquitously dispersed on Earth's crust in form of inorganic minerals. Most minerals contain metals bound with varying elements, creating an overabundance of different mineral types out of one essential metal component. All kinds of bacteria and archaea can interact with these metals and mediate biogenic mineral formation through direct or indirect mechanisms. Interestingly, biologically formed minerals can have identical structures to geochemically formed minerals [9]. Information about various and well preserved biominerals/organic fossils can be vital to comprehend and reconstruct the evolution of life during different geological periods on Earth. The archaeon *Sulfolobus acidocaldarius* for instance can be,

when subjected to Fe-phosphates in the growth medium, encrusted by amorphous iron on the outer S-layer of the cell. While the encrusting cells were exposed to thermal treatments (to mimic diagenetic conditions) the Fe-phosphates evolved into lipscombite crystals, but only in the presence of archaea [10]. To redraw the geological history and evolution of first life on the early Earth, it is crucial to assess if microstructures found in rocks are of biological origin which makes the investigation and constitution of biosignatures essential. Nevertheless, assigning biogenicity to a certain structure or signature in ancient rocks remains very challenging due to probable degradation of microbial remains during diagenesis or microbial-like morphologies being produced abiotically [11]. Some microbial species favour to live in extreme environments, they colonize the pore space of rocks and are highly adapted to this endolithic lifestyle. This unusual habitat might be considered a low-nutrient (oligotrophic) one, but these small endolithic microbial communities obtain their nutrients from the boulder, thereby directly or indirectly altering their host rock. A secreted extracellular polymeric substance (EPS) as well as EPS-associated molecules are facilitating archaeal biofilm formation on rocks and minerals [12]. Biofilm formation and microbial coverage of the minerals/rocks correlate with the metal leaching ability of acidophilic archaeal species since they are involved in dissolution of rocky materials [12, 13].

Extracting and recovering precious metals from minerals and rocks via microorganisms presents an alternative technology to current prevalent techniques such as pyrometallurgy or hydrometallurgy. From an ecological and economical point of view, “biomining” as an arising method of harvesting metals is more tolerable than conventional ones. To recover base metals from a low-grade ore out of a rock, bioleaching methods are already applied nowadays [14].

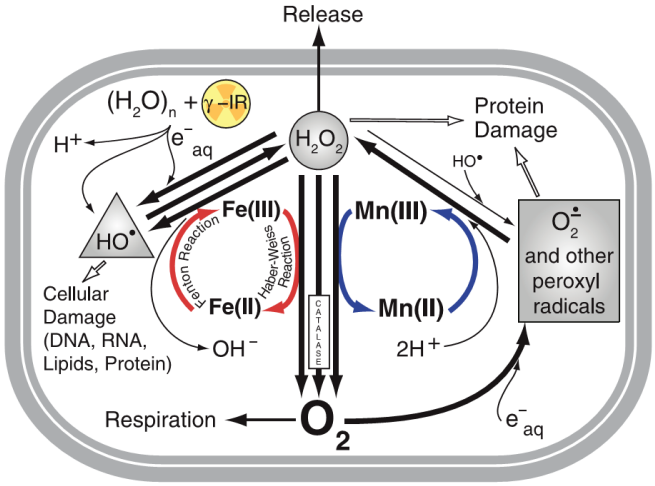

Fig. 1: Manganese and iron cycle induced upon irradiation. In γ-radiolysis, water releases solvated electrons (e^-_{aq}) which react with O_2 to form the superoxide radical $O_2^{\bullet-}$. The radicals can in turn, react with Mn(II) ions and protons (H^+) to form H_2O_2 and Mn(III). Mn-recycling occurs when Mn(III) is reduced back to Mn(II) by receiving an electron from H_2O_2. Hydroxyl ($HO^{\bullet}$) and peroxyl radicals ($R\text{-}O_2^{\bullet}$) are the primary oxygen radicals which are generated by the radiolysis of water. During irradiation, Fe(II,III) redox cycling with respective reactions such as the Fenton or Haber-Weiss reaction are thought to generate $HO^{\bullet}$ snd $O_2^{\bullet-}$ whereas Mn (II,III) redox cycling is thought to scavenge radicals without producing toxic byproducts [19].

Bioleaching uses the marvellous tools of microorganisms to solubilise metal cations from ores, industrial interests hereby drive the conversion of insoluble sulphides into soluble sulphates. These processes usually require an acidic pH ranging from 0.5-2.0 and variable mesophilic (35-40°C) to thermophilic (< 50°C) temperatures [15]. Most of the organisms capable of biomining or bioleaching exhibit similar metabolisms, they usually oxidise iron and/or sulphur and grow autotrophically at an acidic pH in their natural habitats. Biomining

operations at elevated temperatures (< 60°C) favour thermophilic sulphur and iron oxidising archaea deriving from the genera *Sulfolobus, Acidianus, Metallosphaera* and *Sulfurisphaera*, mainly to leach copper from different sources [16].

Certain metals (Mn, Zn, Co) play a key role in defending reactive oxygen species (ROS) when implemented as a cofactor into enzymes. An enzyme called superoxide dismutase (SOD) is allegedly crucial to protect cells against oxidative stress in form of different radicals [17]. The production of ROS can be induced metabolically, either upon exposure to chemical or physical agents, desiccation, ionizing radiation or UV radiation and can cause lipid peroxidation, protein oxidation and DNA damage [18]. Extreme resistance against ionizing radiation (IR) and desiccation of the gram-positive bacterium *Deinococcus radiodurans* is suggested to be based on intracellular Mn-accumulation to protect against protein degradation and subsequent cell death [19]. IR resistant *Deinococci* cells contained approximately 300 times more Mn compared to IR-sensitive *Shewanella oneidensis* cells which in contrary exhibit a high intracellular Fe concentration [20].

Even though metals fulfil vital tasks to keep a cell alive and viable, the concentration of (heavy) metals as well as the adaptation and subsequent development of strategies to cope with them is of great importance. Overconcentration or the general toxicity of some metals for certain organisms are a threat to their viability, therefore different systems of detoxification evolved and can be observed (Fig. 2). Heavy metal resistant bacteria such as *Cupriavidus metallidurans* which were isolated from a zinc decantation tank, [21] utilize efflux transporters to expel these lethal concentrations out of the cell [22]. Similar resistance systems have been characterised in *E. coli* concerning arsenite and in *S. aureus* concerning cadmium, both are protected by efflux systems based on ion-pumping ATPases [23]. An alternative solution against toxic metal compounds is the release of chelators into extracellular surroundings or intracellular sequestration. The high metal biosorption ability of extracellular fungal and bacterial chelating pigments (e.g. melanin) is carried out through

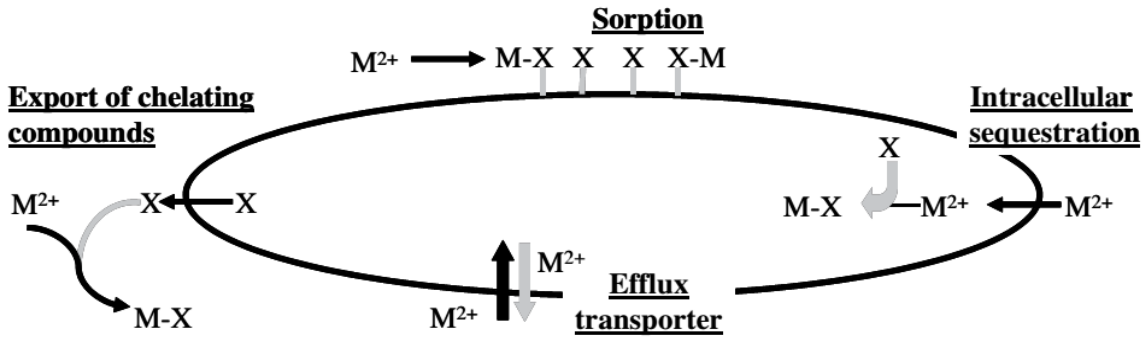

Fig. 2: Mechanisms of microbial metal resistance. X = cell compounds interacting with metal; M = metal cation [21]

the anionic function of carboxyl and hydroxyl groups of this secondary metabolite. Furthermore, the structure of the cell envelope can bind a high concentration of metals through biosorption, preventing them to enter the cell [17].

To completely understand the interactions and specific interplay between metals and microbes requires a multidisciplinary knowledge and experimental approaches of different disciplines. On one hand, microorganisms are able to immobilize, absorb, solubilize, sequester and precipitate supplemented or naturally occurring metals, hence cleaning

polluted habitats or make precious metal resources more accessible for industrial or technological use. The other side of metal-microbe interactions are possible toxic effects when they are overconcentrated in their environment and the release of toxic metals into surrounding soils. Geological processes, metallic environments and microbial activity seem to be intertwined into a cycle which shaped and still shapes life on planet Earth and possibly beyond.

2.1.1. *Metallosphaera sedula*

Unicellular organisms such as archaea which constitute the third domain of life, are often found in harsh and extreme environments and exhibit a rather multifaceted way of life. The branch of thermoacidophilic archaea grow optimally at temperatures > 45°C and a low, acidic pH. Natural habitats of these extremophilic microbes include volcanos and solfatara fields where acid solutions are generated through the interaction of gases and seawater [24]. A prominent representative is the extreme thermoacidophile *Metallosphaera sedula* which flourishes under hot (optimally at 73°C) and acidic conditions (around pH 2.0), mobilizes metal ions from pyrite (FeS_2) and chalcopyrite ($CuFeS_2$) about 10 times faster than other relatives and may be suited for *in situ* leaching of geothermally heated ore resources. Originally isolated from a hot, sulfidic water pond at Pisciarelli Solfatara in Italy, about half of the round-shaped cocci (Fig. 3) growing on ores were attached to the particles, displaying a characteristic wiggling movement [7]. Deeper investigations into the microbes physiology uncovered that *M. sedula* can assimilate organic and inorganic carbon sources, it grows heterotrophically when the medium is supplemented with peptides, autotrophically by fixing CO_2 as well as on metal sulphides and $FeSO_4$ [25]. The mixotrophic life style of *M. sedula* makes it distinguishable from its phylogenetic relatives, *Sulfolobus solfataricus* and *S. acidocaldarius,* which only thrive under chemoheterotrophic conditions despite having a similar genetic constitution. Another feature of this microbe is its unusual heavy metal resistance, especially concerning cupric ions (Cu^{2+}) compared to other *Sulfolobales* species [26]. Testing the boundaries of *Metallosphaera* growing in a metallic environment, the cells were

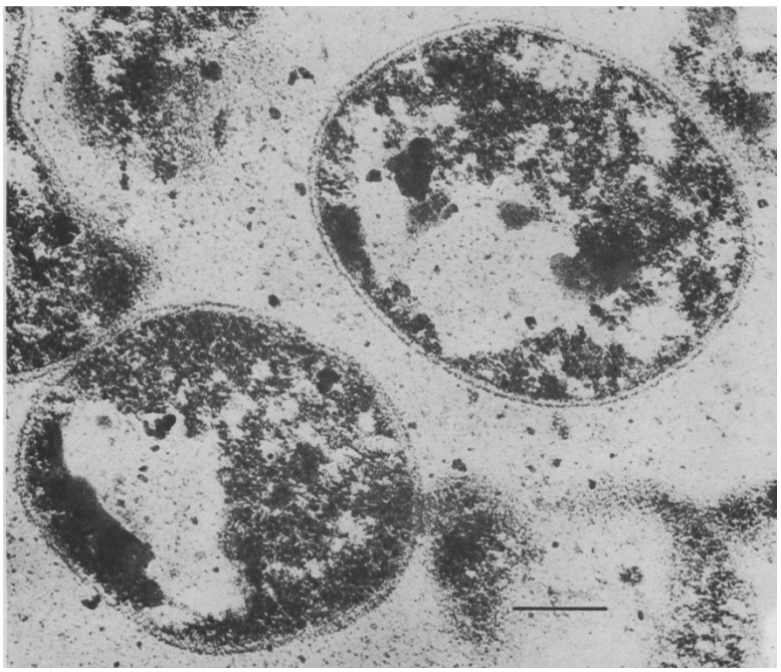

Fig. 3: Transmission Electron Micrograph of *M. sedula* cells [7].

subjected to an artificial low dosage and high dosage "metal shock" (Co^{2+}, Cu^{2+}, Ni^{2+}, UO_2^{2+}, Zn^{2+}) at sub-inhibitory and inhibitory levels. Metal supplemented high dosage cultures were still growing up to 60% compared to the control cultures where no metals were added to the medium. Transcriptomic analyses reveal that *M. sedula* rapidly senses and responds with upregulating several open reading frames which respond to a single metal, dealing with these toxic conditions [27].

Investigations on how microbes are able to flourish and propagate in these hot and acidic environments have elucidated some of their survival strategies. Dealing with metal-laden surroundings and recovering from metal-induced stress involves mechanisms similar to coping with oxidative stress as well as the self-limitation of toxic metal concentration. Even though these microbes are constantly subjected to low pH and high temperatures, they still must protect themselves against acidification of the cytosol and cold/heat shock. This interesting lifestyle makes *M. sedulas* bioleaching and biomining properties appealing for industrial use to release precious metals (gold, copper) from sulphide ores (pyrite or chalcopyrite) [28]. Dissimilatory oxidation processes of iron and sulphur with subsequent electron transport through the microbe's membrane constitute the key activity of bioleaching [29]. Optimising these biocatalytic operations for global purposes includes the biological removal of inorganic sulphur from coal [30]. The creation of "clean coal" implies its desulphurisation before combustion to avoid the production of sulphur dioxide (SO_2) which is a threat to general human health [31]. *Metallosphaera sedula* can oxidise mineral pyrite about ten times faster than *Acidianus brierleyi* when the medium is supplemented with yeast extract, making an impact on novel coal cleaning strategies [32].

Extremophilic organisms are not only interesting for the development of new technology concerning our environment, they can also contribute massively to study the origin of life on earth and bygone or recent life on other planets. The study of extreme environments interacting with microbial life and the thorough investigation of subsequent biogeochemical signals can help us to gain a deeper insight into microbial-mineral co-evolution on earth over geological timescales and might also enrich our knowledge of biosignatures for a search of life on other celestial bodies such as Mars. If life by our definitions ever occurred on a planet as Mars, it probably would have happened during a time when liquid water was a part of this planet [33]. The early Martian geological period (pre-Noachian) was marked by extensive hydrothermal events similar to the early Earth where photosynthesis was the next hallmark of evolution. In contrary to Earth, Mars became a hyperarid planet with an oxidized surface and is therefore described as inhabitable. In the search for ancient and bygone life on Mars, one needs to take a look into the subsurface of the rusty planet to find biogenic evidence in form of biosignatures or specific fingerprints [34]. The creation of a biosignature requires a sole biological origin and cannot be recreated abiotically under the exclusion of once viable microbes. As a preserved evidence of bygone life, stony biosignatures will be subjected to environmentally caused degradation, mineralization and are in the best case embedded and fossilized in the local rock record [35]. Iron-oxidizing archaea such as *M. sedula*, also grows chemolithoautotrophically and occupies a certain niche in our environment where oxygen

and nutrient levels are lower than in other habitats. To identify such distinct metabolisms, the evaluation and detection of metabolic biosignatures help us gain insight into the formation of specific fingerprints (e.g. Archean-aged banded iron formations) on Earth and putative similar structures on other rocky planets in our solar system [36]. *Metallosphaera sedula* was chosen to work with due to its diverse physiology, ability to tolerate and solubilize metals from ores and minerals and to study astrobiological implications of this organism.

2.1.2. *Deinococcus radiodurans*

Originally named *Micrococcus radiodurans*, this gram-positive, red-pigmented, mesophilic bacterium was startling researchers from the day of its discovery with unique capacities to survive massive doses of ionizing radiation (IR). After 16S rRNA analysis, *M. radiodurans* was phylogenetically re-placed in its own family, the Deinococcaceae and the species was renamed to *Deinococcus radiodurans* ("strange berry" in greek)[18]. Since its discovery as a meat spoilage organism even after sterilising doses of irradiation (by Anderson et al., 1956), the robustness and underlying survival mechanisms of *Deinococcus radiodurans* have been studied extensively. *D. radiodurans* quickly became a prime candidate to study peculiarities of the DNA and its effective repair and protection mechanisms which transported a DNA-centred view into the studies of radiobiology and associated survival strategies. Surprisingly, several experimental analyses have shown that *D. radiodurans'* genome is as sensitive to radiation-induced breakage as the genomes of other bacteria [37]. Despite not being the primary answer to this microbe's survival strategy, the DNA of *D. radiodurans* repairs ionizing radiation induced double strand breaks by sequential actions of two mechanisms - fragments are reassembled by "extended synthesis-dependent strand annealing" (ESDSA) followed by homologous recombination [18]. Surviving high doses of ionizing radiation and desiccation pose a severe struggle on living cells and subsequently break the genome into hundreds of fragments. The newly discovered ESDSA mechanism requires at least two identical copies of the genome to successfully reassemble *D. radiodurans'* DNA. Via overlapping homologous segments which are used as primers and templates, complementary strands are produced. Through synthesis of complementary strands, adjacent sticky DNA fragments are joined together first into long and linear double-stranded intermediates which are then, with the help of RecA-dependent crossover, matured into circular chromosomes [38]. *Deinococci* cells show no loss of viability when exposed to 5000 Gy of gamma radiation, surviving cells have been recovered even after exposure to 20 kGy. Since the highest measured background radiation on Earth does not exceed 175 mGy/year (Guarapari, Brazil), researchers are debating which evolutionary force has been acting on these cells to make them extremely resistant to factors like radiation and desiccation. Mattimore and Battista (1996) argue that both traits are functionally interrelated phenomena and radiation resistance "accidentally" arose. These claims are based on experimental data of more than 40 ionizing radiation-sensitive mutants which were found to be more sensitive to desiccation than radiation-resistant wild types [39]. A hypothetical

approach concerning *D. radiodurans'* evolution suggests that these microbes originally evolved on Mars and infected Earth at some point, travelling through space on a meteorite. The authors claim that bacteria, e.g. *E. coli* and *Bacillus spp.*, which are much more sensitive to irradiation, can be "trained" in cycles of irradiation and regeneration. By repeating cycles of exposing cells to 150 Gy/min and letting the survivors re-grow at 37°C in rich medium, each following cycle of irradiation required increasing dosages to kill most of the new generation. Furthermore, Mars would provide natural circumstances of increased irradiation and microbial re-growth to accumulate high radiation dosage over a long period of time [40].

To unravel the microbe's enigmatic survival strategies, different hypotheses have been proposed over time, most of them putting DNA protection into the focus of experimental investigations. Reactive oxygen species (ROS) and gamma photons impose heavy damage on cells if they are not properly scavenged and neutralised. Metal-microbe interactions as a hint to scavenge radicals, comprise intracellular manganese and iron concentrations as well as the ratio to each other [20]. First, it was hypothesized that Mn(II) accumulation is essential to neutralise ROS since it's a crucial cofactor for the Mn-dependent superoxide dismutase (Mn-SOD). However, other bacteria such as *Lactobacillus plantarum* which is radiation resistant up to 0.69 kGy [41] utilizes and incorporates Mn(II) as detoxification agent instead of Mn-SOD [20]. Since the DNA of resistant and sensitive bacteria is equally broken up into many small fragments by ionizing radiation, a dogmatic shift from DNA protection to protein protection took place. Researchers around Daly et al. (2007) proposed the idea that accumulation of intracellular manganese favours radiation resistance by protecting cells from protein oxidation by IR-driven Fe-cycling and the production of superoxide- ($O_2^{\cdot-}$) and hydroxyl radicals ($HO^{\cdot}$) (Fig. 1). Manganese accumulation mitigates the destructive effects of Fe-redox cycling in resistant bacteria which usually express fewer proteins with attackable Fe-S clusters.

Mn(II) does not specifically neutralise $HO^{\cdot}$ but the Fe(III) driven Haber-Weiss reaction is able to generate relatively unreactive $O_2^{\cdot-}$ which in turn produces protein oxidising alkoxyl- and peroxyl radicals [19]. Free Mn(II) ions are poor $O_2^{\cdot-}$ scavengers but complexed into different phosphate ligands, they can act as a Mn-SOD mimic [42]. Manganese complexed with molecules as succinate and lactate acts as a strong $O_2^{\cdot-}$ scavenger, whereas Mn(II) with

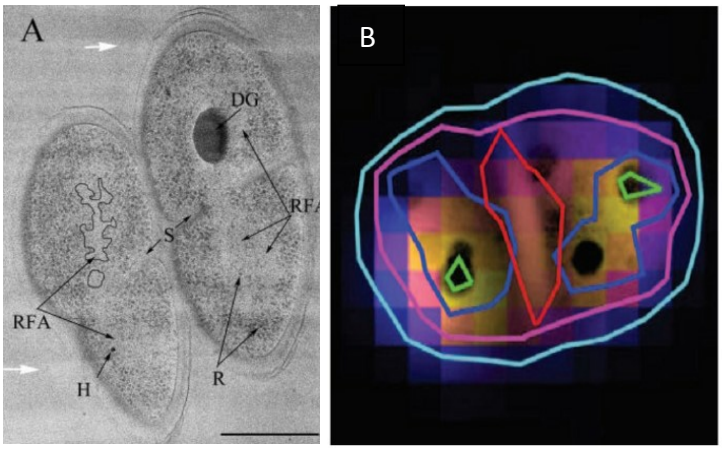

Fig. 4A: Transmission electron section of *D. radiodurans* tetrads. (DG) = Electron dense granule as a dark, large spot in the centre of the cell. **[43]**

Fig. 4B: Overlaid transmission electron-, light microscopy and X-ray fluorescence picture of *D. radiodurans* diplococci. Green circle emphasizes EDG with highest manganese deposition. Red circle shows Fe distribution among the septum [19].

bicarbonate takes over the disproportionation of H_2O_2. [19]. In silico approaches to determine the potential Mn-proteome and key players in ROS of *D. radiodurans* defence unveiled that the most abundant molecule was Mn-SOD. While this molecule catalyses the disproportionation of $O_2^{\cdot-}$ to O_2 and H_2O_2, an unusually high activity level of the catalase enzyme drives the conversion from cell damaging H_2O_2 into harmless H_2O and O_2. [43] The highest intracellular Mn concentration in *Deinococci* cells is located in frequently observed electron-dense granules (EDG), whereas the cell envelope is the least surrounded by manganese-associated ions and complexes (Fig. 4) [19, 44].

Extremophiles such as *D. radiodurans* which developed an outstanding robustness, shed light on strategies to reduce oxidative-related stress that also plays a big role in age-related diseases and cancer in humans. Experimentally, protein-free *D. radiodurans* extracts already exhibited a significant radioprotective effect on *E. coli* and human Jurkat T cells which is lost upon removal. Future tasks involve using these antioxidants to reduce disease-related protein damage and DNA mutations and ongoing studies of combating oxidative stress resistance in respect of medicine and public health [18].

2.2. ASTROBIOLOGICAL IMPLICATIONS OF METAL-MICROBE-INTERACTIONS

2.2.1. Biominerals & Chemolithotrophy

Mineral formation is usually associated with inorganic, physical and chemical processes which result under the right parameters, in the production of specific crystalline material. Even though these processes are mainly of non-microbial origin, some bacteria and archaea are involved in the deposition and formation of mineral material actively or passively [45]. Biogenically precipitated minerals and crystals (biominerals) can help us to decipher the processes and nature of how and when first cellular life arose on Earth. Furthermore, we can imply this knowledge for the search for extinct or extant life and its biogenically derived signatures on Earth and other celestial bodies. The search for traces of ancient and bygone life in rocks and minerals is easily justified by the fact that so far, the oldest signs of microbial life (3.5-3.8 Ga) have been identified in sedimentary rocks of the Barberton Greenstone Belt in South Africa and in the Isua and Akilia Greenstone Belts in Greenland [46]. Microorganisms, which lived and thrived in these unusual habitats, are usually characterized as biomineralized microfossils organized into colonies, microbial mats and stromatolites to withstand the harsh conditions of the early Earth as a unity [47]. Biomineralized and fossilized microbes serve as an important mineral biosignature for the search of traces of past life on iron-mineral-rich planets such as Mars. Milder global conditions during early Martian Noachian and Hesperian periods promoted the emergence of extensive valleys and sedimentary rocks and might have hosted liquid water at the surface. It is proposed that mudstone rich in silica and iron-bearing clays are the hot spots to look for microfossils on Mars since they represent environments with a range of redox states that serve and feed

microbial metabolisms and offer probable biomineralization sites [48]. When it comes to search for life on planets as Mars, it is vital to confirm the (past) presence of not only water but also energy providing building blocks of life (carbon, hydrogen, nitrogen, sulfur, phosphorous - CHNOPS) as well as trace elements. Thorough on-site investigations on Mars by NASA's Curiosity rover showed that locations such as Gale crater was once filled by a lake and is a well-suited study site to search for bygone chemolithoautotrophic life and might resemble a past habitable environment [49]. Chemolithotrophy represents one of the most ancient metabolisms considering the origin of life on Earth. Iron-oxidizing and sulfur-reducing organisms such as *Acidithiobacillus ferrooxidans* and *Leptospirillum ferrooxidans* are able to grow on iron meteorites and utilize inorganic resources of the iron-nickel alloy to promote growth followed by precipitation of biogenic Fe(III) oxides as goethite [50].

2.2.2. Interplanetary Transfer of Life & Tanpopo Orbital Mission

A detailed and scientific formulation that microscopic life could be transferred through space has already been proposed in 1903, by the Swedish scientist Svante Arrhenius although the term "panspermia" has been mentioned first by the Greek philosopher Anaxagoras in the 5th century [51, 52]. Heavy and intense bombardment of planets and moons by comets caused the ejection of a considerable amount of soil and rocks which began to orbit around the sun until they again impacted another planetary body or were excluded from the solar system. Endolithic microorganisms would be able to travel through space since they are encased in rocky material, protected from the complex and harsh outer space environment and the subsequent impact on another rocky planet [53]. The panspermia theory is an objective of ongoing investigation and has been tested experimentally with different microorganisms since the 1960s. A variety of microbes has been exposed to the outer space environment on the International Space Station (ISS) in low Earth orbit (LEO). To find any active form of life in a surrounding characterized by low pressure (10^-14 Pa), low temperature (4K), solar and galactic radiation is highly unexpected [54], the most detrimental effect on spores of *Bacillus subtilis* exposed to a variety of space conditions was the accumulation of radiation damage and cell death. Space traveling spores would be able to repair the damage when they again reach conditions which allow them to recover [55]. Prior to the start of the "Tanpopo"

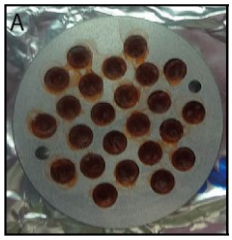

Fig. 5: Aluminium wells with dried *Deinococci* cells (red) inside. These aluminium plates are used in real space exposure experiments where multi-layers of cells will be exposed up to three years.

(Dandelion in Japanese) space mission, Yamagishi et al. were able to catch airborne microbes using aircrafts and balloons. Upon this mission, various radiation resistant *Deinococci* species were chosen for exposure to the outer space environment on the ISS [56]. In a previous space mission named EURECA, a single layer of cells did not survive under argon or space

vacuum. Two *Deinococci* species have been isolated from the high atmosphere and exhibit an equal or even higher resistance to irradiation than *D. radiodurans*. To prepare the cells for the space mission, liquid cultures were collected, dried and placed as multi-layers into aluminium plates containing cylindrical wells (Fig. 5).

Lithopanspermia describes the interplanetary transfer of microbes inside of rocks which provides sufficient protection from UV radiation. Aggregations of *Deinococci* cells are highly resistant to low Earth orbit conditions and provoked the concept of "massapanspermia" (Massa is mass in Latin) in frames of the Japanese Tanpopo mission [51]. This experiment will not only examine the possibility of panspermia but will also provide information on DNA damage response and survival mechanisms supporting life in space.

3. RESULTS SYNOPSIS - PUBLICATION 1 (AS MAIN AUTHOR)

3.1. Growth and Identification of *M. sedula* grown on Martian Regolith simulants

To examine if *M. sedula* can thrive on four different kinds of Martian Regolith Simulants (MRSs – JSC-1A, S-MRS, P-MRS, MRS07/52) and use them as the sole energy source, cells were fixed and subsequently hybridized with a specifically designed 16S rRNA probe which exclusively binds to *M. sedula* cells. After 21 days of chemolithoautotrophic growth cells were positively identified by a specific fluorescent signal. These results were obtained using Multi-labelled fluorescence *in situ* hybridization (MiL-FISH).

3.2. Metal Release into the Medium by *M. sedula*

In all four tested MRSs, *M. sedula* mobilized S, K, Ca, Mg, Si and Na from the substrate into the medium after three weeks of incubation. Manganese was released into the leachate solution from JSC-1A, P-MRS and S-MRS whereas Fe, Ni, Zn and Al concentrations were elevated in MRS07/52 compared to the abiotic control cultivation without *M. sedula* cells. Increased Ni and Mn was detected in S-MRS, Zn and Al in JSC-1A and Sr leaching was observed in the supernatants of P-MRS, S-MRS and MRS07/52. Phosphorous levels dropped in all four cultures, iron was precipitated in JSC-1A, P-MRS and S-MRS probably due to the formation of insoluble iron oxyhydroxides. These results were obtained using inductively-coupled plasma optical emission spectroscopy (ICP-OES).

3.3. Alterations of the Solid Mineral Phase upon *M. sedulas* Growth

After the cultivation was completed, remnants of the liquid culture were left to air dry for several weeks until they were completely dried up. Visual and spectroscopic investigations of the solid mineral phase led to the observation that the surface of all four MRSs was altered after microbial incubation. Our analysis revealed the presence of sphere-like precipitates of variable size in three MRSs (JSC-1A, P-MRS, S-MRS) and coupled spectral analysis indicates that the hemispheroidal morphologies are mainly composed of aluminium and chlorine with a very low carbon content. In MRS07/52 these structures could not be observed but a biofilm layer was distributed over the mineral layer. All newly formed structures/biofilm layer were not observed on corresponding abiotic controls. These results were obtained via scanning electron microscopy coupled to electron dispersive spectroscopy.

3.4. Spectroscopic inspection of the Solid Mineral Phase upon *M. sedulas* Growth

Paramagnetic manganese and iron species were identified via electron paramagnetic resonance (EPR). All four MRSs were examined as well as respective abiotic controls and raw mineral material. All samples (except raw material) were measured at 90K and 273K. Abiotic samples of JSC-1A and P-MRS contained a Mn^{2+} signal which was diminished or altered in biogenic *M. sedula* grown solid material. Furthermore, these samples contained characteristic Fe^{3+} signals in a high spin state while the *M. sedula* grown spectral amplitudes were shifted or reduced. Spectra obtained at 90K inhabited signals of low spin Fe^{3+}. Sample JSC-1A at 273K exhibits an identical g-signal for all three samples (biogenic, abiotic, raw) but a continuously narrowing linewidth (ΔH) is specific to the *M. sedula* grown sample and has already been observed in other microbial samples. In S-MRS a unique signal was observed indicating the presence of tetrahedral Mn^{2+} species which is absent in the abiotic control. Low and high spin Fe^{3+} species were identified in MRS07/52 and no manganese signals.

4. RESULTS SYNOPSIS – PUBLICATION 2 (AS CO-AUTHOR)

4.1. Effects of UVC/vacuum on cellular integrity of *D. radiodurans*

Desiccated *D. radiodurans* cells were investigated via Scanning Electron microscopy to check on the cellular morphology after cells were exposed to simulated space conditions. Our results show that there is no visible cell damage in irradiated samples, typical diplococci and tetracocci aggregates were observed compared to control cells.

5. PUBLICATION 1 AS MAIN AUTHOR

5.1. Contribution of the Author

The author composed table 1, 2 and 4 as well as figures 2 and four. The author conducted EPR and SEM-EDS experiments and interpreted the overall data together with author 7 and EPR with author 2.

Exploring fingerprints of the extreme thermoacidophile *Metallosphaera sedula* grown on synthetic Martian regolith materials as the sole energy sources

Denise Kölbl[1], Marc Pignitter[2], Veronika Somoza[2], Mario P. Schimak[3], Oliver Strback[4], Amir Blazevic[1], Tetyana Milojevic[1*]

[1]Department of Biophysical Chemistry, University of Vienna, Althanstrasse 14, A-1090 Vienna, Austria.

[2]Department of Nutritional and Physiological Chemistry, Faculty of Chemistry, University of Vienna, Althanstraße 14, 1090 Vienna, Austria.

[3]Max Planck Institute for Marine Microbiology, Celsiusstrasse 1, D-28359 Bremen, Germany

[4]Biomedical Center Martin, Jessenius Faculty of Medicine in Martin, Comenius University in Bratislava, Mala Hora 4, 036 01 Martin, Slovakia

*Correspondence to: Tetyana Milojevic tetyana.milojevic@univie.ac.at

ABSTRACT

The biology of metal transforming microorganisms is of a fundamental and applied importance for our understanding of past and present biogeochemical processes on Earth and in the Universe. The extreme thermoacidophile *Metallosphaera sedula* is a metal mobilizing archaeon, which thrives in hot acid environments (optimal growth at 74°C and pH 2.0) and utilizes energy from the oxidation of reduced metal inorganic sources. These characteristics of *M. sedula* make it an ideal organism to further our knowledge of the biogeochemical processes of possible life on extraterrestrial planetary bodies. Exploring the viability and metal extraction capacity of *M. sedula* living on and interacting with synthetic extraterrestrial minerals, we show that *M. sedula* utilizes metals trapped in the Martian regolith simulants **(**JSC Mars 1A; P-MRS; S-MRS; MRS07/52) as the sole energy sources. The obtained set of microbiological and mineralogical data suggests that *M. sedula* actively colonizes synthetic Martian regolith materials and releases free soluble metals. The surface of bioprocessed Martian regolith simulants is analyzed for specific mineralogical fingerprints left upon *M. sedula* growth. The obtained results provide insights of biomining of extraterrestrial material as well as of the detection of biosignatures implementing in life search missions.

Keywords: *Metallosphaera sedula*, Martian Regolith Simulants, EPR spectroscopy, microbe-mineral interactions, biosignatures

INTRODUCTION

Chemolithoautotrophy has been indicated as the most primordial form of microbial metabolism on the early Earth (Blöchl et al., 1992; Wächtershäuser, 1992; Stetter et al., 2006) and proposed as a possible metabolic form for other iron-mineral-rich planets like Mars (Grotzinger et al., 2014; Hurowitz, et al., 2017). Recent Mars exploration missions have provided a comprehensive analysis of the physical and geochemical environment of Mars (Grotzinger et al., 2014, 2013; Hurowitz, et al., 2017) aiming to identify potential habitats that bear the energy sources available on this planet to support chemolithotrophic life. The rich content of iron and sulfur minerals on Mars makes iron and sulfur transforming microorganisms the prime candidates for considering as models for putative Martian extant or extinct life forms (Amils et al., 2007; Nixon et al., 2012). In the hydrogeological and atmospheric oxygen-rich past of Mars (>3 Ga ago), such metabolically similar microorganisms might have contributed in redox cycling of elements from Martian regolith and deposition of the mineral sediments of hydrated sulfates and ferric oxide content (Amils et al., 2007). The detection of a stable redox-stratified water body along with recent mineralogical, geochemical and sedimentological investigations point to an ancient habitable fluvio-lacustrine environment at Yellowknife Bay in the Gale crater of Mars that would have been suited to harbor a Martian biosphere based on chemolithoautotrophy (Grotzinger et al., 2013, 2014; Hurowitz et al., 2017). The present atmosphere of Mars contains traces of oxygen at a concentration of 0.146% (Mahaffy et al., 2013), ruling out the consideration of Mars as an environment where only anaerobic metabolism can be expected, while mineralogical analysis points to a plausible redox couple for prokaryotic respiration (Grotzinger et al., 2013 and 2014). In this context metal transforming extremophiles represent an exciting field of research for the study of microbe-mineral interactions in order to find the unique biosignatures of life in extreme conditions.

A rock-eating archaeon *Metallosphaera sedula*, originally isolated from a geothermal environment, flourishes in hot and acidic conditions (optimal growth at 74°C and pH 2.0) and exhibits unusual heavy-metal resistance (Auernik et al., 2008; Huber et al., 1989; Peeples and Kelly, 1995). This facultative chemolithotroph is capable of bioleaching, and the key to its chemical attack of metal ores is the redox regeneration of Fe^{3+} from Fe^{2+}. Apart from Fe-oxidizing properties, metabolically versatile *M. sedula* has the ability to use a variety of electron donors, including reduced inorganic sulfur compounds, uranium ores, as well as molecular hydrogen under microaerobic conditions (Auernik and Kelly, 2008; 2010; Maezato et al., 2010; Mukherjee et al., 2012; Wheaton et al, 2016).

In light of future perspectives of space exploration and *in-situ* resource utilization (ISRU) programs, the possible implications of the extreme thermoacidophile *M. sedula* have been already suggested for asteroid biomining (Reed, 2015). A deeper investigation of the physiology of metal transforming microorganisms and mineral-microbial interactions facilitates our understanding of the possible energy production mechanisms of early life forms. Further, it extends our understanding of putative biosignatures that can be detected during missions aiming to uncover evidence of past habitability on planetary bodies.

The main goal of this work was to explore the growth potential and metal extraction capacity of the extremely thermoacidiphilic archeon *M. sedula* cultivated on four different types of Mars regolith simulants - JSC Mars 1A, P-MRS, S-MRS, and MRS07/52 as the sole energy sources, as well as to

investigate the possible biosignatures of mineral-microbial interactions associated with these cases. The different simulants were used to mimic the Martian regolith composition from different locations and historical periods of Mars: a palagonitic tephra (JSC Mars 1A as a close spectral analog to the bright regions of Mars); Early Hydrous or Phyllosilicatic Mars Regolith Simulant (P-MRS, characterized by high clay content); Late Acidic or Sulfatic Mars Regolith Simulant (S-MRS, characterized by the gypsum); the highly porous Mars Regolith Simulant (MRS07/52 that simulate sediments of the Martian surface). Due to its metal oxidizing metabolic activity, when given an access to these Martian regolith simulants, *M. sedula* released soluble metal ions into the leachate solution and altered their mineral surface leaving behind specific signatures of life.

MATERIALS AND METHODS

Strain and Media Composition

M. sedula (DSMZ 5348) cultures were grown aerobically in DSMZ88 Sulfolobus medium containing 1.3 g $(NH_4)_2SO_4$, 0.28 g KH_2PO_4, 0.25 g $MgSO_4 \cdot 7\ H_2O$, 0.07 g $CaCl_2 \cdot 2\ H_2O$ and 0.02 g $FeCl_3 \cdot 6\ H_2O$ dissolved in 1 L of water. After autoclaving, Allen's trace elements solution was added to 1 L media resulting in 1.80 mg $MnCl_2 \cdot 4\ H_2O$, 4.50 mg $Na_2B4O_7 \cdot 10\ H_2O$, 0.22 mg $ZnSO_4 \cdot 7\ H_2O$, 0.05 mg $CuCl_2 \cdot 2\ H_2O$, 0.03 mg $Na_2MoO_4 \cdot 2\ H_2O$, 0.03 mg $VSO_4 \cdot 2\ H_2O$, and 0.01 mg $CoSO_4$ final concentration. The pH was adjusted to 2.0 with 10 N H_2SO_4. Chemicals of high purity grade were used for media preparation.

Composition of synthetic Martian regolith analogues

In this study, four mineral mixtures of Mars regolith simulants (MRS) were used to examine whether these minerals could provide nutrients/energy sources necessary for lithoautotrophic growth of *M. sedula* (Table 1 and Table 2). The mineral mixtures of synthetic Martian regolith analogues were assembled in accordance to data on the structural and chemical composition of Martian minerals identified in meteorites (McSween, 1994) and by recent orbiter and rover missions (Bibring et al., 2005; Chevrier and Mathé, 2007; Morris et al., 2010; Poulet et al., 2005; Mustard et al., 2009) reflecting current knowledge of environmental changes on Mars (Boettger et al., 2011). JSC Mars-1A Martian Regolith Simulant is a palagonitic tephra (volcanic ash altered at low

TABLE 1 | Chemical composition of the synthetic Martian regolith analogs used in this study.

Major chemical composition	JSC Mars-1A[1]	P-MRS[2]	S-MRS[3]	MRS07/52[4]
	Wt %	Wt %	Wt %	Wt %
Silicon dioxide (SiO_2)	34.5–44	43.6	30.6	34.6
Aluminum oxide (Al_2O_3)	18.5–23.5	11.9	9.2	14.1
Titanium dioxide (TiO_2)	3–4	0.36	0.05	0.1
Ferric oxide (Fe_2O_3)	9–12	19.6	14.9	20.6
Iron oxide (FeO)	2.5–3.5	–	–	–
Magnesium oxide (MgO)	2.5–3.5	4.52	10.3	3.4
Calcium oxide (CaO)	5–6	4.74	17.8	6.1
Sodium oxide (Na_2O)	2–2.5	0.32	1.09	2.5
Potassium oxide (K_2O)	0.5–0.6	1.04	0.13	0.2
Manganese oxide (MnO)	0.2–0.3	0.16	0.3	–
Diphosphorus pentoxide (P_2O_5)	0.7–0.9	0.55	0.05	–
Sulfur trioxide (SO_3)	–	0.2	9.1	5.1
LOI	–	11.8	5.4	–

[1]*Data for JSC Mars-1A obtained from Orbital Technologies Corporation, Madison, WI, United States;* [2,3]*Data for P-MRS and S-MRS were obtained from Boettger et al. (2012);* [4]*Data for MRS07/52 were obtained from Moeller et al. (2008).*

temperatures), produced by Orbital Technologies Corporation, Madison, WI, USA. The only phases detected by x-ray diffraction are plagioclase feldspar and minor magnetite. Iron Mossbauer spectroscopy also detected traces of hematite, olivine, pyroxene and/or glass (Morris et al., 1993). One of the Mars regolith simulants was phyllosilicate-rich (Phyllosilicate Mars Simulant, P-MRS), containing a high percentage of smectite clays like montmorillonite, kaolinite, and chamosite, as well as carbonates (siderite, hydromagnesite). The other mixture (Sulfatic Mars Simulant, S-MRS) was characterized by its high gypsum and goethite content. Both mineral mixtures consist also of pyroxene and plagioclase (gabbro), olivine, quartz, and the anhydrous ferric oxide hematite (Boettger et al., 2011). The mineral composition of P-MRS is modeled based on the phyllosilicate-rich sites on Mars, which formed during an aqueous weathering regime with neutral to alkaline conditions in the Noachian epoch (>3.7 Ga), either on the surface or in the subsurface at hydrothermal areas (Tables 1 and 2) (Bibring et al., 2006; Chevrier et al., 2007; Halevy et al., 2007; Ehlmann et al., 2011). S-MRS represents the Martian sediments with a high sulfate content that presumably correspond to the acidic conditions in the Hesperian epoch (3.7- 3.0 Ga) (Bibring et al., 2006; Bullock and Moore, 2007; Chevrier et al., 2007). The final inorganic mineral mixture investigated in this study was the Martian soil simulate MRS07/52. This sample was supplied by German Aerospace Center and was produced to have comparable constituents to that of the soil on Mars (Moeller et al., 2008) (Tables 1 and 2).

TABLE 2 | Mineral composition of the synthetic Martian regolith analogs used in this study.

Mineral component	JSC 1A[1]	P-MRS[2]	S-MRS[3]	MRS07/52[4]
	Wt %	Wt %	Wt %	Wt %
Plagioclase Feldspar	64	–	–	–
Olivine	12	–	–	-
Magnetite	11	–	–	–
Pyroxene and/or glass	9	–	–	–
Gabbro		3	32	–
Dunite		2	15	–
Quartz		10	3	1
Hematite	5	5	13	20
Montmorillonite		45	–	48
Chamosite		20	–	–
Kaolinite		5	–	10
Siderite		5	–	–
Hydromagnesite		5	–	–
Goethite		–	7	–
Gypsum		–	30	–
Anhydrite		–	–	13
$MgSO_4$		–	–	7
Halite		–	–	1

[1]*Data for JSC Mars-1A were obtained from Morris et al. (1993);* [2,3]*Data for P-MRS and S-MRS were obtained from Boettger et al. (2012);* [4]*Data for MRS07/52 were obtained from Moeller et al. (2008).*

Cultivation Setup

Chemolithoautotrophic cultivation of *M. sedula* was performed in DSMZ88 Sulfolobus medium described above in 1L glassblower modified Schott-bottle bioreactors (Duran DWK Life Sciences GmbH, Wertheim/Main, Germany), equipped with a thermocouple connected to a heating and magnetic stirring plate (IKA RCT Standard/IKA C-MAG HS10, Lab Logistics Group GmbH, Meckenheim, Germany) for temperature and agitation control. Each bioreactor was equipped with three 10 mL graduated glass pipettes, permitting carbon dioxide and air gassing (with the gas flow of 9 mL min-1, adjusted to five bubbles s^{-1} by using 8 mm valves (Serto, Frauenfeld, Switzerland)) and sampling of culture, respectively (Supplementary Figure 1). The graduated pipettes used for gassing were connected by silicon tubing to sterile 0.2 µm filters (Millex-FG Vent filter unit, Millipore, Billerica, USA).

The graduated pipettes used for sampling were equipped with a Luer-lock system in order to permit sampling with sterile syringes (Soft-Ject, Henke Sass Wolf, Tuttlingen, Germany). The offgas was forced to exit via a water-cooled condenser (Ochs GmbH, Bovenden, Germany). For the cultivations of *M. sedula* at 73°C the temperature inside the bioreactors was controlled by electronic thermocouple via the heating and magnetic stirring plates. *M. sedula* inocula were obtained by resuspending a chemolithoautotrophically grown cell pellet formed by centrifugation at 6000 × *g* for 15 min in DSMZ88 media without organic carbon source and inorganic metals/metalloids as energy sources. For chemolithoautotrophic growth cultures with initial pH of 2.0 were supplemented with 1 g/liter Martian regolith simulants, no further pH adjustments were introduced during the cultivation. The minerals were temperature sterilized at 180°C in a heating chamber for a minimum of 24 hours prior to autoclaving at 121°C for 20 min. Abiotic controls consisting of uninoculated culture media supplemented with MRSs were included in all the experiments. Growth of cells was monitored by phase contrast/epifluorescence microscopy and metal release. Precise cell enumeration was found to be difficult due to the interference with mineral particles of similar size and round shaped morphology and shielding of *M. sedula* by iron mineral precipitates, especially at later stages of the growth. To visualize wiggling cells on solid particles, a modified "DAPI" (4'-6'- Diamidino-2-phenylindole) staining was used (Huber et al., 1985); afterwards the cells were observed and recorded with ProgRes® MF cool camera (Jenoptik) mounted on Nikon eclipse 50i microscope, equipped with F36-500 Bandpass Filterset (ex, 377/50 nm; em, 447/60 nm).

Multi-labelled-Fluorescence in Situ Hybridization (MiL-FISH)

Cultures of *M. sedula* grown on Martian Regolith Simulants (Supplementary Figure 2) were fixed in 2% paraformaldehyde (PFA) at room temperature for 1 hour and subsequently washed three times in 1x PBS (phosphate buffer saline) with centrifugation steps of 3000 ×g for 5 minutes between each exchange. Cells were extracted from sediment after Braun et al. 2016 as follows: 1 ml sediment from each sample was centrifuged at 5000 ×g for 5 minutes, the supernatant discarded, re-suspended in 1.5 ml Mili-Q that included 0.2 ml methanol and 0.2 ml detergent mix (100mM EDTA, 100mM sodium pyrophosphate decahydrate and 1% v:v Tween 80) and shaken at 750 rpm for 60 minutes. To separate cells from sediment particles samples were sonicated at 30% power three times for 15 seconds using an ultrasonic probe. Finally, a gradient centrifugation was applied consisting of three 2 ml Nycodenz layers of 30% 50% and 80% on top of a 2 ml sodium polytungstate solution with a 2.23 g per ml density and centrifuged at 5000 ×g for 2 hours at 4° C. The microbial fraction contained within the supernatant above the sodium polytungsate was extracted with a glass pipette. To further clean the samples from fine sediment particles the gradient centrifugation was repeated a second time in the same manner. *Metallosphaera sedula* 16S rRNA phylotype specific probe was designed with the software package ARB (Ludwig, 2004) and labelled with 4x Atto488 via Click chemistry (biomers.net GmbH, Ulm, Germany) (see Table 3). Cells were mounted on 10 well Diagnostica glass slides (Thermo Fisher Scientific Inc. Waltham, USA) and MiL-FISH conducted directly on slides with 30% formamide and a 3 hour hybridisation time (Schimak et al., 2015). Positive control for the specificity of the phylotype specific probe M.sedula_174 was provided by use of the same *Metallosphaera sedula* DSM5348 culture published in Schimak et al., 2015. After hybridization, slides were washed for 15 minutes at 48 °C according to Manz et al. 1992 (14 to 900 mM NaCl, 20 mM Tris-HCl [pH 8], 5 mM EDTA [pH 8], and 0.01% SDS) at a stringency adjusted to the formamide concentration used

(Manz et al., 1992). DNA staining with DAPI (4=,6-diamidino-2-phenylindole) followed (10 mg/ml) for 10 minutes after which slides were rinsed in distilled water 3 times. Vectashield (Vector Laboratories, Burlingame, U.S.A) mounting medium was applied and slides closed with a coverslip. Fluorescence images were taken with an AxioCam Mrm camera mounted on an Nikon Eclipse 50i illuminated by a Nikon Intensilight C-HGFI light source and equipped with a F36-525 Alexa 488 (ex, 472/30 nm; em, 520/35 nm) filter cube. Images were recorded with the Windows based AxioVision (release 4.6.3 SP1) imaging software and any image-level adjustments made either therein or using the Mac OS X based Adobe Photoshop version 12.0.4. The figure table depicted was composed using Mac OS X based Adobe Illustrator version 15.0.2 and images cropped by use of clipping masks.

Scanning electron microscopy

The mineral precipitates (Supplementary Figure 3) were examined with a Zeiss Supra 55 VP scanning electron microscope (SEM), equipped with a spectroscope of dispersive energy (EDS), which was used for imaging and elemental analysis of precipitates. The samples were coated with a thin Au/Pd layer (Laurell WS-650-23 spincoater). The acceleration voltage applied was 5 kV and the EDS analyses were performed with a 120 µm aperture and a counting time of 50 s. In order to control the beam parameters, cobalt was used as a standard. Conventional ZAF matrix correction was used to calculate the final composition from the measured X-ray intensities. All the sample spots investigated by EDS were chosen randomly and each spot was measured three times. Table 4 represents the chemical composition of aluminum/chlorine containing microspheroids, which was taken as the average of the measurements from 20 randomly chosen spots.

Metal analysis

To determine the extracellular concentrations of metal ions mobilized from the Martian regolith simulants, culture samples were clarified by centrifugation. Samples of the resulting supernatants were filtered (0.44µm pore size) and analyzed by inductively coupled plasma-optical emission spectrometer (ICP-OES) Perkin Elmer Optima 5300 DV. All reported values are averages from duplicate samples.

EPR

The Electron Paramagnetic Resonance (EPR) spectra were recorded on an X-Band Bruker Elexsys-II E500 CW-EPR spectrometer (Bruker Biospin GmbH, Rheinstetten, Germany) at 90 ± 1 and 293 ± 1 K using a high sensitivity cavity (SHQE1119). Solid state EPR measurements were performed setting microwave frequency to 9 GHz, modulation frequency to 100 kHz, center field to 6000 G, sweep width to 12000 G, sweep time to 335.5 s, modulation amplitude to 20.37 G, microwave power to 15 mW, conversion time to 81.92 ms and resolution to 4096 points. The samples were put in EPR quartz tubes (Wilmad-LabGlass, Vineland, New Jersey, USA) and scanned three times, of which the average was used for analysis. The spectrum of an empty control tube was subtracted from all sample spectra. All spectra were analyzed

TABLE 3 | Oligonucleotide probes used in this study.

Probe	Sequence 5′–3′ (reverse complementary)	Target gene	Label	Synthesis	Taxon	Target species	FA %	Colour
M. sedula_174_17mer	AGA UUC CCU UGC CCG CU	16S rRNA	Atto488	Click chemistry	Archaea	*Metallosphaera sedula*	30%	Green

Probe name, nucleotide sequence - underscore indicates nucleotide:fluorochrome conjugates, target gene, label type, label synthesis, target taxon or higher, target species and probe color during imaging.

with the Bruker Xepr software.

Statistical Analysis

For the statistical analysis and graphical representation of the data the Excel 2016 (version 7.0) and Sigma plot (version 13.0) software packages were used.

TABLE 4 | Average metal composition (%) of microhemispheroids detected in mineral precipitates withdrawn from cultures of *Metallosphaera sedula* grown on JSC Mars 1A, P-MRS, and S-MRS.

	C	O	Al	Cl
Mean % (± standard deviation) *n = 20*	6.41 ± 5.01	20.33 ± 7.71	18.18 ± 10.47	7.10 ± 3.85

RESULTS

Chemolithotrophic growth on synthetic Martian regolith

M. sedula was grown under chemolithoautotrophic conditions on MRSs (Table 5), and interaction of cells with the mineral particles was examined. After 21 days of CO_2-supplemented cultivation on MRSs as the sole energy source, phylogenetic identification and visualization of *M. sedula* cells was achieved with Multi-Labeled fluorescence *in situ* hybridization (MiL-FISH). For this purpose a newly designed phylotype specific probe targeting the 16S rRNA (Table 3) was used. The cultures of *M. sedula* grown on all four investigated in this study MRSs (JSA 1A, P-MRS, S-MRS, and MRS07/52) resulted in positive fluorescent signal with Atto488 labeled probes at a 30% formamide concentration (Figure 1). Only cells that show both DAPI and fluorescent signal were considered as positive hybridization with the target organism. Additionally, it was noted that cells of S-MRS and MRS07/52 cultures occur in mucus bound aggregates which can be inferred as extracellular polysaccharide substances (EPS) known for *M. sedula* (Auernik et al., 2008) (Figure 1G – L).investigated in this study MRSs (JSA 1A, P-MRS, S-MRS, and MRS07/52) resulted in positive fluorescent signal with Atto488 labeled probes at a 30% formamide concentration (Figure 1). Only cells that show both DAPI and fluorescent signal were considered as positive hybridization with the target organism. Additionally, it was noted that cells of S-MRS and MRS07/52 cultures occur in mucus bound aggregates which can be inferred as extracellular polysaccharide substances (EPS) known for *M. sedula* (Auernik et al., 2008) (Figure 1G – L).

Metal release

ICP-OES analysis of composition of major elements mobilized from all tested Martian regolith simulants showed the elevated levels of released S, K, Ca, Mg, Si, and Na in the growth medium (leachate solution) (Figure 2). A further change in trace elements (higher released Mn) occurred in cultures of *M. sedula* grown on JSA 1A, P-MRS, and S-MRS. Additionally, in case with MRS07/52 leachate solution was characterized by elevated levels of Fe, Ni, and to lesser extent Al in comparison to abiotic control (Figure 2D). The increased level of released Ni ions was also detected in S-MRS grown cultures. The elevated levels of Sr ions were measured in culture supernatants of *M. sedula* grown on P-MRS, S-MRS, and MRS07/52, while increased soluble Zn was represented in JSC 1A and MRS07/52 grown cultures. The drop in P concentrations was detected in leachate solutions of all the tested MRS. The decrease of total iron

observed in *M. sedula* cultures grown on JSC 1A, P-MRS, and S-MRS could be possibly attributed to the formation of insoluble iron oxyhydroxides which form precipitated mineral phase and therefore are not included in the samples of leachate solution used for the ICP-OES analysis. This phenomenon of 'lost iron' has been already previously reported in case of microbial cultivation on extraterrestrial material (Gronstal et al., 2009).

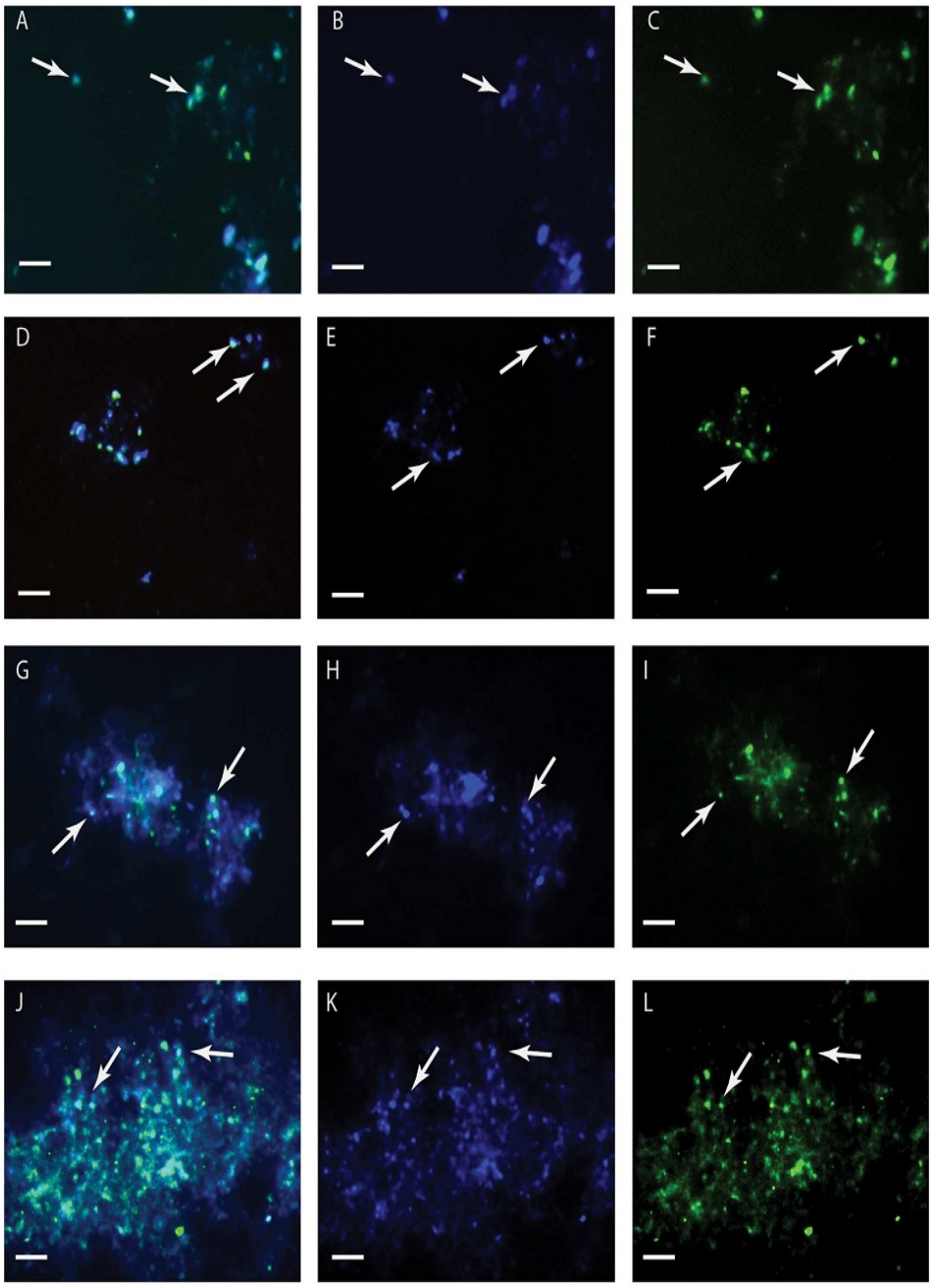

FIGURE 1 | Multi-Labeled-Fluorescence *in situ* Hybridization (MiL-FISH) of *Metallosphaera sedula* cells grown on synthetic Martian regolith materials as the sole energy sources. **(A,D,G,J)** Overlaid epifluorescence images, showing overlap of the specific oligonucleotide probe targeting *M. sedula* with DAPI signals. **(B,E,H,K)** DAPI staining of the same field (blue). **(C,F,I,L)** MiL-FISH images of cells (green) after hybridization with the specific oligonucleotide probe targeting *M. sedula*. Cultures of *M. sedula* were examined with MiL-FISH conducted after Schimak et al. (2015) after 21 days of cultivation with JSC Mars 1A **(A–C)**, P-MRS **(D–F)**, S-MRS **(G–I)**, and MRS07/52 **(J–L)**.

SEM-EDS investigation of solid mineral phase

To further study the interactions of *M. sedula* with the Martian regolith simulants, the surface of these minerals was examined for possible alterations upon *M. sedula* growth. Inspection by SEM of solid mineral phase in cultures of *M. sedula* grown on synthetic Martian regolith revealed the presence of sphere-like particles of variable size (0.3-3 µm). These microhemispheroids were represented in cultures of *M. sedula* grown on JSC 1A, P-MRS, and S-MRS and absent in the corresponding abiotic controls (Figure 3). The results of SEM-EDS analysis indicate that these hemispheroidal morphologies are mainly composed of oxygen, aluminum and chlorine and with no or low carbon content (Table 4, Supplementary Figure 4). The solid mineral phase withdrawn from S-MRS grown cultures of *M. sedula* was especially enriched with aluminum/chlorine containing microspheroids, while both biotransformed JSC 1A and P-MRS had a minor occurrence of these particles. Figure 3C and Supplementary Figure 4 show budding microspheroids represented on biotransformed surface of S-MRS. SEM assisted investigations of a solid phase of biotransformed MRS07/52 showed the biofilm layer distributed over the mineral surface (Figure 3G). Such a deposited biofilm layer was absent in the corresponding abiotic control of MRS07/52 incubated in the growth medium at 73 °C but without *M. sedula* (Figure 3H).

TABLE 5 | Cell densities of *M. sedula* cultures grown on the synthetic Martian regolith analogs at "0" time point and after 21 days of cultivation.

Cultivation time	0 day	21 days
	Cell density [cells/ml]	
JSC 1A	4,93E+06 ± 6,49E+05	1,24E+08 ± 7,40E+07
P-MRS	5,98E+06 ± 3,19E+06	4,77E+08 ± 3,74E+08
S-MRS	5,57E+06 ± 3,10E+06	3,06E+08 ± 3,07E+08
MRS07/52	4,34E+06 ± 2,25E+06	2,02E+08 ± 1,32E+08
Pyrite	9,80E+06 ± 9,45E+05	1,50E+09 ± 2,50E+08
No MRSs added	6,95E+06 ± 7,85E+05	1,48E+05 ± 8,73E+03

Mean and standard deviation of n = 3 biological replicates are represented. When no MRSs were added, cultivation medium was inoculated with cells of M. sedula without additional energy source.

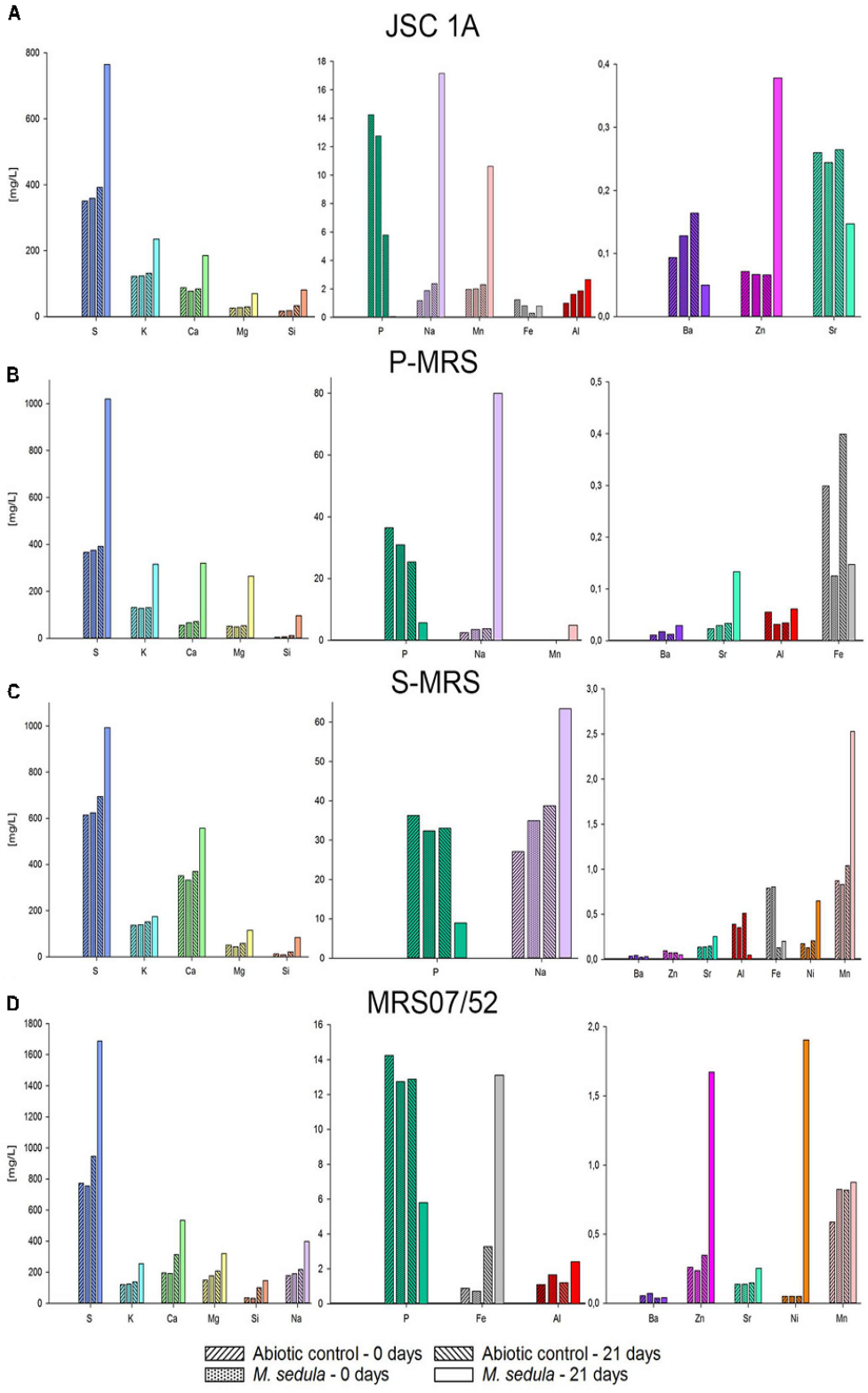

FIGURE 2 | Inductively coupled plasma-optical emission spectrometer (ICP-OES) analysis of released metal ions in supernatant of *M. sedula* cultures grown on the Martian regolith simulants [JSC Mars 1A **(A)**; P-MRS **(B)**; S-MRS **(C)**; MRS07/52 **(D)**] as the sole energy sources. Samples were taken at "0" time point and after 21 days of cultivation of *M. sedula* on the Martian regolith simulants and from corresponding abiotic controls.

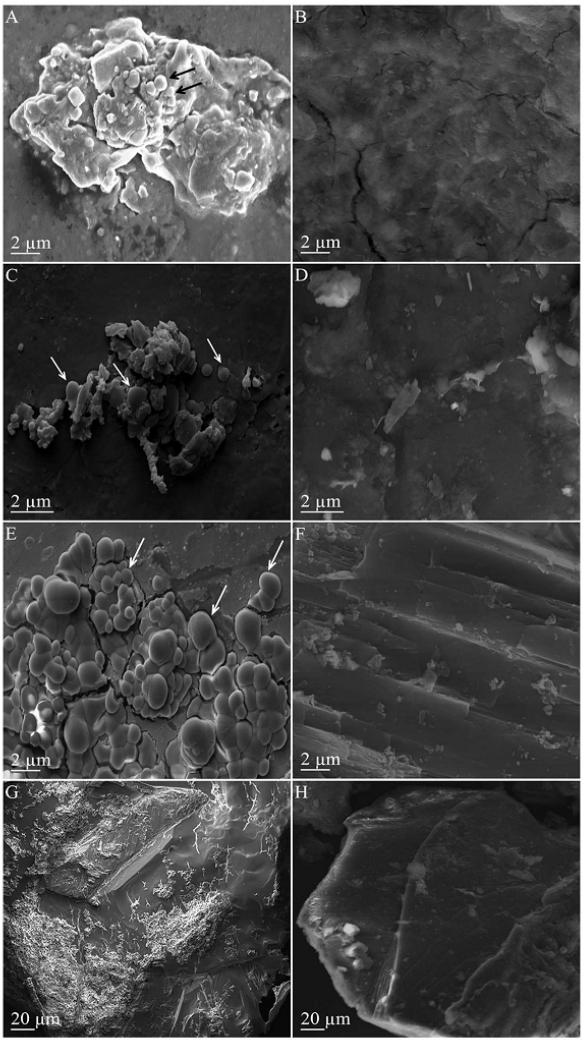

FIGURE 3 | Scanning electron microscopy (SEM) images of the mineral surfaces of synthetic Martian regolith materials. **(A)** Scanning electron image showing a surface of mineral precipitate obtained after the cultivation of *M. sedula* on JSC 1A. **(C)** Scanning electron image showing a surface of mineral precipitate obtained after the cultivation of *M. sedula* on P-MRS. **(E)** Scanning electron image showing a surface of mineral precipitate obtained after the cultivation of *M. sedula* on S-MRS. **(G)** Scanning electron image showing a surface of mineral precipitate obtained after the cultivation of *M. sedula* on JSC 1A. Cultures of *M. sedula* were examined with SEM after 21 days of cultivation on the Martian regolith simulants. Aluminum/chlorine containing microspheroids occurred in mineral precipitates of JSC Mars 1A, P-MRS, and S-MRS after *M. sedula* growth, are depicted with arrows. Images **(B,D,F,H)** represent the corresponding abiotic controls.

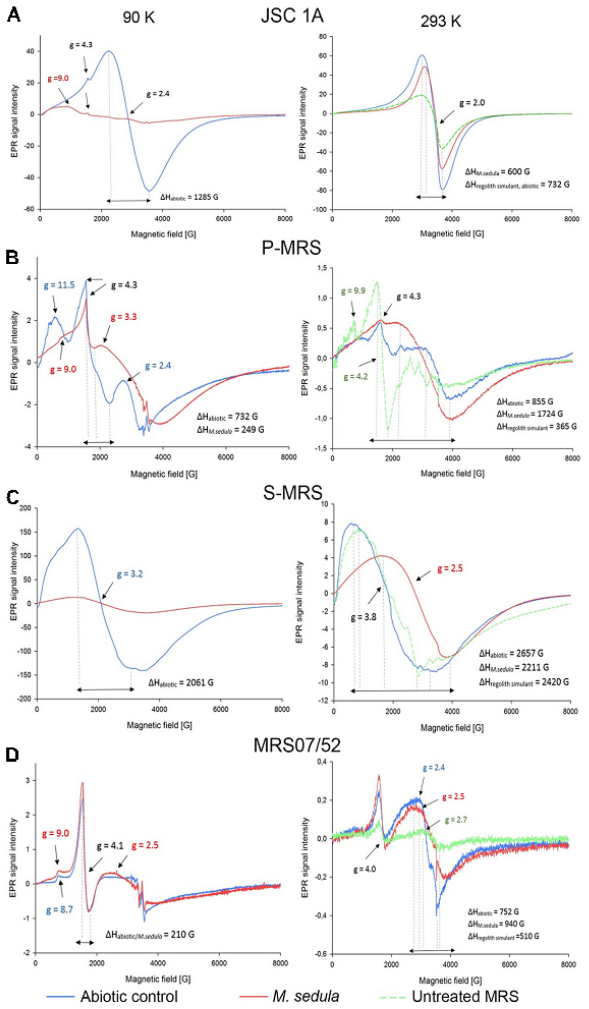

FIGURE 4 | Electron Paramagnetic Resonance (EPR) spectra of raw synthetic Martian regolith materials (green line), synthetic Martian regolith materials bioprocessed by *M. sedula* (red line), and synthetic Martian regolith materials after the treatment with cultivation medium, but without *M. sedula* (abiotic control, blue line). **(A)** EPR spectra of JSC Mars 1A; **(B)** EPR spectra of P-MRS; **(C)** EPR spectra of S-MRS; **(D)** EPR spectra of MRS07/52). Spectra recorded at 90 and 293 K are represented in left and right columns, respectively. *g*- values are depicted with the color code corresponding to the spectra; identical *g*-values are represented in black color. The EPR *g*-values recorded at 90 and 293 K are grouped in Supplementary Table 1. The corresponding EPR Linewidths (ΔH) values are provided in Supplementary Table 2.

EPR investigation of solid mineral phase

EPR measurements were performed to (1) identify paramagnetic species of manganese and iron in the different MRSs samples and to (2) investigate the impact of *M. sedula* on MRSs with a possible effect on the oxidative state of manganese and iron. The four different MRSs mineral mixtures were incubated in cultivation medium in the presence (biotic) or absence (abiotic) of *M. sedula*. The spectra of untreated (raw) MRSs were investigated as well. The abiotic samples of JSC 1A and P-MRS contained Mn^{2+} as evident by a prominent signal at g=2.4 with a broad linewidth of >1200 G (Figure 4, Supplementary Tables 1 and 2) typical for abiotic Mn^{2+} samples (Kim et al., 2011; Ivarsson et al., 2015). For JSC 1A, the biotic sample

revealed an almost complete decline of the Mn^{2+} signal, while for P-MRS an alteration of the g=2.4 signal in the biotic sample resulted to the appearance of a broad signal with g=3.3, indicating dipolar interactions of mixed ionic states (Mn^{3+} and Mn^{4+}) (Ivarsson et al., 2015). In biotic and abiotic samples of JSC 1A and P-MRS, Fe^{3+} could be identified by the characteristic g=4.3 and g=9 signals. A high spin d5 configuration of the Fe^{3+} can be inferred from the positions of these resonance signals. Figure 4B shows that the amplitude of high spin Fe^{3+} g=4.3 signal is slightly lower in biotic P-MRS than in the corresponding abiotic sample, while the signals g=11.5 and g=9.9 measured at 90K and 293 K, respectively, are clearly diminished after *M. sedula* cultivation. Independent of the incubation conditions, the EPR spectra of all four MRSs samples recorded at 90 K revealed small signals with g-values in the range of 2.0 and 2.7, which were assigned to Fe^{3+} with low spin electron configuration. No significant changes were detected between the biotic and abiotic samples measured at 90 K with regard to the Fe^{3+} in the low spin state. In opposite, a continuously narrowing resonance signal g=2 was recorded at 293 K in JSC 1A samples after cultivation with *M. sedula*. The linewidth (ΔH) remained unaltered for raw and abiotic JSC 1A (732 G) and decreased to 600 G after the cultivation with *M. sedula* (Figure 4 and Supplementary Table 2).

The EPR spectrum of the abiotic S-MRS sample exhibits a prominent resonance at g=3.2 with a broad linewidth of 2061 G, which is absent in the EPR spectra of all the other MRSs samples measured at 90 K. This specific resonance is obtained from samples containing tetrahedral Mn^{2+} species (J. Xu et al., 1999). A pronounced decrease of the g=3.2 resonance signal could be demonstrated for the biotic sample of S-MRS compared to the corresponding abiotic sample. In MRS07/52, Fe^{3+} species in the low and high spin state were identified based on the characteristic EPR signals as mentioned above. No manganese could be detected in MRS07/52. The minor difference in biotic and abiotic MRS07/52 samples occurred at the area of low spin Fe^{3+}, which is even more detectable in spectra recorded at 293 K (Figure 4D). The slightly increased amplitude of high spin Fe^{3+} signal along with the shift of g value from 8.7 for abiotic to 9 for biotic samples was also observed at 90K. The strong resonance line at g=4.1 which can be assigned to Fe^{3+} located in orthorhombic positions (Polikreti and Maniatis, 2002) is not altered in biotic and abiotic MRS07/52 samples (Figure 4D).

DISCUSSION

Evolutionally diversified metal-solubilizing microorganisms with their fascinating metabolic pathways have developed an exquisite set of capabilities for manipulating minerals by dissolving them to access useful metals. We tested the ability of *M. sedula* to grow chemolithoautotrophically in four different types of synthetic Martian regolith. As growth was detected in all four MRS, we concluded that *M. sedula* is capable of chemolithotrophic growth using the synthetic Martian regolith as the sole energy source. Further, our results indicated that *M. sedula* is able to solubilize metals from the synthetic Martian regolith (e.g., S, K, Ca, Na, Mg, Si, Mn, Fe, Zn, Ni, Sr) into the growth medium (leachate solution). Interestingly, in all four tested MRSs, the amount of detected phosphorus decreased in the biogenic samples after 21 days of cultivation, possibly indicating phosphorous consumption by *M. sedula* in order to maintain the growing population of the cells, which can explain a decreased amount of P in leachate solutions (Figure 2). The observed metabolic activity coupled to the release of free soluble metals from

the synthetic Martian regolith can certainly pave the way to asteroid biomining, launching the biologically assisted exploitation of raw materials from asteroids, meteors and other celestial bodies.

However, insufficient evidence exists to confidently identify which metal/or metals in all tested MRSs serve as electron donors utilized by *M. sedula* to satisfy its bioenergetics needs. Due to its versatile metal-oxidizing capacities (Mukherjee et al., 2012; Maezato et al., 2012; Huber et al., 1989; Auernik and Kelly, 2010; Wheaton et al., 2016), the fact that *M. sedula* can potentially respire on a combination of different elements represented in MRSs cannot be ruled out. It would seem beneficial for *M. sedula* to attach preferentially to those minerals containing useable substrates such as reduced iron or sulfur compounds. Fe^{2+} as a constitutive element is represented in variety of minerals, including olivine ($(Mg, Fe^{2+})_2SiO_4$) (11% in JSC 1A, 2% in P-MRS, 15% in S-MRS), and siderite ($Fe(CO_3)$, 5% in P-MRS), or bound to the smectite clay chamosite ($(Fe^{2+},Mg)_5Al_2Si_3O_{10}(OH)_8$, 20% in P-MRS) (Table 2). The comparison of the obtained EPR spectra of raw and abiotic samples (Figure 4, green and blue lines, correspondingly) with the mineralogy and chemical composition of all MRSs we tested suggested that the recorded signals are most likely due to Mn^{2+} and Fe^{3+} ions. The obvious alteration of the width of EPR signals g=2 detected in JSC 1A samples at 293 K after *M. sedula* growth might well reflect the oxidation of Fe^{2+} into Fe^{3+} (Presciutti et al., 2005; Mangueira et al., 2011). Interestingly, no ΔH alteration of g=2 signal was observed for abiotically treated JSC 1A compared to raw JSC 1A material (Fig. 4A and Supplementary Table 2). The slight increase of the signal amplitude of high spin Fe^{3+} g=4.1 and g=9 signals along with the appearance of g=2.5 signal in biotic samples of MRS07/52 suggest the accumulation of Fe^{3+} in mineral phase, which also speaks on the account of Fe^{2+} oxidation mediated by *M. sedula* (Figure 4D). Interestingly, MRS07/52 is the only simulant among all tested MRSs, where Fe ions were detected to be released from after 21 days of cultivation with *M. sedula*. In biotic samples of Mn-bearing MRSs (JSC 1A, P-MRS, and S-MRS) the increased signals of mixed ionic states Mn^{3+} and Mn^{4+} and the decrease of Mn^{2+} in tetrahedral positions were observed pointing to a plausible redox couple for *M. sedula* respiration. The accumulation of redox heterogeneous Mn species may occur in the mineral phase due to *M. sedulas* oxidative metabolism, analogously to microbial mediated sulfur oxidation with the wide variety of redox heterogeneous intermediate sulfur compounds (Schippers et al., 1996) and serve as a fingerprint of chemolithoautotrophic life. However, to which extent Mn^{2+} is oxidized to Mn^{3+} and Mn^{4+} by *M. sedula* cannot be elucidated by EPR.

The signal g≅4 assigned for high spin energy Fe^{3+} is well preserved within JSC 1A, P-MRS, and MRS07/52 abiotic and biotic samples, with only small variations in amplitude. This situation indicates that the Fe^{3+} remained associated to orthorhombic positions in the structure of mineral precipices upon *M. sedula* growth. Such an observation is also in line with EPR-characterization of iron-bearing multi-mineral materials under the oxidative conditions of firing temperatures, suggesting that a biologically mediated oxidative effect does not differ from abiotic physical-chemical oxidation in this spectral area. However, changes were detected at signals g=9 (Figure 4A, B, and D; Supplementary Table 1) originating from high-spin rhombic Fe^{3+} centers, supporting the microbial mediated alteration of Fe^{3+} complexes in axial symmetry.

The different composition of mineral phases of MRSs has to be taken into account when assigning a certain resonance signal and the formation of different environments in response to abiotic and biologically mediated oxidation. Nevertheless, the EPR data should be supported by other observations

such as synchrotron assisted X-ray absorption techniques, to obtain a deeper insight into the microbial mediated mineralogical alterations.

The development of the microspheroids described here that overgrow mineral surface of Martian regolith simulants was one of the features mediated by *M. sedula*. Most of the microspheroids were observed in the range of 0,3 to 3 µm in size, with the majority in between 0,5 to 1 µm. Frequently, the microspheroids were characterized by very low carbon content, which did not exceed the background carbon level in surrounding mineral surface according to our EDS analysis and suggested the non-cellular nature of these morphologies (Supplementary Figure 4). Chlorine and aluminum content of the microspheroids has been constantly detected by EDS analysis, with chlorine represented solely in microspheroid structures and absent in the mineral background (Supplementary Figure 4, Table 4). These microspheroid structures tend to cluster into aggregates, which overgrow the mineral surfaces while forming assemblages on underlying structures (Figure 3E, Supplementary Figure 4).

Occurring as single particles (Figure 3A and B), these microstructures expose correctly shaped hemispherical surface. When grouped into aggregates, overgrowing the surface of S-MRS and competing with each other in restricted size area, microspheroids expose overlapping conjoined boundary sides, which results in a distorted hemispherical morphology and "overcrowded" appearance (Figure 3C). The neoformed opaline microhemispheroids of similar morphology were previously described as a part of possibly microbial mediated diagenesis of marine sediments (Monty et al., 1991). Massively deposited chlorine/aluminum microspheroids can be inferred to be self-assembled aggregated clusters that form new nuclei and mineral intermediates as a part of new mineral formation process biologically mediated by *M. sedula*. This fine-scale morphological signature along with leaching of elements as the signs of metabolic activity may serve as indication of chemolithotrophic life in extreme environments.

CONCLUSION

The mineralogical composition of the synthetic Martian regolith analogues supports the chemolithotrophic growth of *M. sedula*, when Martian regolith simulants are used as the sole energy sources. Acquisition of Fe^{2+} and/or Mn^{2+} from these simulants seems to satisfy the bioenergetic needs of *M. sedula*. The obtained results highlight metallophilic life in extreme environments and reveal unique fingerprints of life in the extreme conditions.

AUTHOR CONTRIBUTIONS

D.K, M.P.S., M.P., O.S., A.B., and T.M. performed experiments; D.K. and M.P. planned, performed, and interpreted EPR experiments; all authors provided editorial input. All authors made substantial contributions to the acquisition, analysis, and interpretation of data described in this perspective. All authors critically reviewed the report and approved the final version.

ACKNOWLEDGMENTS

We warmly thank R. Moeller (German Aerospace Center (DLR), Cologne) for providing the synthetic Martian regolith analogues used in this study. We would like to acknowledge T. Hofmann and W. Obermaier (University of Vienna, Department of Environmental Geosciences) for help with ICP-OES and Dr. Pelin Yilmaz for ARB 16S rRNA probe design. The support of Stephan Puchegger (University of Vienna, Physics Faculty Center for Nano Structure Research) with electron microscopy investigations is greatly appreciated. T.M. would also like to thank Frances Westall for fruitful discussions.

Competing financial interests

The authors declare no competing financial interests.

References

Amils, R., et al. (2007). Extreme environments as Mars terrestrial analogs: The Rio Tinto case. *Planet. Space Sci.* **55**(3): 370-381. doi: 10.1016/j.pss.2006.02.006

Auernik, K.S., and Kelly, R.M. (2008). Identification of components of electron transport chains in the extremely thermoacidophilic crenarchaeon Metallosphaera sedula through iron and sulfur compound oxidation transcriptomes. *Appl. Environ. Microbiol*. **74**, 7723–7732. doi: 10.1128/AEM.01545-08

Auernik, K.S. and Kelly, R.M. (2010). Impact of molecular hydrogen on chalcopyrite bioleaching by the extremely thermoacidophilic archaeon Metallosphaera sedula. *Appl. Environ. Microbiol.* **76**, 2668–2672. doi: 10.1128/AEM.02016-09

Auernik, K. S. and R. M. Kelly (2010). Physiological versatility of the extremely thermoacidophilic archaeon Metallosphaera sedula supported by transcriptomic analysis of heterotrophic, autotrophic, and mixotrophic growth. *Appl. Environ. Microbiol.* **76**(3): 931-935. doi: 10.1128/AEM.01336-09

Auernik, K.S., Maezato, Y., Blum, P.H. and Kelly, R.M. (2008). The genome sequence of the metal- mobilizing, extremely thermoacidophilic archaeon Metallosphaera sedula provides insights into bioleaching-associated metabolism. *Appl. Environ. Microbiol*. **74**, 682–692. doi: 10.1128/AEM.02019-07

Bibring J-P., Langevin Y., Gendrin A., Gondet R, Poulet F., Berthe M. et al. (2005). Mars surface diversity as revealed by the OMEGA/Mars express observations. *Science* **307**: 1576-1581. doi: 10.1126/science.1108806

Bibring, J.-P., et al. (2006). Global Mineralogical and Aqueous Mars History Derived from OMEGA/Mars Express Data. *Science* **312**(5772): 400. doi: 10.1126/science.1122659

Bishop, J. L., Dobrea, E. Z., McKeown, N. K., Parente, M., Ehlmann, B. L., Michalski, J. R. et al. (2008). Phyllosilicate diversity and past aqueous activity revealed at Mawrth Vallis, Mars. *Science* **321**(5890): doi: 830-833. 10.1126/science.1159699

Blöchl, E., et al. (1992). Reactions depending on iron sulfide and linking geochemistry with biochemistry. *Proc. Natl. Acad. Sci. U.S.A.* **89**(17): 8117-8120.

Boettger, U., de Vera, J. P., Fritz J, Weber, I., Hübers, H. W., Schulze-Makuch, D. (2012). Optimizing the detection of carotene in cyanobacteria in a martian regolith analogue with a Raman spectrometer for the ExoMars mission. *Planet. Space Sci.* **60**(1): 356-362. doi: 10.1016/j.pss.2011.10.017

Braun, S., et al. (2016). Cellular content of biomolecules in sub-seafloor microbial communities. *Geochim. Cosmochim. Acta* **188**:330-351. doi: 10.1016/j.gca.2016.06.019

Bullock, M. A. and J. M. Moore (2007). Atmospheric conditions on early Mars and the missing layered carbonates. *Geophys. Res. Lett.* **34**(19). doi: 10.1029/2007GL030688

Chevrier, V. and P. E. Mathé (2007). Mineralogy and evolution of the surface of Mars: A review. *Planet. Space Sci.* **55**(3): 289-314. doi: 10.1016/j.pss.2006.05.039

Ehlmann, B. L., et al. (2011). Subsurface water and clay mineral formation during the early history of Mars. *Nature* **479**(7371): 53-60. doi: 10.1038/nature10582

Gooding, J. L. (1978). Chemical weathering on Mars thermodynamic stabilities of primary minerals (and their alteration products) from mafic igneous rocks. *Icarus* **33**(3): 483-513. doi: 10.1016/0019-1035(78)90186-0

Gronstal, A., Pearson, V., Kappler, A., Dooris, C., Anand, M., Poitrasson, F. et al. (2009). Laboratory experiments on the weathering of iron meteorites and carbonaceous chondrites by iron-oxidizing bacteria. *Meteorit. Planet. Sci.* **44**: 233–247. doi:10.1111/j.1945-5100.2009.tb00731.x

Grotzinger, J. P., et al. (2014). A habitable fluvio-lacustrine environment at Yellowknife Bay, Gale crater, Mars. *Science* **343**(6169): 1242777.

Grotzinger, J. P. (2013). Analysis of surface materials by the Curiosity Mars rover. *Science* **341**(6153): 1475. doi: 10.1126/science.1244258

Halevy, I., et al. (2007). A Sulfur Dioxide Climate Feedback on Early Mars. *Science* **318**(5858): 1903. doi: 10.1126/science.1147039

Huber, H., Huber, G. & Stetter, K. O. A modified DAPI fluorescence staining procedure suitable für the visualization of lithotrophic bacteria. *Syst. Appl. Microbiol*. **6**, 105–106 (1985). doi: 10.1016/S0723-2020(85)80021-7

Huber, G., Spinnler, C., Gambacorta, A., and Stetter, K.O. (1989). Metallosphaera sedula gen. and sp. nov. represents a new genus of aerobic, metal-mobilizing, thermoacidophilic archaebacteria. *Syst. Appl. Microbiol*. **12**, 38–47. doi: 10.1016/S0723-2020(89)80038-4

Hurowitz, J. A., et al. (2017). Redox stratification of an ancient lake in Gale crater, Mars. *Science* **356**(6341). doi: 10.1126/science.aah6849

Ivarsson M, Broman C, Gustafsson H, Holm NG (2015). Biogenic Mn-Oxides in Subseafloor Basalts. *PLoS ONE* **10**(6): e0128863. doi:10.1371/ journal.pone.0128863

Kim, S. S., et al. (2011). Searching for biosignatures using electron paramagnetic resonance (EPR) analysis of manganese oxides. *Astrobiology* **11**(8): 775-786. doi: 10.1089/ast.2011.0619

Ludwig, W., et al. (2004). ARB: a software environment for sequence data. *Nucleic Acids Res.* **32**(4): 1363-1371. doi: 10.1093/nar/gkh293

Maezato, Y., Johnson, T., McCarthy, S., Dana, K., and Blum, P. (2012). Metal resistance and lithoautotrophy in the extreme thermoacidophile Metallosphaera sedula. *J. Bacteriol*. **194**, 6856–6863. doi: 10.1128/JB.01413-12

Mahaffy, P. R., et al. (2013). Abundance and Isotopic Composition of Gases in the Martian Atmosphere from the Curiosity Rover. *Science* **341**(6143): 263. doi: 10.1126/science.1237966

Mangueira, G. M., et al. (2011). A study of the firing temperature of archeological pottery by X-ray diffraction and electron paramagnetic resonance. *J. Phys. Chem. Solids* **72**(2): 90-96. doi: 10.1016/j.jpcs.2010.11.005

Manz, W., et al. (1992). Phylogenetic Oligodeoxynucleotide Probes for the Major Subclasses of Proteobacteria: Problems and Solutions. *Syst. Appl. Microbiol.* **15**(4): 593-600. doi: 10.1016/S0723-2020(11)80121-9

McCarthy, S., Ai, C., Wheaton, G., Tevatia, R., Eckrich, V., Kelly, R. et al. (2014). Role of an archaeal PitA transporter in the copper and arsenic resistance of Metallosphaera sedula, an extreme thermoacidophile. *J. Bacteriol.* **196**, 3562–3570. doi: 10.1128/JB.01707-14

McSween, H.Y.j., (1994). What have we learned about Mars from the SNC meteorites. *Meteoritics* **29**, 757-779.

Moeller, R., Horneck, G., Rabbow, E., Reitz, G., Meyer, C., Hornemann, U., et al. (2008). Role of DNA protection and repair in resistance of Bacillus subtilis spores to ultrahigh shock pressures simulating hypervelocity impacts. *Appl. Environ. Microbiol.* **74**(21): 6682-6689. doi: 10.1128/AEM.01091-08

Monty C, Westall F, Van Der Gaast S. (1991). Diagenesis of siliceous particles in subantarctic sediments. Hole 699A: possible microbial mediation. *Proc. ODP, Sci. Res.* **114**:685–710. doi: 10.2973/odp.proc.sr.114.121.1991

Morris, R. V., et al. (2010). Identification of carbonate-rich outcrops on Mars by the Spirit rover. *Science* **329**(5990): 421-424. doi: 10.1126/science.1189667

Morris, R. V., Golden, D. C., Bell, J. F. III, Lauer, H. V. Jr. and Adams, J. B. (1993). Pigmenting agents in martian soils: inferences from spectral, Mössbauer, and magnetic properties of nanophase and other iron oxides in Hawaiian palagonitic soil PN-9. *Geochim. Cosmochim. Acta* **57**:4597–4609. doi: 10.1016/0016- 7037(93)90185-Y

Mukherjee, A., Wheaton, G.H., Blum, P.H., and Kelly, R.M. (2012). Uranium extremophily is an adaptive, rather than intrinsic, feature for extremely thermoacidophilic Metallosphaera species. *Proc. Natl. Acad. Sci. U.S.A.* **109**, 16702–16707. doi: 10.1073/pnas.1210904109

Mustard, J. F., Ehlmann, R L., Murchie S. L., Poulet, F., Mangold, N., Head, et al. (2009). Composition, Morphology, and Stratigraphy of Noachian Crust around the Isidis basin. *J. Geophys. Res.* **114**, EOOD12. doi:10.1029/2009JE003349

Nixon, S. L., et al. (2012). Limitations to a microbial iron cycle on Mars. *Planet. Space Sci.* **72**(1): 116-128. doi.org/10.1016/j.pss.2012.04.003

Peeples, T.L. and Kelly, R.M. (1995). Bioenergetic response of the extreme thermoacidophile Metallosphaera sedula to thermal and nutritional stress. *Appl. Environ. Microbiol*. **61**, 2314–2321.

Polikreti, K., Maniatis, Y., (2002). A new methodology for the provenance of marble based on EPR spectroscopy. *Archaeometry* **44** 1–21. doi:10.1111/1475-4754.00040

Poulet F., Bibring J-P., Mustard J. F., Gendrin A., Mangold N., Langevin Y , Arvidson R. E., Gondet R and Gomez C. (2005). Phyllosilicates on Mars and implications for early martian climate. *Nature* **438**: doi: 623-627. 10.1038/nature04274

Presciutti, F., et al. (2005). Electron Paramagnetic Resonance, Scanning Electron Microscopy with Energy Dispersion X-ray Spectrometry, X-ray Powder Diffraction, and NMR Characterization of Iron-Rich Fired Clays. *J. Phys. Chem. B* **109**(47): 22147-22158. doi: 10.1021/jp0536091

Reed, C. (2015). Earth microbe prefers living on meteorites. *Science*, doi:10.1126/science.aab2499

Schimak, M. P., et al. (2015). MiL-FISH: Multilabeled Oligonucleotides for Fluorescence In Situ Hybridization Improve

Visualization of Bacterial Cells. *Appl. Environ. Microbiol.* **82**(1): 62-70. doi: 10.1128/AEM.02776-15

Schippers, A., et al. (1996). Sulfur chemistry in bacterial leaching of pyrite. *Appl. Environ. Microbiol* **62**(9): 3424-3431.

Stetter, K. O. (2006). History of discovery of the first hyperthermophiles. *Extremophiles* **10**(5): 357-362. doi: 10.1007/s00792-006-0012-7

Wächtershäuser, G. (1992). Groundworks for an evolutionary biochemistry: The iron-sulphur world. *Prog. Biophys. Mol. Biol.* **58**(2): 85-201. doi: 10.1016/0079-6107(92)90022-X

Wheaton, G. H., Mukherjee, A., Kelly, R. M. (2016). Metal 'shock' transcriptomes of the extremely thermoacidophilic archaeon Metallosphaera sedula reveal generic and specific metal responses. *Appl. Environ. Microbiol*. **82**(15): 4613-4627. doi: 10.1128/AEM.01176-16

Xu, J., et al. (1999). Synthesis and Characterization of Mn-Containing Cubic Mesoporous MCM-48 and AlMCM-48 Molecular Sieves. *Chem. Mater.* **11**(10): 2928-2936. doi: 10.1021/cm990300j

6. PUBLICATION 2 - AS CO-AUTHOR

6.1. Contribution of co-author

The co-author assembled figure 1 and conducted and interpreted the experimental SEM part together with author 8.

Proteometabolomic response of *Deinococcus radiodurans* exposed to UVC and vacuum conditions: initial studies prior to the Tanpopo space mission

Emanuel Ott[1], Yuko Kawaguchi[2], Denise Kölbl[1], Palak Chaturvedi[1,4], Kazumichi Nakagawa[3], Akihiko Yamagishi[2], Wolfram Weckwerth[4,5*], Tetyana Milojevic[1*]

[1]Department of Biophysical Chemistry, University of Vienna, Vienna, Austria

[2]School of Life Sciences, Tokyo University of Pharmacy and Life Sciences, Tokyo, Japan

[3]Graduate School of Human Development and Environment, Kobe University, Kobe, Japan

[4]Department of Ecogenomics and Systems Biology, University of Vienna, Vienna, Austria

[5]Vienna Metabolomics Center (VIME), University of Vienna, Vienna, Austria

[*]Corresponding authors: tetyana.milojevic@univie.ac.at (T. M.) & wolfram.weckwerth@univie.ac.at (W. W.)

Keywords: Panspermia, Space exposure experiments of microbes, Deinococcus, Proteome, Metabolome

ABSTRACT

The multiple extremes resistant bacterium *Deinococcus radiodurans* is able to withstand harsh conditions of simulated outer space environment. The Tanpopo orbital mission performs a long-term space exposure of *D. radiodurans* aiming to investigate the possibility of interplanetary transfer of life. The revealing of molecular machinery responsible for survivability of *D. radiodurans* in the outer space environment can improve our understanding of underlying stress response mechanisms. In this paper, we have evaluated the molecular response of *D. radiodurans* after the exposure to space-related conditions of UVC irradiation and vacuum. Notably, scanning electron microscopy investigations showed that neither morphology nor cellular integrity of irradiated cells was affected, while integrated proteomic and metabolomic analysis revealed numerous molecular alterations in metabolic and stress response pathways. Several molecular key mechanisms of *D. radiodurans*, including the tricarboxylic acid cycle, the DNA damage response systems, ROS scavenging systems and transcriptional regulators responded in order to cope with the stressful situation caused by UVC irradiation under vacuum conditions. These results reveal the effectiveness of the integrative proteometabolomic approach as a tool in molecular analysis of microbial stress response caused by space-related factors.

INTRODUCTION

The Gram positive bacterium *Deinococcus radiodurans* is extremely resistant to several environmental conditions, such as ionizing radiation [57], UV radiation [58], oxidation stress [18] and desiccation [59]. Such a multifaceted resistance of *D. radiodurans* ensures its potential to survive in the harsh outer space environment during interplanetary transfer. The Tanpopo, which means dandelion in Japanese, mission [60] includes a long-term exposure (separate experiments between one to three years) of *D. radiodurans* on the Japan Experimental Module of the International Space Station (ISS) in the low Earth orbit (LEO). It is performed in order to validate the panspermia theory [61] - the possible transfer of life between Earth and extra-terrestrial bodies. To ensure that *D. radiodurans* is suitable for a long term exposure experiment on the ISS, several preliminary exposure experiments have been performed by Kawaguchi, Yang [62]. During these experiments, the different parameters (heavy ion beam radiation, temperature cycles, vacuum and UVC radiation) were adapted to mirror LEO conditions and the following survival tests revealed that UVC radiation had the highest impact on cell survivability [62, 63]. It was shown that, even though *D. radiodurans* possesses high tolerance against UVC radiation, direct exposure of monolayers to LEO conditions results in no survival [60]. However, aggregated *Deinococci* cells exposed to UVC radiation showed that they should withstand solar UV radiation on the ISS for one year as multilayers of dehydrated cells, and survive, wherein upper cellular layers cover and protect underlying inner cells. Approximately 200 µm of cell layers are necessary to shield the inner layers of *D. radiodurans* efficiently from solar UV radiation. Based on these findings, massapanspermia has been proposed, implying that apart from rocks which shield the microbes against solar UV radiation (i.e., lithopanspermia), it is possible for cell-aggregates to function as a protective ark for interplanetary transfer of microbes, where upper layers shield lower layers from the harmful environment [62, 63]. Proving this theory is a part of the Tanpopo mission, as cell aggregates with different thicknesses of *D. radiodurans* are directly exposed to LEO conditions. These factors are microgravity, vacuum down to 10^{-7} Pa, solar UV radiation, galactic radiation, solar cosmic radiation, van Allen Belts and temperature cycles (from -120 °C up to 120 °C every 90 min) [64].

Complementing survivability studies, an approach to unravel the response to LEO conditions on a molecular level is desirable, as it might provide an explanation how it is possible for certain organisms to survive under such extreme conditions. A systems biology approach, especially the combination of several –omics analysis, improves the knowledge of microbial stress response mechanisms and explains how microorganisms respond to environmental changes on the molecular level. Environmental stresses can damage cells due to the formation of reactive oxygen species (ROS), which cause lipid peroxidation, protein oxidation and oxidative DNA damage. Exogenous factors can further interfere with genome integrity as they cause double strand breaks, primarily induced by vacuum and single strand breaks, primarily induced by UVC irradiation [18]. In addition to breaks, three major classes of bipyrimidine photoproducts (BPPs), cyclobutane pyrimidine dimers, pyrimidine 6-4 pyrimidone photoproducts and Dewar isomers, are formed if organic material is exposed to UVC radiation [65]. Although there is no evidence that the DNA damage repair mechanism is very different in *D. radiodurans* compared to *Escherichia coli* [66]. Despite the number of BPPs after UVC irradiation of 500 Jm^{-2} being comparable between *D. radiodurans* and *E. coli*, *D. radiodurians* is about 25 times more resistant to BPPs compared to *E. coli* [67, 68]. The reason for this higher resistance lies in the protection of intracellular proteins against UV induced oxidative damage [18]. However, as the amount of DNA damage caused by UVC irradiation and desiccation is severe, an efficient DNA repair mechanism is still important. Two separate nucleotide excision repair pathways act simultaneously to remove BPPs [69]. The pathways rely on the proteins UV

DNA damage endonuclease (*uvsE*) and UvrABC system protein A (*uvrA*) [68]. Both pathways require the proofreading DNA polymerase I (*polA*), as mutants without the *polA* gene are extremely sensitive to UVC irradiation [70]. Another essential protein for enzymatic repair of DNA damage is RecA, which cleaves the repressor LexA that represses SOS response genes, like DNA repair enzymes [71]. After successful excision, recombinational repair is performed. The genome repair does not rely on a new pathway for double-strand break repair, caused by desiccation stress, but is rather a set of recombinational DNA repair functions which can be observed in many other species [72]. Important proteins for the recombination process are gyrases (*gyrA* and *gyrB*), which cause negative supercoils to favor strand separation, DNA replication, transcription, recombination and repair [73]; PprA to stimulate the end-joining reaction catalyzed by DNA ligases [74] and the different single-stranded DNA binding proteins DdrA [75], DdrB [76], DdrC [77] and DdrD [77] for RecA independent genome reconstruction processes.

The aim of this study was to decipher the molecular response of *D. radiodurans* to space-related conditions of UVC radiation and vacuum using the experimental set-up of Tanpopo orbital project. Here we present an integrative proteometabolomic approach applied to reveal key components of the molecular mechanism of *D. radiodurans* survivability in response to UVC irradiation under vacuum conditions.

MATERIALS AND METHODS

Cultivation and preparation of dehydrated *D. radiodurans* cells

D. radiodurans R1 (ATCC 13939) was cultured 15 h in mTGE medium (1 %(w/V) tryptone, 0.6 %(w/V) beef extract, 0.2 %(w/V) glucose) at 30 °C in an incubator with shaking speed of 150 rpm until it reached the anaphase of the logarithmic phase. Liquid cultures of *D. radiodrans* R1 were washed in 10 mM phosphate buffer (PB). This step was repeated three times. Aluminum plates containing cylindrical wells (2.0 mm diameter, 2 mm depth) with flat floor were used as sample holders [63]. Twelve microliter of a cell suspension ($2.9*10^9$ cells/mL) were dropped into 4 wells and dried up under $3.3*10^{-2}$ atm in a desiccator at room temperature under sterile conditions. These steps were repeated 6 times. The amount of deinococcal cells was $3.5*10^7$ cells per well corresponding to a multilayer of 200 µm thickness (S1 Fig). The cells were dried up under $3.3*10^{-2}$ atm for 16 h.

UVC and vacuum exposure

A mercury lamp 254 nm was used to irradiate deinococcal cells in the vacuum chamber. The setup of the UVC-irradiation experiment was described previously [62]. The aluminum plates containing dehydrated cells of *D. radiodurans* were exposed to $UVC_{254\,nm}$ dose 862.0 kJ/m^2 under approximately 400 Pa. Control samples were only dehydrated cells kept in a desiccator at room temperature.

Survival assay

After the exposure to UVC and vacuum, cells were recovered from wells of aluminum plate using PB 10 mM. The cell suspension was serial diluted with PB 10 mM and the diluted cell suspension was dropped on mTGE agar plates [62]. The plates were incubated at 30 °C for 1.5 days. Surviving fractions were determined from the ratio of N/N_0, with N being the number of colony formation unit (cfu) of the irradiated cells and N_0 being the CFU of the control samples.

Scanning Electron Microscopy

The morphology and cellular integrity of the dehydrated cells of *D. radiodurans* deposited on aluminum plates were examined with a Zeiss Supra 55 VP scanning electron microscope. The dehydrated cells were coated with a thin Au/Pd layer (Laurell WS-650-23 spin coater). The imaging of dehydrated clustered cell layers and single cells was performed with the acceleration voltage of 5 kV.

Cultivation conditions

For cultivation of the dehydrated *D. radiodurans* cells, two wells were resuspended in 100 µL phosphate buffer (10 mM K_2HPO_4, 10 mM KH_2PO_4, pH 7) to inoculate 10 mL of mTGB medium. In total 4 biological replicates of the control non-irradiated cells and 4 biological replicates of the UVC/vacuum-irradiated cells were incubated at 30 °C with an agitation rate of 150 rpm for 5 hours. The growth of the cells was monitored by cell counting using a hemacytometer.

Integrative Extraction of Proteins and Metabolites

Extraction and analysis of metabolites and proteins from one sample was performed according to Weckwerth, Wenzel [78] with slight modifications (for a detailed version of the extraction protocol see dx.doi.org/10.17504/protocols.io.j3bcqin). The cells were harvested (3000 g, 5 min, 4 °C), washed with 10 mM phosphate buffer three times and finally resuspended in ice-cold 1 mL MCW (methanol:chloroform:water 2.5:1:0.5). 0.5 g of FastPrepTM lysing matrix B (MP Biomedicals, Santa Ana, USA) was added to the mixture and the cells were homogenized with a FastPrepTM-24 Instrument (MP Biomedicals, Santa Ana, USA) at 3x4.5 m/s for 30 s with a 5 min cooldown on ice between the cycles. After centrifugation (21000 g, 15 min, 4 °C) the supernatant, which contained the metabolites was transferred into a new tube. The pellet, which contained the precipitated proteins was stored at 4°C for the subsequent extraction. Phase separation was induced by adding 200 µL of water. The phases were separated in different tubes and dried in a vacuum concentrator.

Derivatisation and analysis of the metabolites with GC-TOF-MS

Polar metabolites were dissolved in 10 µL of 40 mg mL-1 methoxyamine-hydrochloride in pyridine through shaking at 650 rpm at 30 °C for 90 min. Subsequently, 40 µL of a silylation mix (1 mL N-methyl-N-trimethylsilyltrifluoroacetamid spiked with 30 µL of a mix of even-number alkanes (C10-C40)) was added and the mixture was incubated for 30 min at an agitation rate of 650 rpm at 37 °C. After centrifugation (14000 g, 2 min), the supernatant was transferred into a glass vial and 1 µL of it was injected into the GC (Agilent® 6890 gas chromatograph) in splitless injection mode.

For separation of the metabolites, an Agilent HP-5MS column (30 m length, 0.25 mm diameter and 0.25 µm film) was used. Further parameters were set as following: flow rate 1 mL min^{-1}; injection temperature 230 °C; column temperature started at 70 °C for one minute, then heated up to 330 °C in 9 min, where it was hold for 8 min; recorded masses in the LECO Pegasus® 4D GC×GC-TOF spectrometer were set between 40-700 m/z. Apart from the samples, a house intern standard mix of certain metabolites was measured to get level 1 identifications of common primary metabolites.

Identifications of the metabolites were based on matching the obtained MS-spectra and retention times with an in-house library (extended gmd database). Peak integration was performed with the LECO ChromaTOF® software. Metabolites which were also identified in the standard mix were considered a level 1 identification, the ones which were not present in the mix, but the retention index and the mass spectrum was similar to one of the database were considered a level 2 identification. The measured areas were normalized against the number of cells, used for the extraction.

Protein Extraction

The pellets were suspended in 400 µL of a protein extraction buffer (100 mM NaCl, 100 mM Tris-HCl pH 7.5, 10 % (v/v) Glycerol, 3 % SDS (m/v)) and an equal amount of phenol (saturated with Tris-HCl, pH 7.0, Roth) was added to the suspension. The mixture was vortexed, centrifuged (20000 g, 2 min, 4 °C) and the lower, phenolic phase was transferred into a new tube. To precipitate the proteins, five volumes of ice-cold 0.1 M ammonium acetate in methanol was added. After keeping the suspension at -20 °C overnight, it was centrifuged (5000 g, 30 °C, 4 °C) and the pellet was washed twice with methanol and once with acetone.

Protein Quantification and In-gel Digestion

Protein analysis was performed according to Chaturvedi, Ischebeck [79] with slight modifications. The pellet was dissolved in approximately 30 µL of urea buffer (6 M urea, 5 % SDS). The proteins were quantified with a BCA (bicinchoninic acid) assay kit with a BSA standard. A total amount of 100 µg protein for each sample was mixed with 5x Laemmli buffer, heated at 95 °C for 5 min and applied on a SDS-polyacrylamide gel (separation gel 12 %, stacking gel 5 %). A voltage of 40 V was applied until the samples reached the interphase between the gels. Then the voltage was switched to 80 V until the bromophenol blue run approximately one centimeter into the separation gel. Gel staining was performed with 40 % (V/V) methanol, 10 % acetic acid (V/V), 0.1 % (w/V) Coomassie R-250 in milliQ-water for 30 min, followed by four 20-min destaining (40 % (V/V) methanol, 2 % (V/V) acetic acid). Finally, the gel was washed in milliQ-water for half an hour and all protein lanes for each replicate were cut out of the gel.

For further analysis, the gel bands were cut into small pieces around 1 mm^3 and 1 mL 200 mM AmBic (ammonium bicarbonate) in 50 % ACN (acetonitrile) solution was added to each replicate. The samples were incubated (37 °C, 30 min, agitation rate 650 rpm) and the supernatant was discarded. This process was repeated until the colour of the gel pieces completely disappeared. Afterwards, 500 µL of 50 mM AmBic in 5 % ACN were added, incubated (37 °C, 15 min, agitation rate 650 rpm) and the supernatant was discarded. Finally, 500 µL of ACN were added to the gel pieces, incubated (37 °C, 10 min, agitation rate 650 rpm) and the supernatant was discarded. Gel pieces were air-dried and 12.5 ng/µL trypsin (Roche; in

25 mM AmBic, 10 % ACN, 5 mM CaCl2) was added until all gel pieces were covered by the solution. Tryptic digestion took place at 37 °C for 16 h without shaking.

Peptide Extractions and Desalting

For the peptide extraction, 150 µL of 50 % ACN with 1 % formic acid were added to each tube, incubated for 5 min at room temperature, sonicated shortly in a low intensity ultrasound bath and the supernatant was transferred to a new tube. The procedure was repeated once. Ultimately, 100 µL 90 % ACN with 1 % formic acid were added, incubated 5 min at room temperature and the supernatant was transferred to the same tube again. Extracted peptides were dried down in a vacuum concentrator.

The peptides were suspended in 4 % ACN, 0.25 % formic acid and applied on C18-Bond Elut 96-well plates (Agilent Technologies). They were washed five times with 400 µL of water, whereby the first flow through was kept for another desalting step with graphite. Washed peptides were eluted with 400 µL methanol. Graphite spin column (MobiSpin Column F, MoBiTec) desalting with the first flow through was performed according to the manufacturer's manual (Thermo scientific, Pierce® graphite spin columns). The desalted eluates from the plates and the columns were combined for each sample and dried down in a vacuum concentrator.

Shotgun Proteomics with HPLC nESI-MS/MS

Peptides were dissolved in 2 % ACN with 0.1 % formic acid to a theoretical concentration of 0.2 µg μL^{-1} based on the amount of protein which was loaded on the gel. 1 µg of each sample (4 biological replicates for UV and control) was applied on a C18 reverse phase column (Thermo scientific, EASY-Spray 500 mm, 2 µm particle size). Separation was achieved with a 180 min gradient from 100 % solution A (0.1 % formic acid) to 40 % solution B (90 % ACN and 0.1 % formic acid) with a flow rate of 300 nL min^{-1}. nESI-MS/MS measurements were performed on an Orbitrap Elite (Thermo Fisher Scientific, Bremen, Germany) with the following settings: Full scan range 350–1800 m/z resolution 120000, max. 10 MS2 scans (activation type CID), repeat count 1, repeat duration 30 sec, exclusion list size 500, exclusion duration 30 sec, charge state screening enabled with rejection of unassigned and +1 charge states, minimum signal threshold 500.

Protein Identification and LFQ (Label Free Quantification)

For identification, a Uniprot database (last updated 2015-06-20) containing the annotation of 3088 proteins for *D. radiodurans* was used. The received Thermo raw files from the instrument were identified and quantified in MaxQuant (version 1.5.7.0) with the following parameters: first search peptide tolerance 20 ppm; main search peptide tolerance 4.5 ppm; ITMS MS/MS match tolerance 0.6 Da; a minimum of 7 amino acid were required for the peptide identification and a minimum of two peptides for the protein identification; a maximum of two missed cleavages were allowed; a maximum of five modifications (oxidation of methionine and acetylation of the N-term) were allowed per peptide; a retention time window of 20 min was used to search for the best alignment function and identifications were matched between runs in a window of 0.7 min; a revert decoy database was used to set a cut-off at a FDR of 0.01. LFQ with a minimum ratio of two was performed when at least one MS2 identification was present.

Statistical Evaluation

Key metabolite pathways and protein abundance differences between the control cells and the cells exposed to UVC/vacuum conditions was analyzed with Perseus. PCAs and heatmaps were created with the R packages heatmaps.2 and ggplots. Cytoscape was used for the combined analysis of metabolomics and proteomics data. For all analysis, the LFQ intensity values which were calculated by MaxQuant, were used. First, the fold changes between the proteins were calculated. Proteins which weren't identified in at least three of the four replicates in at least one condition were excluded from the list. After z-transformation of the values, a Welch's T-test was performed between the two conditions. For all

proteins with known annotations, different gene ontologies (cellular compartment, biological process, molecular function) and KEGG pathways were added as categorical columns. With these columns, a Fisher exact test (p-value < 0.02) was performed to identify gene ontologies/KEGG pathways with an unusual representation of proteins within the T-test.

RESULTS

Effects of UVC/vacuum conditions on cellular integrity, growth and survivability of dehydrated *D. radiodurans.*

Survival assays after exposure to UVC irradiation under vacuum showed an average survival rate of $6.5*10^{-1}$ (0.04 s.d.) compared to non-exposed control cells. In order to investigate cellular integrity after UVC irradiation under vacuum conditions, the surface of dehydrated clustered cell layers of *D. radiodurans* deposited on aluminum plates was examined with scanning electron microscopy (Fig 1 and S1 Fig). The observed typical morphology of diplococci and tetracocci of *D. radiodurans* is shown in Fig 1. In line with the extreme desiccation resistance of *D. radiodurans*, there was no detectable damage of cell surface and morphology of *D. radiodurans* observed after drying procedure under the control conditions (Fig 1 A,C,E and S1 Fig). UVC irradiation under the vacuum conditions neither affected morphology, nor cellular integrity of dehydrated cells of *D. radiodurans* (Fig 1 B,D,F and S1 Fig). Correspondingly, the analysis of survivability of cells using standard microbiological plating techniques and counts of colony forming units showed a relative survival rate of 65 % for UVC/vacuum exposed cells compared to control conditions (S1 Table).

Functional analysis of identified proteins of *D. radiodurans*

The LC-Orbitrap Elite™ measurements identified 1661 proteins in at least one sample, comprising 54 % of *D. radiodurans* genome. 59 proteins were only found in at least one of the UV irradiated replicates. GO (Gene Ontology) annotations were assigned using the PANTHER (Protein ANalysis THrough Evolutionary Relationships, http://pantherdb.org, V 11.1) online tool with the latest GO database (released 2017-04-24). The tool was able to map 1452 Uniprot IDs and provide the corresponding GO annotation in case there was one. In total the molecular functions of 865, the biological processes of 954 and the cellular compartments of 332 were annotated on the second hierarchical level of gene ontology annotations (Fig 2). Regarding their biological process, the three most dominant categories were metabolic process (38 %), cellular process (19 %) and localization (4 %). 47 % of the proteins from the category metabolic process belonged to primary metabolic processes. Overall, the most dominant protein classes were transferases (21 %), hydrolases (16 %), oxidoreductases (15 %) and nucleic acid binding (12 %). Apart from that, 553 proteins could be assigned to at least one KEGG pathway.

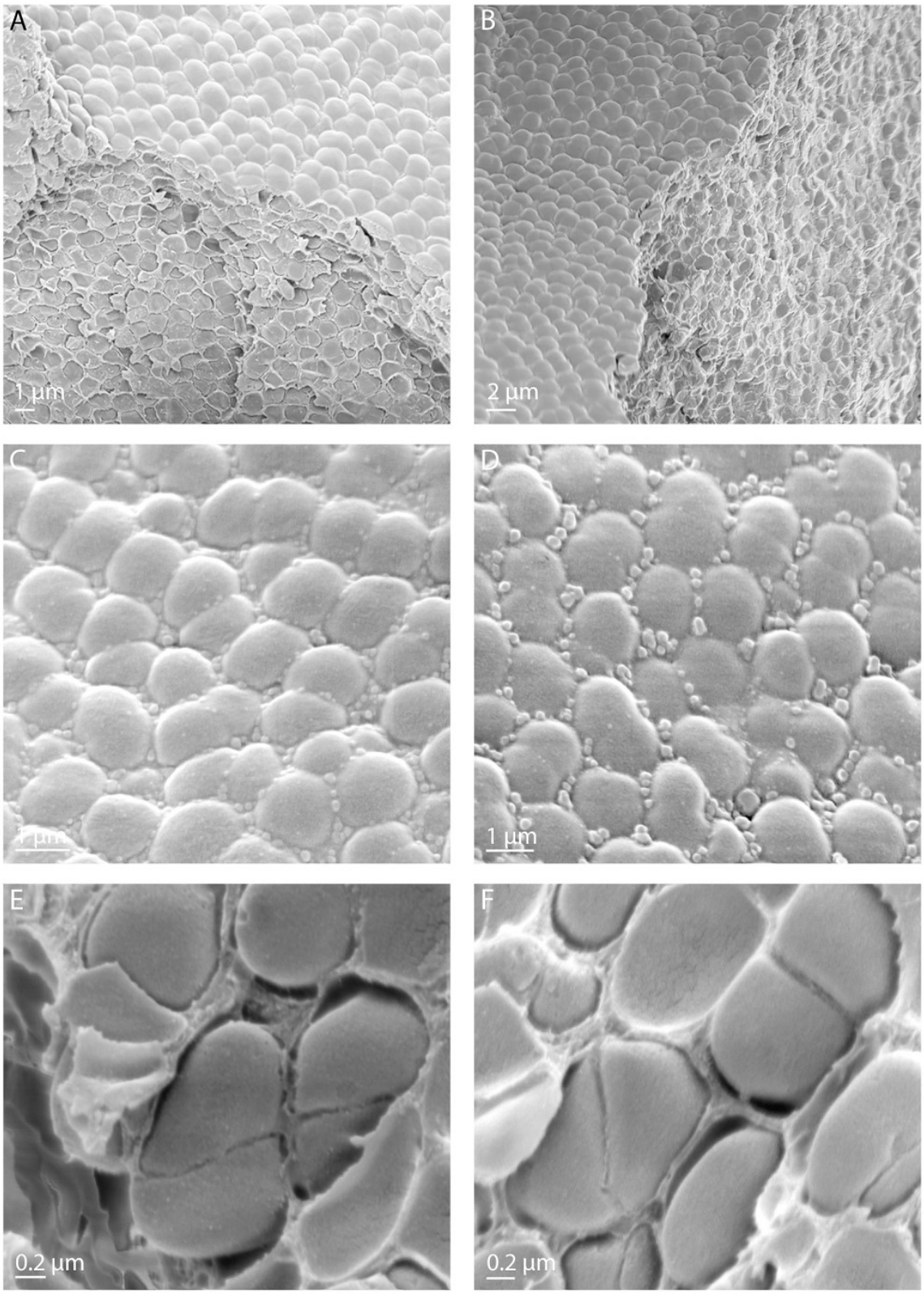

Fig 1. Scanning electron microscopy images of dehydrated cells of *D. radiodurans* deposited on aluminum plates and used in experimental set up of Tanpopo mission. (**A**, **B**) Scanning electron microscopy images, showing upper surface and inner content of multilayers of dehydrated *D. radiodurans* cells deposited on aluminum plates. (**C**, **D**) Higher magnification images displaying upper surface of multilayers of dehydrated cells of *D. radiodurans*. (**E**, **F**) Magnified images of tetracocci and diplococci of *D. radiodurans* taken from the inner part of dehydrated multilayers. (**A**, **C**, **E**) control cells of *D. radiodurans*; (**B**, **D**, **F**) cells of *D. radiodurans* exposed to UVC-vacuum conditions.

https://doi.org/10.1371/journal.pone.0189381.g001

Differences in the proteome between UVC/vacuum exposed and control cells

For quantitative analysis, only proteins which were identified in at least three out of four replicates in at least one of the conditions were used (1457 in total) (S2 Table). The LFQ intensities were z-scored and the PCA-scores (Fig 3) for all four biological replicates showed a clear separation between control and UVC treated cells on component 1.

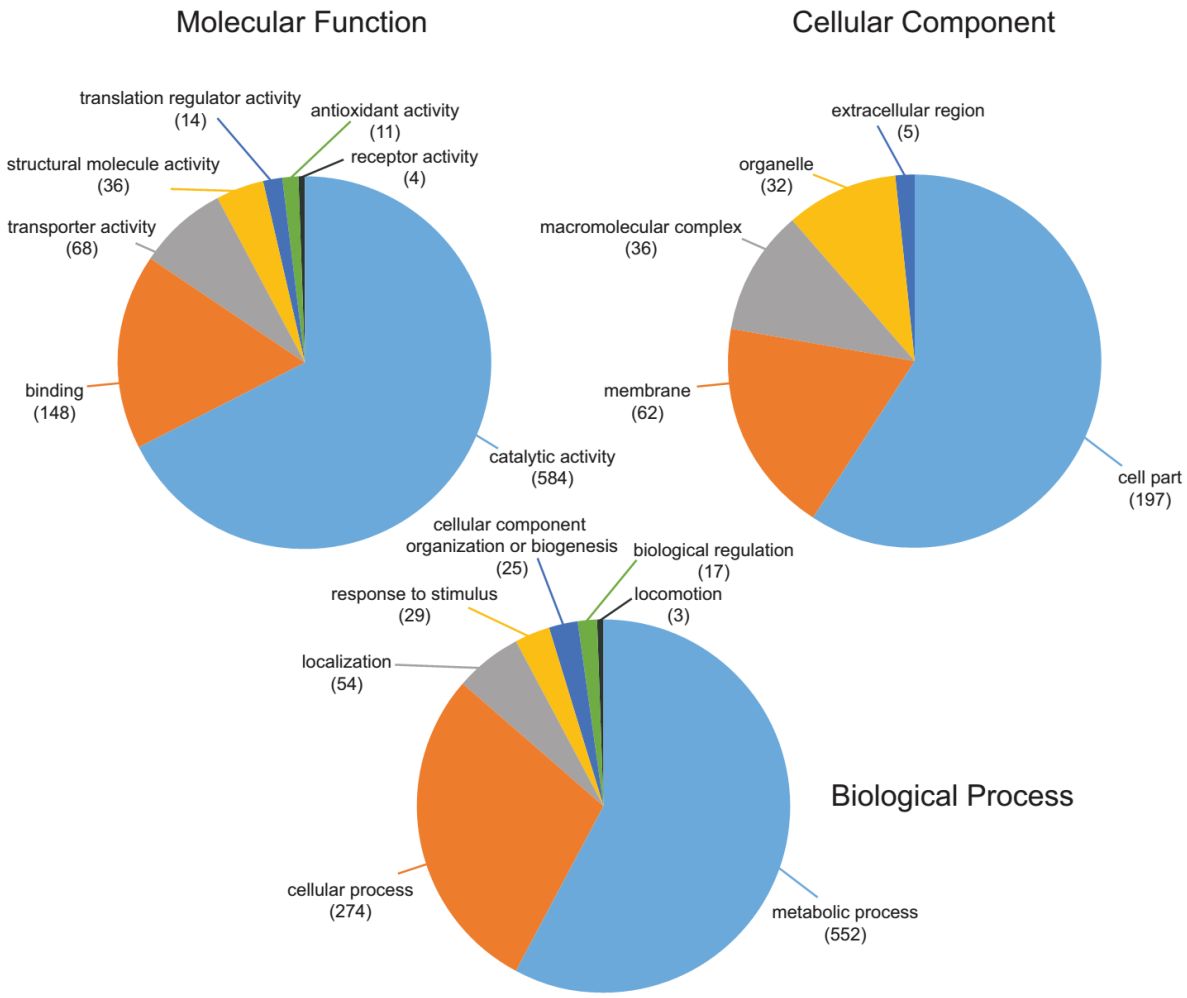

Fig 2. First two levels of gene ontology annotations of all proteins of *D. radiodurans*, which were identified in at least three out of four replicates in at least one condition.

https://doi.org/10.1371/journal.pone.0189381.g002

A Welch's t-test (p-value < 0.05) identified 209 proteins as more abundant in the control cells and 357 in the cells exposed to UVC/vacuum conditions. With these proteins, a Fisher exact test for the KEGG categories was performed. The categories with an unusually high amount of proteins in one of the conditions are shown in Fig 4. Only categories with at least five identified proteins and a minimum enrichment factor of two in at least one condition are shown.

An enrichment factor of zero means that not a single protein in this category was upregulated in the displayed condition.

Annotations and overrepresentation studies provide an overview of pathways which might be affected by the applied stress condition. However, the majority of proteins (> 99.2 %; May 2017) in the gene ontology database are annotated based on automatic algorithmic sequence similarity search instead of manual curation. Therefore, a deeper comparison to the literature and described proteins is inevitable. Fig 5 shows boxplots of mainly manually curated proteins/genes related to DNA damage and oxidative stress response. Most of these proteins (8 out of 11 of selected DNA damage response proteins and 10 out of 11 of selected oxidative stress response proteins) show a significantly higher abundance in the UVC/vacuum exposed cells of *D. radiodurans*. Variances and number of outliers between the two conditions are similar

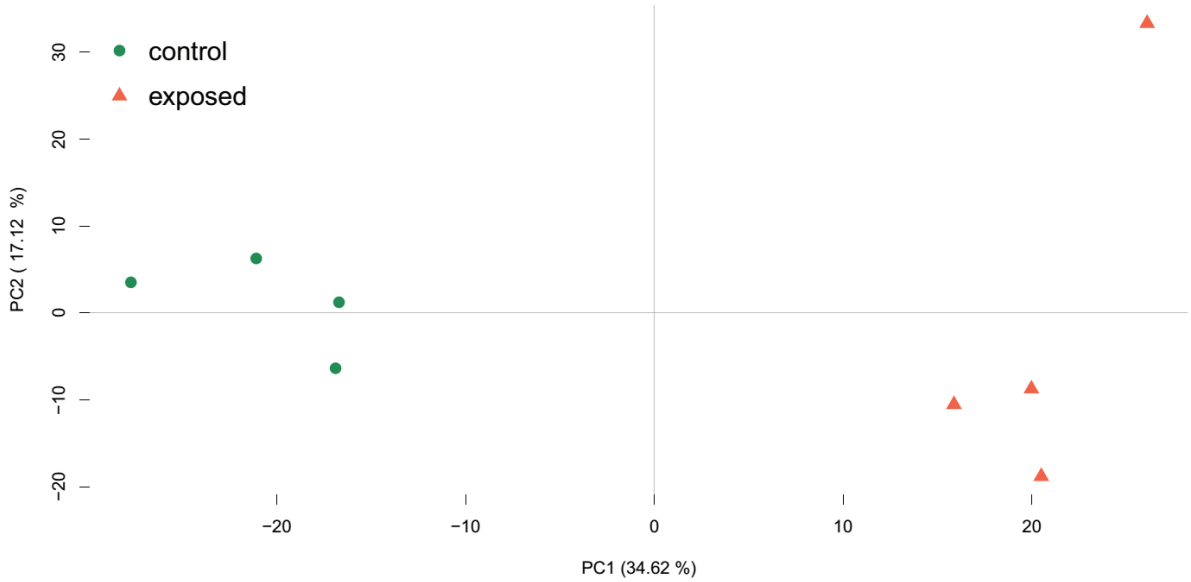

Fig 3. PCA score-plot of the z-scored label free quantification intensities. A clear separation can be observed on the PC1 level, which explains 34.62% of the data's variance, between the UVC/vacuum treated samples (red) and the control samples (green).

https://doi.org/10.1371/journal.pone.0189381.g003

for the chosen proteins.

Metabolomic analysis of *D. radiodurans*

Metabolite analysis from the same cells revealed 31 metabolites which were chosen for quantification. Analysis with GC-TOF usually leads to identification of primary metabolites associated with the primary metabolism. For statistical analysis, only metabolites which were present in at least three out of four replicates in at least one of the conditions were used. The normalized areas were z-scored and compared with a Welch's t-test (p-value < 0.05). 24 metabolites, which abundances were considered different between the two conditions, were blotted as a heatmap (Fig 6). Six of them (O-Palmitoyl-L-Carnitine chloride, octadecanoic acid, ethanolamine, folic acid, mannosamine and cytidine-5-triphosphate disodium salt) were identified on level 2, all the others were identified on level 1 [80]. The majority of metabolites were more present in the control cells of *D. radiodurans* (S3 Table).

Proteometabolic analysis of the TCA cycle

After exposure to stress conditions, additional energy is required to recover the cells. The TCA cycle provides large amounts of energy. Most TCA cycle related proteins showed a higher abundance in the

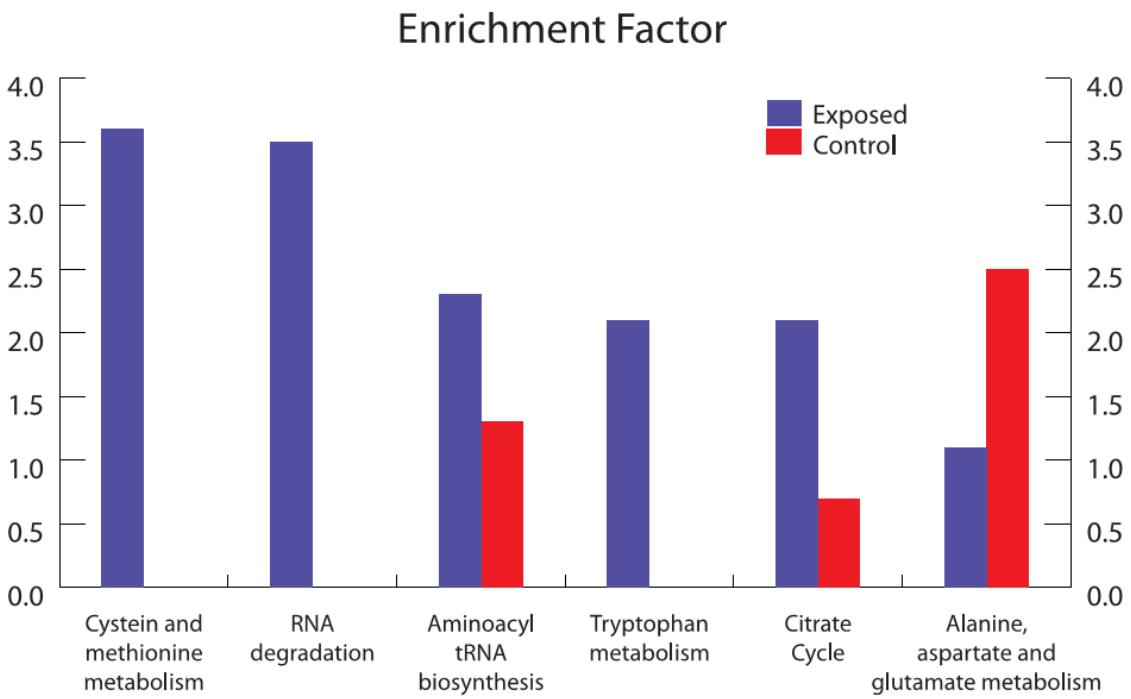

Fig 4. Bar plot of KEGG categories (x-axis) with corresponding enrichment factors (y-axis). Categories with a minimum enrichment factor of two for either UVC/vacuum (blue) treated or control (red) conditions are mapped. An enrichment factor of zero means that not a single protein in this category was upregulated in the displayed condition.

https://doi.org/10.1371/journal.pone.0189381.g004

UVC/vacuum exposed cells of *D. radiodurans* according to the LC-MS measurements. Accordingly, organic acids such as succinic acid, fumaric acid and malic acid were identified (at level 1) and quantified by GC-time of flight (TOF)-MS. Other metabolites were either not identified (limit of detection) or not abundant enough for quantification (limit of quantification).

Fig 7 shows a basic version of the TCA cycle of *D. radiodurans* according to the KEGG website including quantitative proteomics and metabolomics data. The pyruvate dehydrogenase complex, which is responsible for the connection between glycolysis and TCA cycle as it converts pyruvate to coenzyme A, consists of three subunits. The E1 component (aceE) shows a high abundance in the irradiated cells, whereas the dihydrolipoamide acetyltransferase (DR_0032) is more abundant in the control cells. However, according to the KEGG database, another acetyltransferase DR_0256 (S2 Table), which is more abundant in the irradiated cells, is also active in the pyruvate dehydrogenase complex. The third subunit, dihydrolipoamide dehydrogenase (DR_2370) is not significantly higher abundant in any of the two conditions. Further identified and quantified proteins, which are all part of the TCA cycle, are citrate synthase (gltA), aconitate hydratase (acn), isocitrate dehydrogenase (DR_1540), 2-oxoglutarate dehydrogenase (sucA), dihydrolipoamide succinyltransferase (DR_0083), succinate-CoA ligase (sucC), succinyl-CoA synthetase (sdhB), fumarate hydratase (fumC) and malate dehydrogenase (mdh).

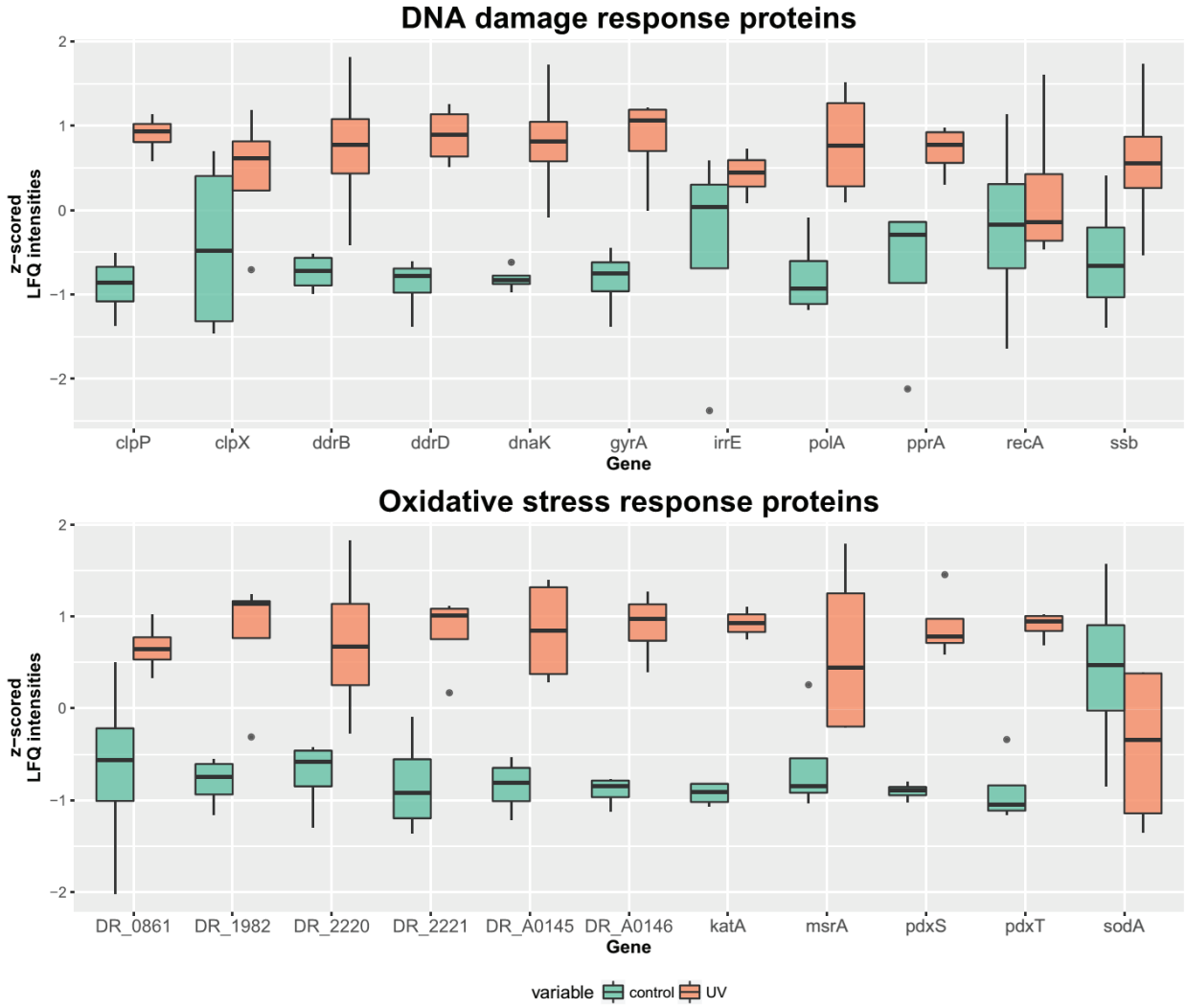

Fig 5. Boxplot of genes encoding important damage response proteins in *D. radiodurans* under the conditions of UVC/vacuum exposure. For every gene, the z-scored LFQ intensities are compared between the control and UVC/vacuum condition. The lower and the upper hinges correspond to the first and the third quartiles. The whiskers extend a maximum of 1.5 times the inter-quartile range. Outliers are indicated as dots. Proteins which are encoded by the mapped genes: Clp protease subunits (clpP and clpX), DNA damage response proteins (ddrB and ddrD), chaperone (dnaK), DNA gyrase subunit A (gyrA), radiation response metalloprotease (irrE), DNA polymerase (polA), DNA repair protein (pprA), recombinase (recA), single-stranded DNA-binding protein (ssb); catalase (katA), uncharacterized protein (DR_A0146), superoxide dismutase (sodA), phytoene dehydrogenase (DR_0861), Pyridoxal 5'-phosphate synthase (pdxS and pdxT), thioredoxin reductase (DR_1982), putative peroxidase (DR_A0145), peptide methionine sulfoxide reductase (msrA), tellurium resistance protein (DR_2220 and DR_2221).

https://doi.org/10.1371/journal.pone.0189381.g005

DISCUSSION

Overall alterations in the proteome of *D. radiodurans* after UVC/vacuum exposure

Proteomic analysis revealed that functional categories of cysteine, methionine and tryptophan metabolism, RNA degradation, aminoacyl-tRNA biosynthesis were overrepresented in *D. radiodurans* exposed to UVC/vacuum conditions compared with the control cells (Fig 4). A previous study [81] showed similar categories of differentially expressed genes after gamma-irradiation. In opposite, the proteins of alanine, aspartate and glutamine metabolism were downregulated in irradiated cells of *D. radiodurans*. Methionine and cysteine as sulfur-containing amino acids greatly contribute to the antioxidant defense system and are key constituents in the regulation of cell metabolism. Apart from structural and catalytic role in proteins, cysteine chemistry is important to the enzymatic mechanism of the thiol-disulfide oxidoreductases of the thioredoxin superfamily, such as thioredoxins, glutaredoxin, and protein disulfide isomerase [82]. The levels of the proteins involved in cysteine biosynthesis, including thioredoxin reductase and thiosulfate sulfurtransferase, were highly upregulated in irradiated cells of *D. radiodurans*

(S2 Table). Surface exposed methionines serve as potent endogenous antioxidants to protect other functionally essential residues from oxidative damage [83]. Methionines are readily oxidized to methionine sulfoxide by many ROS. Methionine sulfoxides can be then subsequently converted back to methionines with the help of methionine sulfoxide reductases Msr [83]. Significant upregulation (p-value 0.043) of MsrA was observed after the exposure of cells to UVC/vacuum conditions as one of the most obvious responses of *D. radiodurans* to oxidative damage (S2 Table, Fig 5).

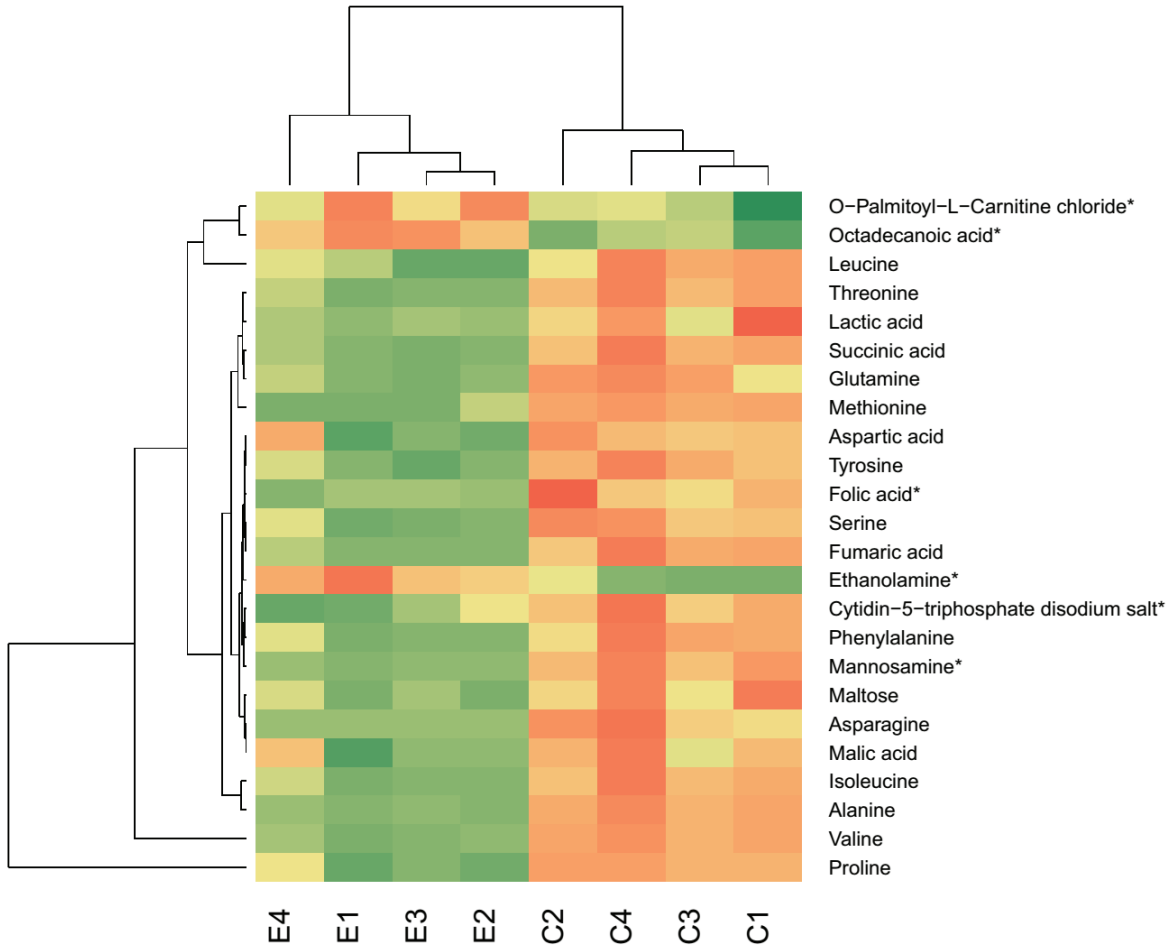

Fig 6. Heatmap of metabolites, which were considered different between cells of *D. radiodurans* exposed to UVC/vacuum and non-exposed control cells. Eucledian distance was used for calculating the dendrogram. *Identification was based on database research and not on a reference substance.

https://doi.org/10.1371/journal.pone.0189381.g006

The Fisher Exact test revealed a high enrichment factor for proteins connected to the TCA cycle and different amino acid pathways (Fig 4). Apart from that, RNA degradation enzymes, which dispose the damaged RNA, are enriched in the UVC irradiated under vacuum conditions cells of *D. radiodurans*. Finally, proteins related to the aminoacyl-tRNA biosynthesis are enriched in the irradiated cells too, indicating an increased demand of protein synthesis. These proteins catalyze the esterification of a specific amino acid to its appropriate tRNA to form an aminoacyl tRNA. In the ribosome, the amino acid is transferred from the corresponding tRNA to a growing peptide strain.

Energy Metabolism

The Fisher Exact Test indicated proteins, which are more abundant in the cells of *D. radiodurans* exposed to UVC/vacuum, belonging to the TCA-cycle. Nearly all key enzymes of the TCA cycle are more abundant in the cells of *D. radiodurans* exposed to UVC/vacuum conditions. Citrate synthase, which is responsible for the condensation of acetyl-CoA and oxaloacetate to form citrate and CoA-SH as well as aconitate

hydratase, which isomerize citrate into isocitrate and isocitrate dehydrogenase, which is allosterically activated by high ADP concentrations and 2-oxoglutarate dehydrogenase (both subunits) are significantly more abundant in the irradiated cells too. Apart from succinate-CoA ligase (hydrolyse of succinyl-CoA into succinate and CoA), all other key enzymes (succinate dehydrogenase for the oxidation of succinate into fumarate, fumarate hydratase, which catalyzes the trans addition of water to produce malate and malate dehydrogenase which oxidizes malate to oxaloacetate) were found in a significantly (p-value below 0.05) higher abundance in the cells of *D. radiodurans* exposed to UVC/vacuum conditions (Fig 7).

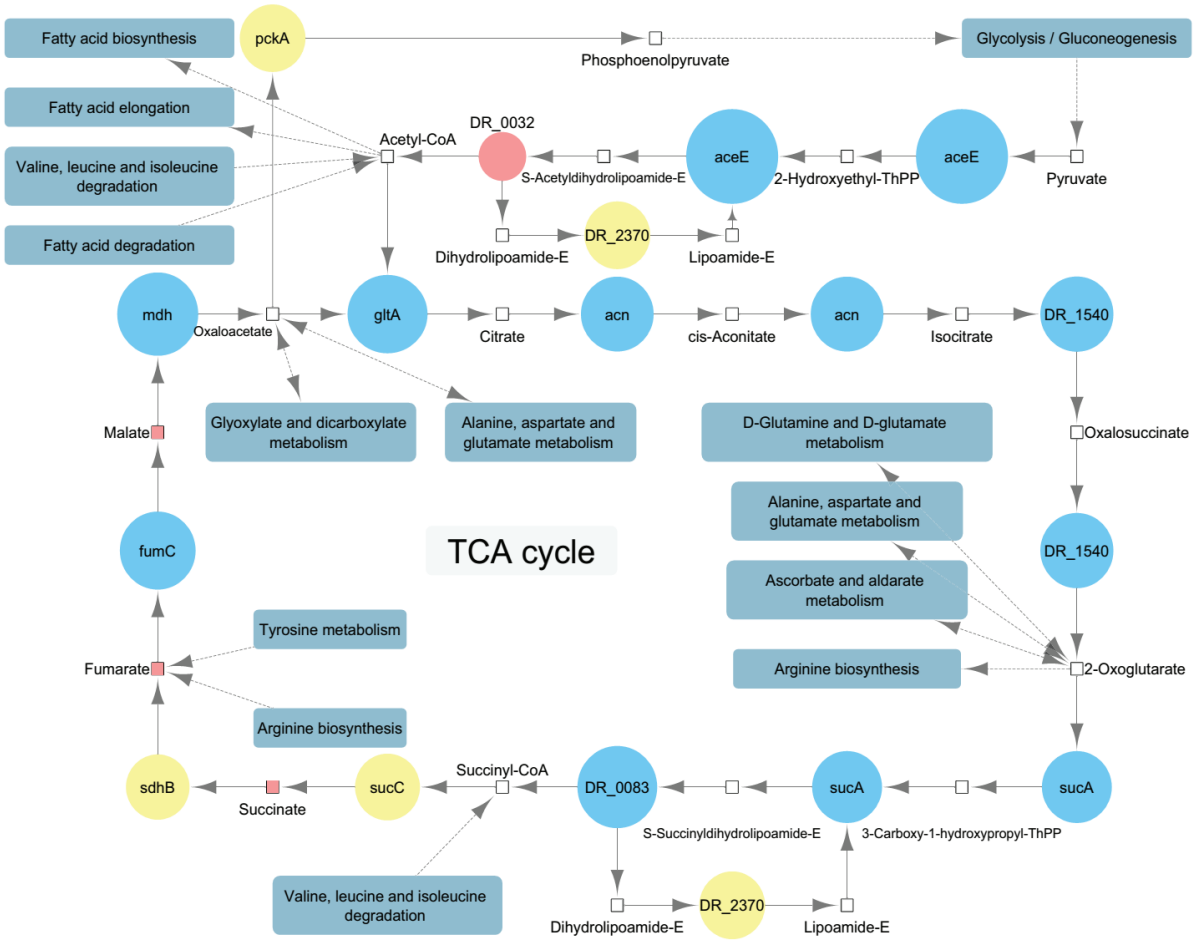

Fig 7. Main components of the TCA cycle in *Deinococcus radiodurans* connected to related pathways under the conditions of UVC/vacuum exposure. Metabolites are shown as rectangles. The areas of the proteins, which are shown as circles, correspond to the fold change between cells of *D. radiodurans* exposed to UVC/vacuum conditions and control non-exposed cells. The color shows whether the average protein or metabolite level was more abundant in the UVC/vacuum exposed cells (blue), the control cells (red), none of both conditions (yellow) or not measured/not abundant enough (colorless).

https://doi.org/10.1371/journal.pone.0189381.g007

Apart from enzymes directly involved into the TCA cycle, all four proteins involved in the pathway that generates pyruvate from D-glyceraldehyde 3-phosphate were more abundant in the cells exposed to UVC/vacuum. Pyruvate dehydrogenase E1 which contributes to the transformation of pyruvate to acetyl CoA for the first step in the TCA cycle was as well upregulated in the UVC/vacuum exposed *D. radiodurans*. Glyceraldehyde 3-phosphate can be obtained from sugars or as a by-product in the tryptophan metabolism [84]. Several proteins of the tryptophan metabolism were significantly upregulated in the UVC/vacuum exposed cells.

Daly [85] reported a higher manganese to iron ratio in *D. radiodurans* compared to other bacteria. Manganese contributes to the resistance against various extreme environmental conditions through the formation of ROS scavenging complexes with orthophosphate and peptides [86]. After application of these complexes, a mouse model showed increased survivability after exposure to ionizing radiation [87].

Furthermore, manganese was proposed to influence glucose incorporation into the DNA after UV exposure [88]. It was shown that glucose is solely metabolized by the pentose phosphate pathway, which augments the DNA excision repair system as it provides adequate metabolites for DNA mismatch repair [89]. Therefore, mutants which lack important pentose phosphate pathway genes, as glucose-6-phosphate-dehydrogenase (*zwf*) are more sensitive to conditions that induce DNA excision repair, such as UV irradiation [89]. Our data supports the assumption that *zwf* might participate in stress response, as it was significantly more abundant in the UVC/vacuum treated cells, which experienced DNA damage.

As there are many upregulated proteins which are directly or indirectly connected to the energy metabolism it can be assumed that more energy for regeneration is required for the UVC/vacuum exposed cells of *D. radiodurans* compared to the control cells. Joshi, Schmid [90] observed a degradation and resynthesis of several proteins after ionizing irradiation. The high abundance of various aminoacyl ligases in the irradiated cells indicates that the resynthesis most likely occur after the exposure to UVC/vacuum as well. The attachment of an amino acid to its tRNA which is catalyzed by these enzymes, is an energy demanding reaction which consumes one ATP per amino acid. At the same time the free amino acid pool in the UVC/vacuum exposed cells is lower than in the control cells also suggesting that protein resynthesis is a highly abundant process during recovery of the cells (Fig 6). The increased energy demand of the irradiated cells is also necessary to cope with the nucleic acid damage which is triggered by upregulation of a number of ribonucleases (S2 Table).

DNA damage response

D. radiodurans wild type strain is approximately 25 times more resistant to UVC irradiation than *E. coli* wild type [66]. Early experiments with the mutagen N-methyl-N'-nitro-N-nitrosoguanidine revealed mutant strains of *D. radiodurans* which are more sensitive to UVC irradiation [91-93]. In 1994, Gutman, Carroll [94] confirmed a lower resistance to UVC in the *recA* and the *polA* [70] mutants. The IrrE mutant showed that the IrrE (also named *pprI*) gene function as a regulator for the expression of DNA repair and oxidative stress response proteins, like *recA* and *pprA* [95, 96]. *pprA*, which encodes a protein that can protect DNA ends from degradation and stimulate DNA-ligase activities, despite its function, seems to play a lesser role in UVC resistance, although it was upregulated in a previous UVC study [97]. Bauermeister, Bentchikou [98] showed in a comparison study that the UVC energy needed to kill 90 % of a *D. radiodurans* culture was 1.5 times lower for the *pprA* mutant, 8 times lower for the *irrE* mutant and 20 times lower for the *recA* mutant compared to the wild type. In our proteomics analysis, *polA* (p-value 0.006) and *pprA* (p-value 0.027) were significantly more abundant in the irradiated cells, while *recA* and *irrE* levels showed no significant difference. Previous shotgun proteomic measurements of *Deinococci spp.* were primarily performed with a combination of two dimensional gel electrophoresis and MALDI-TOF after γ-irradiation. In a study conducted by Dedieu, Sahinovic [99] SSB, PprA, RecA, GyrA/B, UvrD, DdrB and DdrD showed upregulation after ionizing irradiation was applied on *Deinococcus deserti*. Another study [100] found only SSB and PprA among these proteins to be upregulated in *D. radiodurans* after γ-irradiation. However, in a transcriptional approach, Tanaka, Earl [77] showed an upregulation of *recA*, *gyrA/B* and also for the DNA damage response genes *ddrB* and *ddrD* in *D. radiodurans*. In our experiment, a higher abundance of PprA, GyrA/B (both p-values 0.002), DdrB (p-value 0.022) and DdrD (p-value $1.7*10^{-4}$) was observed in irradiated cells, while RecA was present constitutively at high levels in both control and irradiated cells (Fig 5, S2 Table). As our cells were incubated in TGB medium for 5 h after exposure, this fits to a kinetic study [101], which showed that RecA was upregulated for two hours after irradiation, but changed back to basal expression after four hours. Different proteomics/transcriptomics experiments showed some consistency in which DNA damage response proteins were upregulated [77, 99-101]. Differences can be explained due to a number of variable experimental parameters, e.g., dose and type of irradiation, cells dried or in suspension and recovery time. However, as shown in Fig 5, a lot of manually curated DNA damage response proteins were upregulated in our experiment, indicating that the

severe DNA damage, which can be caused by UVC irradiation and desiccation stress, increases the synthesis rate of such proteins.

Contrary to the well-characterized radiation-induced damage, the strategies by which cells of *D. radiodurans* protect their DNA integrity in response to vacuum damage are poorly understood. Along with rapid dehydration of bacterial cells and changes in membrane permeability, DNA damage and mutagenesis have been previously described in microorganisms exposed to space vacuum [102]. Interestingly, the *gyrA* gene, coding for DNA gyrase subunit A has been reported to carry the majority of mutations induced by exposure of spores of *B. subtilis* to high and low vacuum [103, 104]. As suggested by our comparative proteomics analysis, GyrA protein (DR_1913) was upregulated (p-value 0.002) in UVC-irradiated cells of *D. radiodurans* under vacuum conditions, which can be also potentially attributed to the influence of vacuum.

Furthermore, the exposure of *D. radiodurans* to UVC/vacuum stress conditions triggered a suit of proteins involved in detoxification process and aimed to remove damaged nucleotides from the cell. The proteomics experiments revealed that UvrB, helixase subunit of the DNA excision repair endonuclease complex, was significantly more abundantly represented in cells of *D. radiodurans* in conditions of UVC/vacuum stress. The upregulated UvrB binds to DNA, searches it for potential lesions and interacts with other proteins to repair them [105]. MutT/nudix family protein (DR_0550) and MutS2 (DR_1976) involved in mismatch excision repair were upregulated in response to UVC/vacuum exposure. Some members of the Nudix family, such as MutT of *E. coli*, limit mutations by hydrolyzing oxidized nucleotide metabolism products, which are mutagenic once misincorporated into the genome [106, 107]. MutS2 in *D. radiodurans* is involved in ROS detoxification and the repair of ROS-induced DNA damage [108]. Thus, induction of Mut and Nudix family members may be one of the important protective responses to UVC/vacuum stress. Expression of the proteins (recQ and ruvABC) involved in recombinational DNA repair was also significantly induced (S2 Table).

The Mrr restriction system protein (DR_0508) that belongs to a yet unknown pathway showed high abundance (p-value 0.043) in UVC/vacuum exposed cells (S2 Table). Type IV restriction Mrr (methylated adenine recognition and restriction) endonucleases with specificity for methylated DNA have been reported to restrict DNA containing N6-methyladenine and also DNA with C5-methyl-cytosine residues [109]. Contrary to well-characterized Mcr restriction endonucleases, the physiological role of Mrr like nucleases in the cell has been less clarified. Recently, the Mrr restriction system was shown to implement into the peculiar piezophysiology of *E. coli*. Mrr endonuclease activity was linked to cellular filamentation and prophage induction in response to sub-lethal high-pressure shock in *E. coli* K12 [109, 110]. Hence, the observed up-regulation of Mrr restriction protein in *D. radiodurans* under the influence of UVC/vacuum conditions might assign a novel role for this less studied protein in response to space-related stress

stimulus.

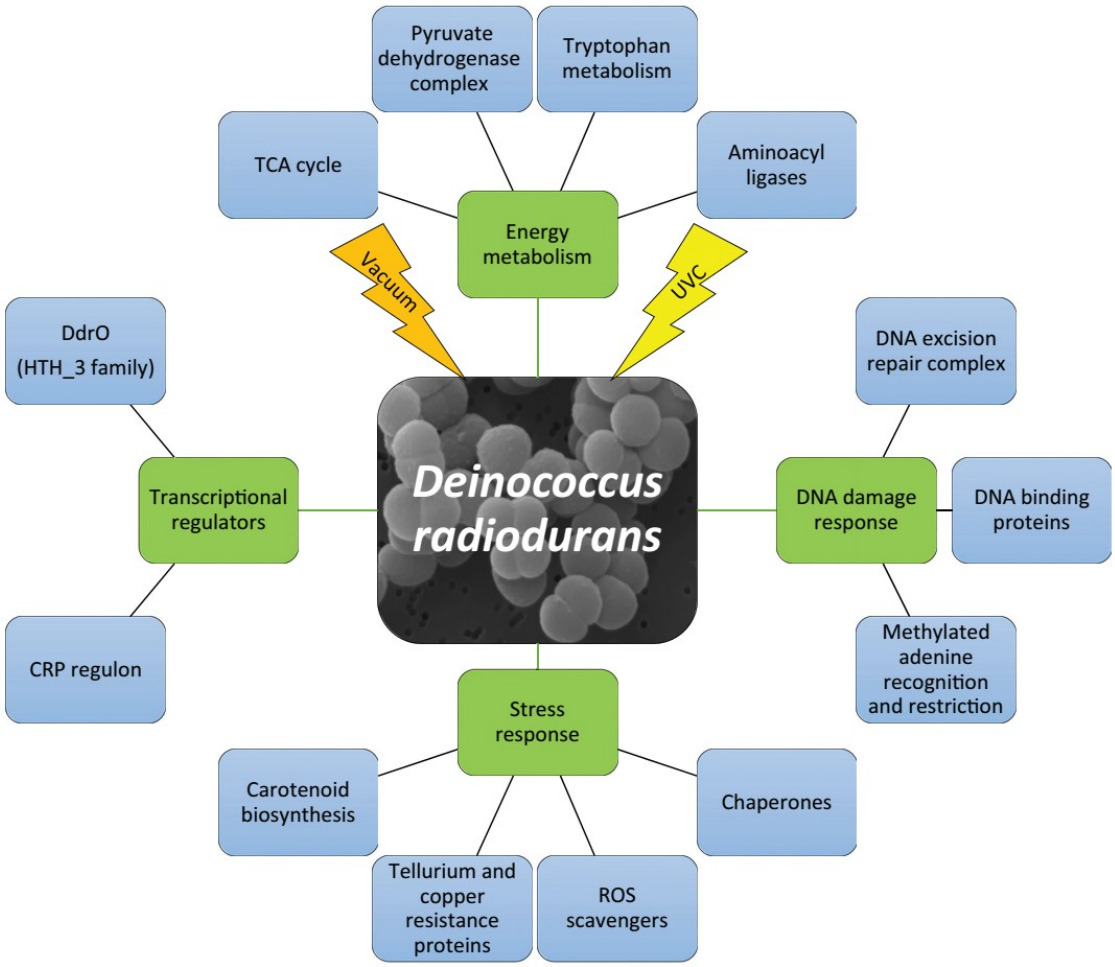

Fig 8. Molecular response of *D. radiodurans* experienced under UVC and vacuum conditions. First two levels of molecular pathways are represented which are affected by UVC irradiation under vacuum conditions.

https://doi.org/10.1371/journal.pone.0189381.g008

Molecular systems of stress response

Our comparative proteomic analysis revealed a number of differentially abundant proteins in UVC/vacuum exposed cells of *D. radiodurans* that belong to the functional machinery of general stress response and oxidative stress response. Proteins of general stress response function to protect and repair damage to cellular structures, such as DNA, the cell envelope and proteins, and to provide microorganisms the ability to recuperate from the stress they experience. Overexpression of a number of chaperons occurred in UVC/vacuum exposed cells of *D. radiodurans*. Heat shock protein that belongs to HSP20 family (DR_1114) and chaperonins hslO (DR_0985) and groL (DR_0607), which are involved in various metabolic processes and responsible for protein folding, were upregulated in UVC/vacuum exposed cells (S2 Table). Chaperone proteins ClpB (Q9RVI3), DnaJ (Q9RUG2) and DnaK Q9RY23 were as well more abundantly represented in UVC/vacuum exposed cells of *D. radiodurans* (S2 Table). By binding to proteins, which are misfolded and damaged in response to various environmental stresses, these molecular chaperones can direct the misfolded proteins to the associated proteases for degradation. The elevated level of several proteases (Lon proteases Q9RXG4 and Q9RSZ5 and ATP-dependent Clp protease ClpA (DR_0588)) in irradiated cells indicates the involvement of quality monitoring and proteolytic regulation in response to combined UVC/vacuum stress.

Comparative proteomics analysis revealed a number of universal reactive oxygen species (ROS) scavengers, e.g., catalase, and redox active proteins (pyridoxal 5'-phosphate synthase, peroxidase, sulfoxide reductase MsrA, thioredoxin reductase) induced in cells of *D. radiodurans* exposed to UVC radiation under vacuum conditions, manifesting the upregulation of antioxidant defense mechanisms in response to these factors (Fig 5). The extreme resistance of *D. radiodurans* against radiation and oxidative damage relies on the high levels of constitutive catalase activity and superoxide dismutase (SOD) activity [18]. These enzymatic systems are devoted to the protection of cells against toxic reactive oxygen species. Out of three known catalases (DR1998, DRA0146, and DRA0259) in genome of *D. radiodurans*, our data show the elevated levels of two of them: catalase katA (p-value $1.1*10^{-6}$) and predicted protein with catalase function DR_A0146 (p-value $4.3*10^{-4}$) in UVC/vacuum exposed *D. radiodurans* (Fig 5). The sodA protein was constitutively represented in both irradiated and control cells (Fig 5). UVC irradiation under vacuum caused 2-fold elevated expression of the pyridoxine biosynthesis proteins PdxS and PdxT (Fig 5) which are singlet oxygen resistance proteins involved in the synthesis of vitamin B_6, an efficient singlet oxygen quencher and a potential antioxidant [111]. The upregulated upon UVC/vacuum-irradiation thioredoxin reductase/alkyl hydroperoxide reductase (DR_1982) (Fig 5) is encoded by the gene *trxB/ahpF*, which is a key determinant of thiol redox sensing antioxidant enzymatic system in *D. radiodurans*. Thioredoxin reduces oxidized cysteine sulfur groups in proteins and is subsequently reverted from its oxidized form by thioredoxin reductase in an NADPH-dependent manner [18, 112]. A putative iron-dependent peroxidase (DRA_0145), enzyme that may implement in defense against oxidative stress by providing protection against toxic hydroperoxides [113], was also among upregulated proteins in response to UVC/vacuum stress. This unique putative peroxidase has very few orthologs among bacteria [113] and is listed among predicted systems of protection against oxidative stress [114].

Among significantly upregulated proteins in response to UVC/vacuum irradiation was also the peptide methionine sulfoxide reductase MsrA (DR_1849) (Fig 5, S2 Table) that shares similarity with *E. coli*'s methionine sulfoxide reductase and performs repair of oxidized proteins reducing protein-bound methionine sulfoxide back to methionine via a thioredoxin-recycling process [114]. Reduction of oxidized methionine residues in proteins is essential mechanism for cells survival under oxidative stress [113] and loss of MsrA sensitizes *E. coli* to hydrogen peroxide [115]. The induction of the gene *msrA* has been reported after ionizing irradiation of *D. radiodurans* [77]. Thiosulfate sulfurtransferase (DR_0217), a rhodanese superfamily enzyme was as well more abundantly represented in exposed cells of *D. radiodurans*. Proteins containing a single rhodanese-like domain are generally considered to mediate different forms of stress response [106]. The level of thiosulfate sulfurtransferase has been earlier reported as significantly increased after ionizing irradiation [101].

Oxidative stress-responsive proteins within tellurium resistance operon TerB (DR2220) and TerD (DR2221) were upregulated in cells of *D. radiodurans* exposed to UVC/vacuum conditions (Fig 5, S2 Table). The homologous tellurium resistance proteins contribute to the resistance of *E. coli* to various damaging agents, such as heavy metal ions and UVC radiation, and to the maintenance of the intracellular reducing environment, possibly by directly reversing disulfide bonds [18]. Several reports suggest oxidative stress as major determinant of tellurite toxicity in tellurite sensitive organisms, including *D. radiodurans* [116]. The genes encoding tellurium resistance have been specifically upregulated in a-proteobacterium *Rhodospirillum rubrum* followed by space exposure at ISS in frames of MELiSSA project, as well as significant differentially expressed under the conditions of modeled microgravity [117, 118]. The genes encoding TerB and TerE tellurium resistance proteins in *D. radiodurans* were shown to respond to acute ionizing radiation [119]. Moreover, the genes encoding TerB and TerZ proteins were found to be

upregulated immediately after gamma-irradiation of *D. radiodurans* [77], while tellurium resistance proteins TerB and TerD were also alleviated during gamma radiation in another study [101], implementing an adaptation to oxidative stress. Apart from tellurium resistance proteins, putative copper resistance protein (DR_A0299) with the predicted function of response to stress stimulus was found more abundant in UVC-irradiated cells of *D. radiodurans* (S2 Table). Such an observed involvement of tellurium resistance elements in the response to radiation or factors related to space environment may be part of a metal sensing stress response system, as well as inner membrane oxidative stress response.

The red-pigmented *D. radiodurans* encodes a set of genes involved in biosynthesis of carotenoids [18, 106]. Carotenoid pigments have also been shown to contribute in protection against oxidative stress damage. Our comparative proteomic data analysis shows that phytoene desaturase (DR_0861), enzyme of carotenoid biosynthetic pathway in *D. radiodurans*, was more abundantly represented (p-value 0.043) in UVC-vacuum stressed cells (Fig 5). The arrest of lycopene synthesis and the accumulation of phytoene along with enhanced sensitivity to acute ionizing radiation and oxygen stress have been reported to the colorless DR0861 gene knockout strain, while complementation of the mutant with a heterologous or homologous gene restored pigmentation and resistance [120]. Increased abundance of phytoene desaturase in UVC-irradiated cells of *D. radiodurans* indicates the contribution of the carotenoid synthesis pathway to the radioresistance and oxidative stress tolerance of *D. radiodurans*.

Other upregulated enzymes with a possible role in oxidative stress response were probable manganese-dependent inorganic pyrophosphatase ppaC (DR_2576) involved in oxidative phosphorylation and FrnE dithiol-disulfide isomerase (DR_0659) that catalyzes formation of protein disulfide bonds and is involved in sulfur metabolism. FrnE was induced in response to ionizing radiation [77]. This thioredoxin fold protein is included in predicted radiation and desiccation resistance regulon of *Deinococci* [121].

Transcriptional regulators

A number of transcriptional regulators and repressors have been identified in our proteomic analysis as constitutively expressed in both UVC-irradiated under vacuum conditions and control cells of *D. radiodurans*. The expression level of transcriptional regulators and repressors of TetR, MerR, GntR and AsnC families remained unaltered in irradiated cells of *D. radiodurans*, being constitutively represented under the control and UVC/vacuum conditions (S2 Table). The transcriptional regulator of FNR/CRP family (DR_0997) was significantly more abundantly represented in cells of *D. radiodurans* after UVC radiation under vacuum conditions. Cyclic AMP (cAMP) repressor proteins (CRP) act as global transcriptional regulators involved in many cellular pathways in various bacteria, including adaptation to starvation and extreme conditions [122-125]. The genome of *D. radiodurans* encodes four predicted CRP family proteins, including DR_0997, DR_1646, DR_2362, and DR_0834 (64). Recently, the gene encoding DR_0997 was shown to regulate stress response of *D. radiodurans* on the transcriptional level and loss of the Dr_0997 gene sensitized *D. radiodurans* toward H_2O_2, ultraviolet radiation, ionizing radiation, and mitomycin C [125]. Interestingly, our comparative proteomic analysis showed the upregulation of DR_0997 along with the upregulation of several proteins, encoded by genes, which belong to CRP regulon [125] in *D. radiodurans* under UVC-vacuum combined stress conditions (S2 Table). Among them are Lon proteases (DR_0349 and DR_1974), DNA repair protein PprA (DR_A0346), UvrABC system protein B UvrB (DR_2275), catalase katA (DR_0146) and tellurium resistance protein TerB (DR_2220). Thus, DR_0997 might act as a positive regulator in response to combined UVC-vacuum stress in *D. radiodurans*.

DdrO, a transcriptional regulator of HTH_3 family (DR_2574) was 2.6-fold downregulated in UVC-irradiated cells of *D. radiodurans* under vacuum conditions (S2 Table). Acting as a transcriptional repressor of Radiation Desiccation Response (RDR), DdrO binds 17 bp palindromic sequence called Radiation

Desiccation Response Motif (RDRM) in 21 RDRM-promoters of *D. radiodurans in vitro* [126] and represses a variety of DNA Damage Response (DDR) genes. We have also found that a number of RDR proteins comprising DdrO regulon were upregulated in UVC-irradiated cells of *D. radiodurans* under vacuum conditions. Among them are DNA gyrase B subunit GyrB (DR_0906), Tkt transketolase (DR_2256), RecQ helicase (DR_1289), UvrD superfamily I helicase (DR1775), urocanate hydratase (DRA0151) and FrnE uncharacterized DsbA-like thioredoxin fold protein (DR_0659) (S2 Table). Apparently, DdrO as a global master regulator serves to control reprogramming of microbial physiology in order to permit the adaptation of *D. radiodurans* to combined UVC-vacuum stress.

Metabolic Regulation

Our approach focuses on the identification and quantification of polar, primary metabolites. These are involved in growth, development and reproduction - parameters which are affected by UVC/vacuum stress. The metabolite analysis showed a significantly reduced abundance of overwhelming majority of identified polar metabolites in the irradiated cells of *D. radiodurans* (Fig 6). As *D. radiodurans* is a bacterium with a proteolytic life-style, it uses amino acids as preferred carbon source [127, 128]. Ethanolamine was one of the very few metabolites, which were more abundant in the UVC-irradiated cells of *D. radiodurans* (Fig 6). Splitting ethanolamine into ammonia and acetaldehyde can serve as a cellular supply of reduced nitrogen as well as a precursor for acetyl CoA [129], sustaining the necessary levels of these compounds in irradiated cells. Interestingly, the elevated level of a palmitoyl-derivative of carnitine was observed in the UVC-vacuum exposed cells of *D. radiodurans* (Fig 6). Apart from its nutritional function, a quaternary amine compound carnitine has various physiological effects. As a compatible solute, carnitine is important osmoprotectant, and can also enhance thermotolerance, cryotolerance and barotolerance, impacting bacterial survival in extreme conditions [130]. At the same time, osmotic stress has been described as a part of stress response which microorganisms experience exposed to the outer space environment or to its individual simulated factors [117, 131-133] In this context, the observed upregulation of O-Palmytoyl-L-Carnitine chloride (Fig 6) may suggest the role of this quaternary amine compound responsible for adaptation to extreme conditions [125] in the protection of *D. radiodurans* against combined stress conditions of UVC and vacuum. Moreover, carnitine as a compatible solute might be potentially necessary to overcome damaging desiccation effects of vacuum [102, 134] by binding additional water molecules, helping to stabilize proteins and cell membranes, and thus preventing complete desiccation of the cell.

The amount of octadecanoic (stearic) acid, which has been described as a minor component of *D. radiodurans* [75], was significantly increased in vacuum/UVC-irradiated cells of *D. radiodurans* (Fig 6). The surface-active compound stearic acid was identified in biosurfactants of several bacterial species [76, 77]. Decreased levels of stearic acid associated with the dramatic reduction in biofilm formation of *Streptococcus sanguinis nox* mutant [78], suggesting its involvement in stress-related reactions. Stearic acid can potentially be involved in covering the cells of *D. radiodurans* by a layer less permeable to water, thereby preserving the structural integrity of cell membranes in conditions of vacuum-induced dehydration. Although the cells of *D. radiodurans* do not naturally produce stearic acid in big quantities under non-stressed conditions [75], the observed accumulation of this biofilm-associated compound may potentially lead to the high survival of *D. radiodurans* in dry multilayers under UVC/vacuum combined stress.

Our study shows that response to UVC/vacuum combined stress and the enzymatic repair caused by the damage after ionizing radiation have overlapping molecular components in *D. radiodurans*. The combination of proteomic with metabolomic analysis of cells after UVC-irradiation under vacuum

condition reveals that the response is a multilayer process (Fig 8). It requires a high amount of energy in order to initiate stress defense mechanisms necessary to alleviate cell damage.

Acknowledgments

We greatly appreciate support of S. Puchegger (University of Vienna, Physics Faculty Center for Nano Structure Research) with electron microscopy investigations.

7. *METALLOSPHAERA SEDULA* - INTERACTIONS WITH A STONY METEORITE

7.1. Introduction

Deciphering microbial-mineral interactions such as biomineralization and fossilization processes can support our knowledge in redrawing the history of the early Earth and using analogue sites, also on other planetary bodies. Therefore, it is critical to assess if microfossils found in rocks and minerals are of biological origin [135]. Microbe-mediated mineralization implies the formation and deposition of a newly appearing mineral phase whereby minerals can either be deposited intracellularly, in the cell envelope, at the cell surface or they may form externally from the cell in the bulk phase [45]. Organisms, which are susceptible to mineralization, usually follow one of three known mechanisms: Biologically Controlled Mineralization, Biologically Induced Mineralization and Biologically Influenced Mineralization [11, 136]. Nevertheless, assigning biogenicity to a certain structure or signature in ancient rocks remains very challenging due to probable degradation of microbial remains during diagenesis or microbial-like morphologies being produced abiotically [137]. The potential to endure and promote biomineralization as well as subsequent fossilization has been examined using different bacterial and archaeal strains, even though only a few reports exist elucidating archaeal-mineral interactions. To gain deeper insight of what drives microbial mineralization and subsequent preservation, microbes from the *Bacteria* and *Archaea* kingdoms have been artificially mineralized since the 1970. In the first published fossilization trial by Oehler and Schopf, cyanobacteria have been successfully silicified leading to the microbes being well preserved and thoroughly embedded in a crystalline silica matrix [138]. The first experimental silicification of archaeal strains was performed with two strictly anaerobic and hyperthermophilic microorganisms, *Methanocaldococcus jannaschii* and *Pyrococcus abyssi* that could have lived in hydrothermal environments on the early Earth and possibly the early Mars. The obtained observations demonstrated that not all (micro)organisms are susceptible to biomineralization and fossilization, they behave differently even though they are closely related phylogenetically. Although both strains possess similar cell wall structures, most *M. janaschii* cells could not withstand silicification and lysed quickly, whereas *P. abyssi* cells were well preserved and silica precipitated on the cell wall [139]. Cell wall structures also serve as a mineral nucleation sites and might enhance the biomineralization process by providing a surface that promotes adsorption or precipitation of metals. A homogenous proteinaceous surface layer (S-layer) commonly found in prokaryotes is able to adsorb metals and radionuclides and to nucleate carbonate and sulfate minerals in Cyanobacteria [140]. Cells of the extreme thermoacidophilic archaeon and *M. sedula* relative *Sulfolobus acidocaldarius* were experimentally exposed to

amorphous Fe-phosphates, which encased the S-layer of the cells continuously after exposure time of 24h. Consequently, the Fe-phosphates encrusting *S. acidocaldarius* evolved into crystalline lipscombite, which was associated with microbial activity upon thermal treatment [141].

The extreme thermoacidophilic archaeon *Metallosphaera sedula* is a metal-mobilizing organism able to catalyze redox transformations of minerals while growing chemolithoautotrophically on a variety of metal-bearing substrates [7, 26, 142]. Investigating the interactions of this extreme metallophilic microorganism with mineral substrates of extraterrestrial origin and analogue sites, we have observed its selective cell surface biomineralization and preservation of cellular integrity under the desiccation conditions [143]. Here we describe the trial of archaeal-meteorite interactions using an ordinary chondrite to feed *M. sedula* with, during cultivation. Quantitative compositional analysis of the meteorite NWA 1172 shows an iron amount >50% along with silica, magnesium and traces of metallic compounds such as nickel, cobalt, chromium and manganese [144].

The study of extreme conditions interacting with microbial life and the thorough investigation of subsequent biogeochemical signals can help us to gain a deeper insight into microbial-mineral co-evolution on Earth over geological timescales and to enhance our knowledge of biosignatures for a search of life on other celestial bodies.

7.2. Materials & Methods

7.2.1. Strain and Media Composition

M. sedula (DSMZ 5348) cultures were grown aerobically in DSMZ88 Sulfolobus medium containing 1.3 g $(NH_4)_2SO_4$, 0.28 g KH_2PO_4, 0.25 g $MgSO_4 \cdot 7\ H_2O$, 0.07 g $CaCl_2 \cdot 2\ H_2O$ and 0.02 g $FeCl_3 \cdot 6\ H_2O$ dissolved in 1 L of water. After autoclaving, Allen's trace elements solution was added to 1 L media resulting in 1.80 mg $MnCl_2 \cdot 4\ H_2O$, 4.50 mg $Na_2B4O_7 \cdot 10\ H_2O$, 0.22 mg $ZnSO_4 \cdot 7\ H_2O$, 0.05 mg $CuCl_2 \cdot 2\ H_2O$, 0.03 mg $Na_2MoO_4 \cdot 2\ H_2O$, 0.03 mg $VSO_4 \cdot 2\ H_2O$, and 0.01 mg $CoSO_4$ final concentration. The pH was adjusted to 2.0 with 10 N H_2SO_4. Chemicals of high purity grade were used for media preparation.

7.2.2. Cultivation Setup

Chemolithoautotrophic cultivation of *M. sedula* was performed in DSMZ88 Sulfolobus medium described above in 1L glassblower modified Schott-bottle bioreactors (Duran DWK Life Sciences GmbH, Wertheim/Main, Germany), equipped with a thermocouple connected to a heating and magnetic stirring plate (IKA RCT Standard/IKA C-MAG HS10, Lab Logistics Group GmbH, Meckenheim, Germany) for temperature and agitation control. Each bioreactor was equipped with three 10 mL graduated glass pipettes, permitting carbon dioxide and air gassing (with the gas flow of 9 mL min-1, adjusted to five bubbles s^{-1} by using 8 mm valves (Serto, Frauenfeld, Switzerland)) and sampling of culture, respectively (Supplementary Figure 1). The graduated pipettes used for gassing were connected by silicon tubing to sterile 0.2 µm filters (Millex-FG Vent filter unit, Millipore, Billerica, USA). The graduated pipettes used for sampling were equipped with a Luer-lock system in order to permit sampling with sterile syringes (Soft-Ject, Henke Sass Wolf, Tuttlingen, Germany). The off gas was forced to exit via a water-cooled condenser (Carl Roth GmbH, Germany). For the cultivations of *M. sedula* at 73°C the temperature inside the bioreactors was controlled by electronic thermocouple via the heating and magnetic stirring plates. *M. sedula* inocula were obtained by resuspending a chemolithoautotrophically grown cell pellet formed by centrifugation at 6000 × *g* for 15 min in DSMZ88 media without organic carbon source and inorganic metals/metalloids as energy sources. For chemolithoautotrophic growth cultures with initial pH of 2.0 were supplemented with 5 g/liter of meteoritic NWA 1172, no further pH adjustments were introduced during the cultivation. The meteorite material was temperature sterilized at 180°C in a heating chamber for a minimum of 24 hours prior to autoclaving at 121°C for 20 min. Abiotic control consists of uninoculated culture media supplemented with NWA 1172 which was included in the spectroscopic experiments.

Growth of cells was monitored by manual counting with an improved Neubauer chamber. Precise cell enumeration was found to be difficult due to the interference with mineral particles of similar size and round shaped morphology and shielding of *M. sedula* by mineral precipitates, especially at later stages of growth.

7.2.3. EPR Analysis

The Electron Paramagnetic Resonance (EPR) spectra were recorded on an X-Band Bruker Elexsys-II E500 CW-EPR spectrometer (Bruker Biospin GmbH, Rheinstetten, Germany) at 90 ± 1 and 293 ± 1 K using a high sensitivity cavity (SHQE1119). Solid state EPR measurements were performed setting microwave frequency to 9 GHz, modulation frequency to 100 kHz, center field to 6000 G, sweep width to 12000 G, sweep time to 335.5 s, modulation amplitude to 20.37 G, microwave power to 15 mW, conversion time to 81.92 ms and resolution to 4096 points. The samples were put in EPR quartz tubes (Wilmad-LabGlass, Vineland, New Jersey, USA) and scanned three times, of which the average was used for analysis. The spectrum of an empty control tube was subtracted from all sample spectra. All spectra were analyzed with the Bruker Xepr software.

7.2.4. SEM Sample Preparation and Analysis

The mineral precipitates obtained after dehydration experiments were examined with a Zeiss Supra 55 VP scanning electron microscope, equipped with a field emission gun (Schottky-FE, DENKA), an energy-dispersive x-ray spectrometer (EDS, Oxford Instruments, X-Max 80), which was used for imaging and elemental analysis of precipitates. The samples were coated with a 3 nm Au/Pd layer (Laurell WS-650-23 spincoater). The acceleration voltage applied was 5 kV and the EDS analyses were performed with a 120-µm condenser aperture and a counting time of 50 s. All the sample spots investigated by EDS were chosen randomly and each spot was measured three times. Table (x) represents the elemental chemical compositions of *M. sedula* cell surfaces, which were taken as the average of the measurements from 20 or more randomly chosen spots. Au, Pd values in EDS spectra, which are due to samples coating with an Au/Pd layer, are not included in the tables.

7.2.5. TEM Sample Preparation and Analysis

TEM samples were primary fixed at 4°C in a 1M Na-Cacodylate buffer containing 2.5% glutaraldehyde. After primary fixation cells were post-fixed for 2h in 1% OsO_4. Cells were washed three times (2x 0.1M Na-cacodylate, 1x dH_2O) and subsequently dehydrated by a gradual ethanol series (30%, 50%, 70%, 90%, abs.), each step with an incubation time of 30 minutes. Cells were spun down after each dehydration step for another 30 minutes and

resuspended for the following ethanol treatment. Samples were embedded in Spurr Low Viscosity Resin (Electron Microscopy Sciences, United States) and polymerized at 60°C for a minimum of 48h. Semi- and ultrathin sectioning were performed via a Reichert-Jung Ultracut E ultramicrotome, 50-70nm ultrathin sections were deposited on formvar/carbon-coated 200 mesh copper grids (Agar Scientific, UK) and examined at the FELMI-ZFE in Graz, Austria. High resolution STEM investigations were performed on a probe corrected FEI Titan G2 60–300 (S/TEM) microscope with an X-FEG Schottky field-emission electron source operated at 300 kV (current of 150 pA, beam diamater of 1Å). The microscope is equipped with a FEI Super-X detector (Chemi-STEM technology), consisting of four separate silicon drift detectors and a Dual EELS - Gatan Imaging Filter (GIF) Quantum. High Angular Annular Dark Field (HAADF) and Annular Dark Field (ADF) detectors were used to acquire micrographs. Conventional and analytical TEM was performed using a FEI Tecnai F20 microscope operated at 200kV under cryo conditions. The microscope is suited with a Schottky emitter, a monochromator, a post-column high resolution Gatan Imaging Filter (GIF) and a Si(Li) X-ray detector with ultrathin window.

7.3. Results

7.3.3. Chemolithotrophic Growth on Meteorite NWA 1172

Metallosphaera sedula was grown in a chemolithotrophic mode to investigate growth capacity, spectroscopic fingerprints and to produce ultrathin cuts for electron microscopy. Chemolithotrophic growth for a total of 12 days was supported by an inorganic CO_2 gasing and supplementation of fine ground meteorite material (5g/L). Manually counted cell densities over a period of 12 days show a steep and exponential increment for 2 days transforming into a stationary phase until harvesting time point (Fig. 6). After conventional cultivation, cells were put for desiccation/dehydration in glass plates under oxic conditions and at room temperature for approximately 60 days to examine possible alterations of the cellular integrity and morphology or the formation of specific inorganic precipitates mediated by *M. sedula*.

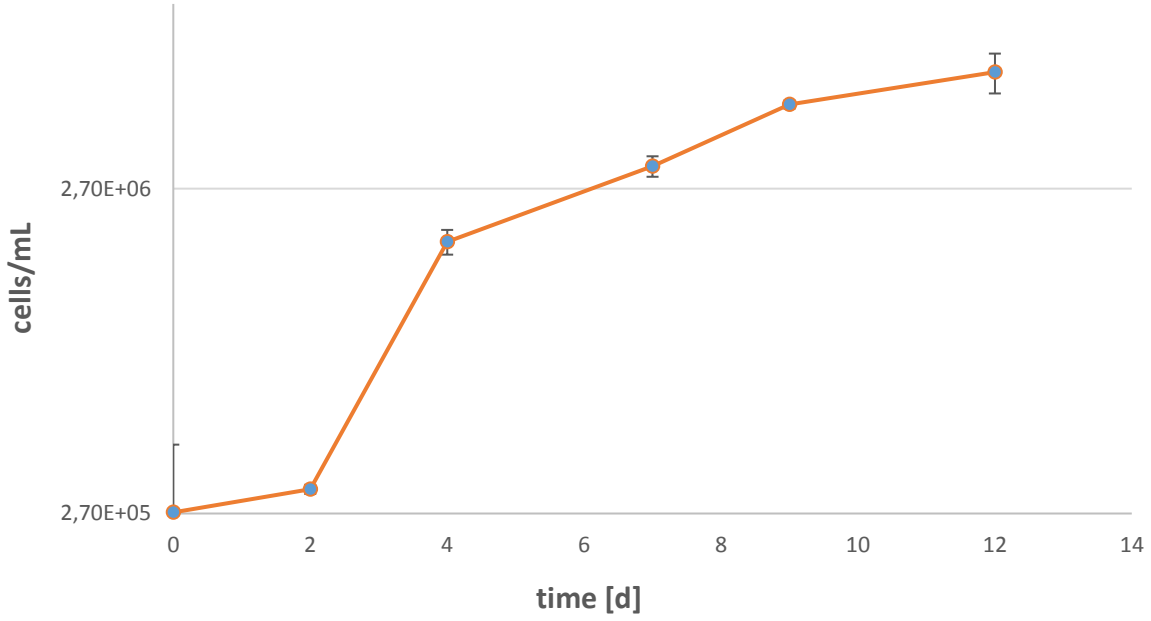

Fig. 6: Logarithmic growth curve of *M. sedula* cultivated in Sulfolobales medium for 12 days, supplemented with 5g/L meteorite material NWA 1172.

7.3.4. EPR of *M. sedula* after cultivation

Electron paramagnetic resonance spectroscopy was applied to identify paramagnetic species after cultivation with *M. sedula*, in the raw meteorite material and the corresponding abiotic

control which consisted of cultivation medium and meteorite but no microbes. Furthermore, this method can help us resolve the putative influence of *M. sedula* on the oxidation state of identified paramagnetic elements. Measurements were performed at room temperature (273 K, Fig. 7B) and 90 K (Fig. 7A) to have a higher chance for unambiguous iron detection.

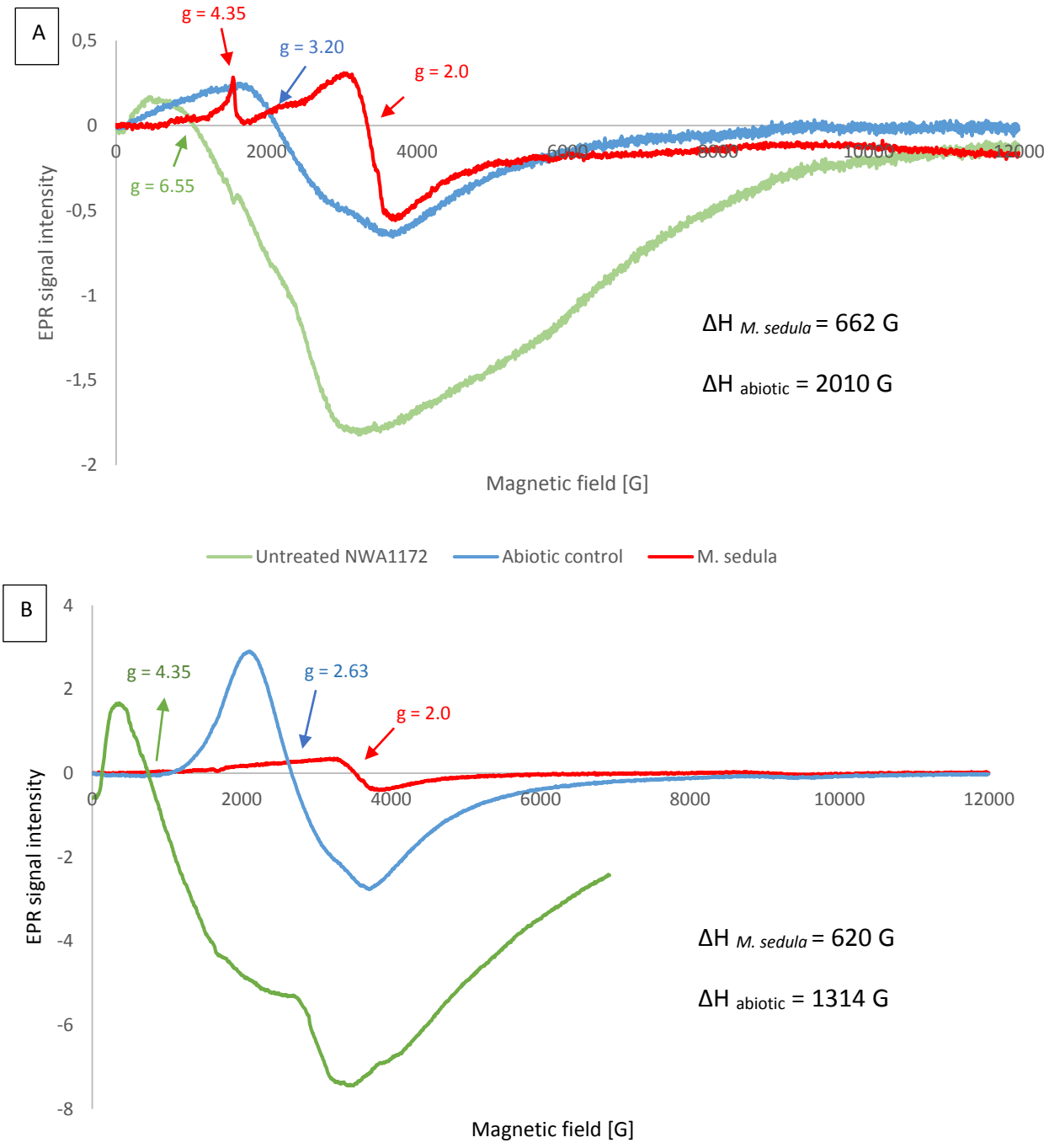

Fig. 7: Electron Paramagnetic Resonance (EPR) measurement of freeze-dried *M. sedula* NWA 1172 culture. (A) Spectra recorded at 90K with assigned linewidth (ΔH) and g-values. (B) Spectra recorded at 273K.

The biogenic sample containing *M. sedula* cells, shows a prominent high spin Fe^{3+} signal with a g-value of 4.35 and a low spin Fe^{3+} signal at g-value 2 (Fig. 7A) as well as a smaller linewidth (ΔH = 662 G) compared to the abiotic sample (ΔH = 2010 G). Previously, it has been shown that for biological samples containing paramagnetic Mn^{2+} species, the reductive shift in linewidth is characteristic upon cultivation with microorganisms [145], [146]. When compared to the raw meteorite material, the appearance of a prominent high spin Fe^{3+} signal (a sharp peak with a g-value of 4.35) along with a low spin Fe^{3+} signal at g-value 2 in biogenic sample may indicate an increase in Fe^{3+} species due to biooxidative activity of *M. sedula*. These characteristic sharp high spin and low spin Fe^{3+} signals are not represented at abiotically treated NWA 1172 (Fig. 7A). The abiotic spectrum is characterized by a shifted g-value 3.20, which cannot be assigned clearly to a specific paramagnetic element due to possible overlay or a mixture of signals. While the distinct high spin Fe^{3+} signal disappears almost completely in the biogenic sample when measured at room temperature (Fig. 7B), the low spin Fe^{3+} signal at g-value 2 appears after cultivation showing us the presence of mineral transforming organisms.

7.3.5. TEM Observations of *M. sedula* cells

To improve our understanding of microbial interactions with meteorite material, it is necessary to further characterize microbial-mineral interface of *M. sedula* grown on NWA 1172. In order to generate cellular samples for elemental ultrastructural analysis, the technical procedure to generate thin sections of *M. sedula* cells grown on NWA 1172 was developed. Obtaining ultra-thin cuts (50-70 nm) from material enriched with fine-grained mineral particles along with attached archaeal cells appeared to be a technically challenging process. The cells of *M. sedula* attached to NWA 1172 represented a kind of hard and brittle biological material that is difficult to cut with a diamond knife in conventional ultramicrotome procedures. To overcome these technical difficulties, we applied a gradient centrifugation approach. A gradient of different cell densities was created before and during embedding the microbial-mineral mixture into a resin matrix. To localize potential biomineralized archaea in the embedded material, semi-thin cuts (~ 500 nm) were produced and examined by light microscopy. By trimming and shaping the area of interest, possible cells were restricted to this selected area. First observations of our ultra-thin cuts reveal round-shaped, irregular cocci with a diameter around 1 µm (Fig. 8). Electron-dense dark areas around the membrane (S-layer) and an extensive dark accumulation in the cytosol will be further resolved in the future by implementing different spectroscopic techniques.

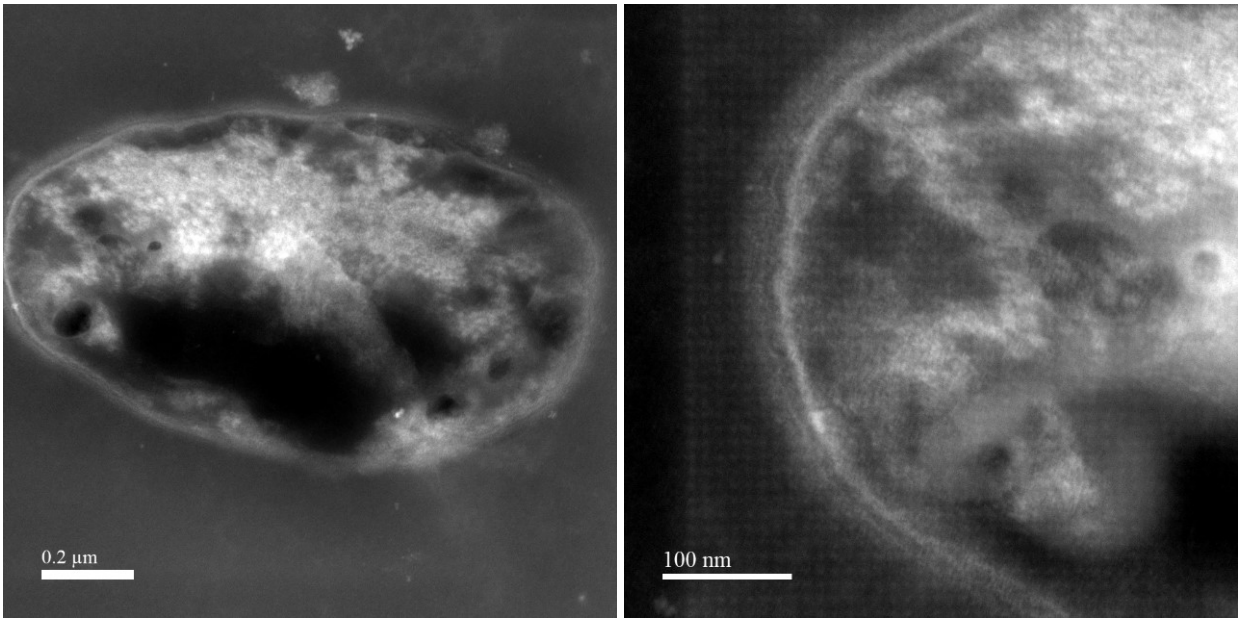

Fig. 8: Tranmission Electron Microscopy (TEM) images of *M. sedula* grown on the stony meteorite NWA 1172. (A) Single cell of *M. sedula* exhibiting areas of varying electron density (bright/dark areas). (B) Magnification of the same cell.

7.4. Conclusion

M. sedula chemolithotrophic growth on a stony meteorite NWA 1172 as the sole energy source was observed. *M. sedula* is capable of utilizing elements and components of NWA 1172 for its own energetic benefits. Iron is the predominant component (51%) of the ordinary chondrite NWA 1172 and its mixed paramagnetic Fe^{3+} species in high and low spin states were identified via electron paramagnetic resonance used in this study. Accumulation of Fe^{3+} in the biogenic sample (90 K) was observed and might be the consequence of extensive Fe^{2+} oxidation of the minerals mediated by *M. sedula*. Within the frames of this thesis a successful establishment of a method to produce ultra-thin sections for transmission electron microscopy was achieved. Examined sections reveal coccoid cells of *M. sedula* with electron-dense dark areas representing metallic accumulations around the S-layer as well as in the cytosol of the cell. The nature of these dense accumulations will be further resolved by nanoanalytical spectroscopy (EELS) or/and synchrotron assisted X-ray spectroscopy (XANES, µXRF, XRD, XAS) to intensify the study of microbial-mineral interactions with terrestrial and extraterrestrial multi-metallic material.

REFERENCES

1. Beveridge, T.J., et al., *Metal-microbe interactions: contemporary approaches.* Adv Microb Physiol, 1997. **38**: p. 177-243.
2. Sterritt, R.M. and J.N. Lester, *Interactions of heavy metals with bacteria.* Sci Total Environ, 1980. **14**(1): p. 5-17.
3. Beveridge, T.J. and R.G. Murray, *Sites of metal deposition in the cell wall of Bacillus subtilis.* J Bacteriol, 1980. **141**(2): p. 876-87.
4. Yilmaz, E.I., *Metal tolerance and biosorption capacity of Bacillus circulans strain EB1.* Res Microbiol, 2003. **154**(6): p. 409-15.
5. Kang, C.H., Y.J. Kwon, and J.S. So, *Bioremediation of heavy metals by using bacterial mixtures.* Ecological Engineering, 2016. **89**: p. 64-69.
6. Krzmarzick, M.J., et al., *Diversity and Niche of Archaea in Bioremediation.* Archaea-an International Microbiological Journal, 2018.
7. Huber, G., et al., *Metallosphaera sedula gen, and sp. nov. Represents a New Genus of Aerobic, Metal-Mobilizing, Thermoacidophilic Archaebacteria.* Systematic and Applied Microbiology, 1989. **12**(1): p. 38-47.
8. Mukherjee, A., et al., *Uranium extremophily is an adaptive, rather than intrinsic, feature for extremely thermoacidophilic Metallosphaera species.* Proc Natl Acad Sci U S A, 2012. **109**(41): p. 16702-7.
9. Gadd, G.M., *Metals, minerals and microbes: geomicrobiology and bioremediation.* Microbiology-Sgm, 2010. **156**: p. 609-643.
10. Miot, J., et al., *Experimental maturation of Archaea encrusted by Fe-phosphates.* Sci Rep, 2017. **7**(1): p. 16984.
11. Gaboyer, F., et al., *Mineralization and Preservation of an extremotolerant Bacterium Isolated from an Early Mars Analog Environment.* Sci Rep, 2017. **7**(1): p. 8775.
12. Walker, J.J. and N.R. Pace, *Endolithic microbial ecosystems.* Annu Rev Microbiol, 2007. **61**: p. 331-47.
13. Zhang M. Sc, R., *Biofilm formation and extracellular polymeric substances of acidophilic metal/sulfur-oxidizing archaea*. 2016.
14. Schippers, A., et al., *Biomining: metal recovery from ores with microorganisms.* Adv Biochem Eng Biotechnol, 2014. **141**: p. 1-47.
15. Mikkelsen, D., et al., *Archaeal diversity in two thermophilic chalcopyrite bioleaching reactors.* Environ Microbiol, 2006. **8**(11): p. 2050-6.
16. Donati, E.R., C. Castro, and M.S. Urbieta, *Thermophilic microorganisms in biomining.* World Journal of Microbiology & Biotechnology, 2016. **32**(11).
17. Miriyala, S., et al., *Manganese superoxide dismutase, MnSOD and its mimics.* Biochim Biophys Acta, 2012. **1822**(5): p. 794-814.
18. Slade, D. and M. Radman, *Oxidative stress resistance in Deinococcus radiodurans.* Microbiol Mol Biol Rev, 2011. **75**(1): p. 133-91.
19. Daly, M.J., et al., *Protein oxidation implicated as the primary determinant of bacterial radioresistance.* PLoS Biol, 2007. **5**(4): p. e92.
20. Daly, M.J., et al., *Accumulation of Mn(II) in Deinococcus radiodurans facilitates gamma-radiation resistance.* Science, 2004. **306**(5698): p. 1025-8.
21. Nies, D.H., *Efflux-mediated heavy metal resistance in prokaryotes.* FEMS Microbiol Rev, 2003. **27**(2-3): p. 313-39.
22. Haferburg, G. and E. Kothe, *Microbes and metals: interactions in the environment.* Journal of Basic Microbiology, 2007. **47**(6): p. 453-467.
23. Nies, D.H., *The Cobalt, Zinc, and Cadmium Efflux System Czcabc from Alcaligenes-Eutrophus Functions as a Cation-Proton Antiporter in Escherichia-Coli.* Journal of Bacteriology, 1995. **177**(10): p. 2707-2712.

24. Amend, J.P. and E.L. Shock, *Energetics of overall metabolic reactions of thermophilic and hyperthermophilic Archaea and bacteria.* FEMS Microbiol Rev, 2001. **25**(2): p. 175-243.
25. Auernik, K.S. and R.M. Kelly, *Physiological Versatility of the Extremely Thermoacidophilic Archaeon Metallosphaera sedula Supported by Transcriptomic Analysis of Heterotrophic, Autotrophic, and Mixotrophic Growth.* Applied and Environmental Microbiology, 2010. **76**(3): p. 931-935.
26. Maezato, Y., et al., *Metal Resistance and Lithoautotrophy in the Extreme Thermoacidophile Metallosphaera sedula.* Journal of Bacteriology, 2012. **194**(24): p. 6856-6863.
27. Wheaton, G.H., A. Mukherjee, and R.M. Kelly, *Transcriptomes of the Extremely Thermoacidophilic Archaeon Metallosphaera sedula Exposed to Metal "Shock" Reveal Generic and Specific Metal Responses.* Applied and Environmental Microbiology, 2016. **82**(15): p. 4613-4627.
28. Auernik, K.S., C.R. Cooper, and R.M. Kelly, *Life in hot acid: Pathway analyses in extremely thermoacidophilic archaea.* Current Opinion in Biotechnology, 2008. **19**(5): p. 445-453.
29. Auernik, K.S. and R.M. Kelly, *Impact of molecular hydrogen on chalcopyrite bioleaching by the extremely thermoacidophilic archaeon Metallosphaera sedula.* Appl Environ Microbiol, 2010. **76**(8): p. 2668-72.
30. Peeples, T.L. and R.M. Kelly, *Bioenergetics of the Metal Sulfur-Oxidizing Extreme Thermoacidophile, Metallosphaera-Sedula.* Fuel, 1993. **72**(12): p. 1619-1624.
31. Lin, C.K., et al., *A Global Perspective on Sulfur Oxide Controls in Coal-Fired Power Plants and Cardiovascular Disease.* Sci Rep, 2018. **8**(1): p. 2611.
32. Clark, T.R., F. Baldi, and G.J. Olson, *Coal Depyritization by the Thermophilic Archaeon Metallosphaera sedula.* Appl Environ Microbiol, 1993. **59**(8): p. 2375-9.
33. Westall, F., et al., *Biosignatures on Mars: What, Where, and How? Implications for the Search for Martian Life.* Astrobiology, 2015. **15**(11): p. 998-1029.
34. Michalski, J.R., et al., *Groundwater activity on Mars and implications for a deep biosphere.* Nature Geoscience, 2013. **6**(2): p. 133-138.
35. Hays, L.E., et al., *Biosignature Preservation and Detection in Mars Analog Environments.* Astrobiology, 2017. **17**(4): p. 363-400.
36. Floyd, M.A.M., et al., *Metabolic Processes Preserved as Biosignatures in Iron-Oxidizing Microorganisms: Implications for Biosignature Detection on Mars.* Astrobiology, 2019. **19**(1): p. 40-52.
37. Krisko, A. and M. Radman, *Biology of extreme radiation resistance: the way of Deinococcus radiodurans.* Cold Spring Harb Perspect Biol, 2013. **5**(7).
38. Zahradka, K., et al., *Reassembly of shattered chromosomes in Deinococcus radiodurans.* Nature, 2006. **443**(7111): p. 569-73.
39. Mattimore, V. and J.R. Battista, *Radioresistance of Deinococcus radiodurans: functions necessary to survive ionizing radiation are also necessary to survive prolonged desiccation.* J Bacteriol, 1996. **178**(3): p. 633-7.
40. Pavlov, A.K., et al., *Was Earth ever infected by martian biota? Clues from radioresistant bacteria.* Astrobiology, 2006. **6**(6): p. 911-8.
41. Hastings, J.W., W.H. Holzapfel, and J.G. Niemand, *Radiation resistance of lactobacilli isolated from radurized meat relative to growth and environment.* Appl Environ Microbiol, 1986. **52**(4): p. 898-901.
42. Barnese, K., et al., *Manganous phosphate acts as a superoxide dismutase.* J Am Chem Soc, 2008. **130**(14): p. 4604-6.
43. Peana, M., et al., *A Model for Manganese interaction with Deinococcus radiodurans proteome network involved in ROS response and defense.* J Trace Elem Med Biol, 2018. **50**: p. 465-473.
44. Eltsov, M. and J. Dubochet, *Fine structure of the Deinococcus radiodurans nucleoid revealed by cryoelectron microscopy of vitreous sections.* J Bacteriol, 2005. **187**(23): p. 8047-54.

45. Ehrlich, H.L., *Microbes as geologic agents: Their role in mineral formation.* Geomicrobiology Journal, 1999. **16**(2): p. 135-153.
46. Westall, F. and R.L. Folk, *Exogenous carbonaceous microstructures in Early Archaean cherts and BIFs from the Isua Greenstone Belt: implications for the search for life in ancient rocks.* Precambrian Research, 2003. **126**(3-4): p. 313-330.
47. Orange, F., et al., *Preservation and Evolution of Organic Matter During Experimental Fossilisation of the Hyperthermophilic Archaea Methanocaldococcus jannaschii.* Origins of Life and Evolution of Biospheres, 2012. **42**(6): p. 587-609.
48. McMahon, S., et al., *A Field Guide to Finding Fossils on Mars.* Journal of Geophysical Research-Planets, 2018. **123**(5): p. 1012-1040.
49. Grotzinger, J.P., et al., *A Habitable Fluvio-Lacustrine Environment at Yellowknife Bay, Gale Crater, Mars.* Science, 2014. **343**(6169).
50. Gonzalez-Toril, E., et al., *Iron meteorites can support the growth of acidophilic chemolithoautotrophic microorganisms.* Astrobiology, 2005. **5**(3): p. 406-414.
51. Kawaguchi, Y., et al., *The Possible Interplanetary Transfer of Microbes: Assessing the Viability of Deinococcus spp. Under the ISS Environmental Conditions for Performing Exposure Experiments of Microbes in the Tanpopo Mission.* Origins of Life and Evolution of Biospheres, 2013. **43**(4-5): p. 411-428.
52. M., O.L., *Anaxagoras and the Origin of Panspermia Theory*. 2008: iUniverse.
53. Mileikowsky, C., et al., *Natural transfer of viable microbes in space.* Icarus, 2000. **145**(2): p. 391-427.
54. Mennigmann, H.D., *Exobiology: Results of Spaceflight Missions.* Advances in Space Research, 1989. **9**(6): p. 3-12.
55. Horneck, G., *Survival of microorganisms in space: a review.* Adv Space Res, 1981. **1**(14): p. 39-48.
56. Yamagishi, A., *TANPOPO: Astrobiology exposure and micrometeorid capture experiments*, in *Transactions of the Japan Society for Aeronautical and Space Sciences, Space Technology Japan*. 2008: Japan.
57. Dainton, F.S., *On the existence of free atoms and radicals in water and aqueous solutions subjected to ionizing radiation.* J Phys Colloid Chem, 1948. **52**(3): p. 490-517.
58. Krisko, A. and M. Radman, *Biology of Extreme Radiation Resistance: The Way of Deinococcus radiodurans.* Cold Spring Harbor Perspectives in Biology, 2013. **5**(7): p. a012765.
59. Potts, M., *Desiccation tolerance of prokaryotes.* Microbiol Rev, 1994. **58**(4): p. 755-805.
60. Yamagishi, A., et al., *Tanpopo: astrobiology exposure and micrometeoroid capture experiments—proposed experiments at the Exposure Facility of ISS-JEM.* Transactions of the Japan Society for Aeronautical and Space Sciences, Aerospace Technology Japan, 2014. **12**(ists29): p. Tk_49-Tk_55.
61. Arrhenius, S., *Die Verbreitung des Lebens im Weltenraum.* Die Umschau, 1903. **7**: p. 481-486.
62. Kawaguchi, Y., et al., *The possible interplanetary transfer of microbes: assessing the viability of Deinococcus spp. under the ISS Environmental conditions for performing exposure experiments of microbes in the Tanpopo mission.* Orig Life Evol Biosph, 2013. **43**(4-5): p. 411-28.
63. Kawaguchi, Y., et al., *Investigation of the Interplanetary Transfer of Microbes in the Tanpopo Mission at the Exposed Facility of the International Space Station.* Astrobiology, 2016. **16**(5): p. 363-76.
64. Horneck, G. and P. Rettberg, *Complete course in astrobiology*. 2007, Weinheim: Wiley-VCH. xx, 413 p.
65. Rastogi, R.P., et al., *Molecular mechanisms of ultraviolet radiation-induced DNA damage and repair.* J Nucleic Acids, 2010. **2010**: p. 592980.
66. Krisko, A. and M. Radman, *Protein damage and death by radiation in Escherichia coli and Deinococcus radiodurans.* Proc Natl Acad Sci U S A, 2010. **107**(32): p. 14373-7.

67. Moeller, R., et al., *Genomic bipyrimidine nucleotide frequency and microbial reactions to germicidal UV radiation.* Arch Microbiol, 2010. **192**(7): p. 521-9.
68. Tanaka, M., et al., *Characterization of pathways dependent on the uvsE, uvrA1, or uvrA2 gene product for UV resistance in Deinococcus radiodurans.* J Bacteriol, 2005. **187**(11): p. 3693-7.
69. Minton, K.W., *DNA repair in the extremely radioresistant bacterium Deinococcus radiodurans.* Mol Microbiol, 1994. **13**(1): p. 9-15.
70. Gutman, P.D., P. Fuchs, and K.W. Minton, *Restoration of the DNA damage resistance of Deinococcus radiodurans DNA polymerase mutants by Escherichia coli DNA polymerase I and Klenow fragment.* Mutat Res, 1994. **314**(1): p. 87-97.
71. Slade, D., et al., *Recombination and replication in DNA repair of heavily irradiated Deinococcus radiodurans.* Cell, 2009. **136**(6): p. 1044-55.
72. Cox, M.M., J.L. Keck, and J.R. Battista, *Rising from the Ashes: DNA Repair in Deinococcus radiodurans.* PLoS Genetics, 2010. **6**(1): p. e1000815.
73. Reece, R.J. and A. Maxwell, *DNA gyrase: structure and function.* Crit Rev Biochem Mol Biol, 1991. **26**(3-4): p. 335-75.
74. Narumi, I., et al., *PprA: a novel protein from Deinococcus radiodurans that stimulates DNA ligation.* Mol Microbiol, 2004. **54**(1): p. 278-85.
75. Harris, D.R., et al., *Preserving genome integrity: the DdrA protein of Deinococcus radiodurans R1.* PLoS Biol, 2004. **2**(10): p. e304.
76. Norais, C.A., et al., *DdrB protein, an alternative Deinococcus radiodurans SSB induced by ionizing radiation.* J Biol Chem, 2009. **284**(32): p. 21402-11.
77. Tanaka, M., et al., *Analysis of Deinococcus radiodurans's transcriptional response to ionizing radiation and desiccation reveals novel proteins that contribute to extreme radioresistance.* Genetics, 2004. **168**(1): p. 21-33.
78. Weckwerth, W., K. Wenzel, and O. Fiehn, *Process for the integrated extraction, identification and quantification of metabolites, proteins and RNA to reveal their co-regulation in biochemical networks.* Proteomics, 2004. **4**(1): p. 78-83.
79. Chaturvedi, P., et al., *Cell-specific analysis of the tomato pollen proteome from pollen mother cell to mature pollen provides evidence for developmental priming.* J Proteome Res, 2013. **12**(11): p. 4892-903.
80. Sumner, L.W., et al., *Proposed minimum reporting standards for chemical analysis Chemical Analysis Working Group (CAWG) Metabolomics Standards Initiative (MSI).* Metabolomics, 2007. **3**(3): p. 211-221.
81. Luan, H., et al., *Genome-wide transcriptome and antioxidant analyses on gamma-irradiated phases of deinococcus radiodurans R1.* PLoS One, 2014. **9**(1): p. e85649.
82. Foloppe, N. and L. Nilsson, *The glutaredoxin -C-P-Y-C- motif: influence of peripheral residues.* Structure, 2004. **12**(2): p. 289-300.
83. Levine, R.L., J. Moskovitz, and E.R. Stadtman, *Oxidation of methionine in proteins: roles in antioxidant defense and cellular regulation.* IUBMB Life, 2000. **50**(4-5): p. 301-7.
84. Sprenger, G.A., *Aromatic Amino Acids*, in *Amino Acid Biosynthesis ~ Pathways, Regulation and Metabolic Engineering*, V.F. Wendisch, Editor. 2007, Springer Berlin Heidelberg: Berlin, Heidelberg. p. 93-127.
85. Daly, M.J., *A new perspective on radiation resistance based on Deinococcus radiodurans.* Nat Rev Micro, 2009. **7**(3): p. 237-245.
86. Daly, M.J., et al., *Small-molecule antioxidant proteome-shields in Deinococcus radiodurans.* PLoS One, 2010. **5**(9): p. e12570.
87. Gupta, P., et al., *MDP: A Deinococcus Mn2+-Decapeptide Complex Protects Mice from Ionizing Radiation.* PLoS One, 2016. **11**(8): p. e0160575.
88. Zhang, Y.M., et al., *Induction of a futile Embden-Meyerhof-Parnas pathway in Deinococcus radiodurans by Mn: possible role of the pentose phosphate pathway in cell survival.* Appl Environ Microbiol, 2000. **66**(1): p. 105-12.

89. Zhang, Y.M., J.K. Liu, and T.Y. Wong, *The DNA excision repair system of the highly radioresistant bacterium Deinococcus radiodurans is facilitated by the pentose phosphate pathway.* Molecular Microbiology, 2003. **48**(5): p. 1317-1323.
90. Joshi, B., et al., *Protein recycling is a major component of post-irradiation recovery in Deinococcus radiodurans strain R1.* Biochem Biophys Res Commun, 2004. **320**(4): p. 1112-7.
91. Moseley, B.E., *The isolation and some properties of radiation-sensitive mutants of Micrococcus radiodurans.* J Gen Microbiol, 1967. **49**(2): p. 293-300.
92. Moseley, B.E. and H.J. Copland, *Isolation and properties of a recombination-deficient mutant of Micrococcus radiodurans.* J Bacteriol, 1975. **121**(2): p. 422-8.
93. Moseley, B.E. and D.M. Evans, *Isolation and properties of strains of Micrococcus (Deinococcus) radiodurans unable to excise ultraviolet light-induced pyrimidine dimers from DNA: evidence for two excision pathways.* J Gen Microbiol, 1983. **129**(8): p. 2437-45.
94. Gutman, P.D., et al., *Sequencing, targeted mutagenesis and expression of a recA gene required for the extreme radioresistance of Deinococcus radiodurans.* Gene, 1994. **141**(1): p. 31-7.
95. Hua, Y., et al., *PprI: a general switch responsible for extreme radioresistance of Deinococcus radiodurans.* Biochemical and Biophysical Research Communications, 2003. **306**(2): p. 354-360.
96. Lu, H., et al., *Deinococcus radiodurans PprI switches on DNA damage response and cellular survival networks after radiation damage.* Mol Cell Proteomics, 2009. **8**(3): p. 481-94.
97. Pogoda de la Vega, U., *Residual Restoration of DNA Lesions in Deinococcus Radiodurans Mutants Indicate Presence of a Bypass UV-repair Process*. 2008.
98. Bauermeister, A., et al., *Roles of PprA, IrrE, and RecA in the resistance of Deinococcus radiodurans to germicidal and environmentally relevant UV radiation.* Arch Microbiol, 2009. **191**(12): p. 913-8.
99. Dedieu, A., et al., *Major soluble proteome changes in Deinococcus deserti over the earliest stages following gamma-ray irradiation.* Proteome Science, 2013. **11**: p. 3-3.
100. Zhang, C., et al., *Proteomic analysis of Deinococcus radiodurans recovering from gamma-irradiation.* Proteomics, 2005. **5**(1): p. 138-43.
101. Basu, B. and S.K. Apte, *Gamma radiation-induced proteome of Deinococcus radiodurans primarily targets DNA repair and oxidative stress alleviation.* Mol Cell Proteomics, 2012. **11**(1): p. M111 011734.
102. Horneck, G., D.M. Klaus, and R.L. Mancinelli, *Space microbiology.* Microbiol Mol Biol Rev, 2010. **74**(1): p. 121-56.
103. del Carmen Huesca Espitia, L., et al., *Base-change mutations induced by various treatments of Bacillus subtilis spores with and without DNA protective small, acid-soluble spore proteins.* Mutat Res, 2002. **503**(1-2): p. 77-84.
104. Munakata, N., et al., *Induction of unique tandem-base change mutations in bacterial spores exposed to extreme dryness.* Mutation research, 1997. **390**(1-2): p. 189-195.
105. Goosen, N. and G.F. Moolenaar, *Repair of UV damage in bacteria.* DNA Repair (Amst), 2008. **7**(3): p. 353-79.
106. Makarova, K.S., et al., *Genome of the Extremely Radiation-Resistant Bacterium Deinococcus radiodurans Viewed from the Perspective of Comparative Genomics.* Microbiology and Molecular Biology Reviews, 2001. **65**(1): p. 44-79.
107. Fowler, R.G. and R.M. Schaaper, *The role of the mutT gene of Escherichia coli in maintaining replication fidelity.* FEMS Microbiol Rev, 1997. **21**(1): p. 43-54.
108. Zhang, H., et al., *Structural and functional studies of MutS2 from Deinococcus radiodurans.* DNA Repair (Amst), 2014. **21**: p. 111-9.
109. Tesfazgi Mebrhatu, M., et al., *Evidence for an evolutionary antagonism between Mrr and Type III modification systems.* Nucleic Acids Research, 2011. **39**(14): p. 5991-6001.
110. Aertsen, A. and C.W. Michiels, *Mrr instigates the SOS response after high pressure stress in Escherichia coli.* Molecular Microbiology, 2005. **58**(5): p. 1381-1391.

111. Bilski, P., et al., *Vitamin B6 (pyridoxine) and its derivatives are efficient singlet oxygen quenchers and potential fungal antioxidants.* Photochem Photobiol, 2000. **71**(2): p. 129-34.
112. Obiero, J., et al., *Thioredoxin system from Deinococcus radiodurans.* J Bacteriol, 2010. **192**(2): p. 494-501.
113. Omelchenko, M.V., et al., *Comparative genomics of Thermus thermophilus and Deinococcus radiodurans: divergent routes of adaptation to thermophily and radiation resistance.* BMC Evolutionary Biology, 2005. **5**: p. 57-57.
114. Ghosal, D., et al., *How radiation kills cells: survival of Deinococcus radiodurans and Shewanella oneidensis under oxidative stress.* FEMS Microbiol Rev, 2005. **29**(2): p. 361-75.
115. Moskovitz, J., et al., *Escherichia coli peptide methionine sulfoxide reductase gene: regulation of expression and role in protecting against oxidative damage.* J Bacteriol, 1995. **177**(3): p. 502-7.
116. Anaganti, N., et al., *Depletion of reduction potential and key energy generation metabolic enzymes underlies tellurite toxicity in Deinococcus radiodurans.* Proteomics, 2015. **15**(1): p. 89-97.
117. Mastroleo, F., et al., *Experimental design and environmental parameters affect Rhodospirillum rubrum S1H response to space flight.* Isme j, 2009. **3**(12): p. 1402-19.
118. Mastroleo, F., et al., *Modelled microgravity cultivation modulates N-acylhomoserine lactone production in Rhodospirillum rubrum S1H independently of cell density.* Microbiology, 2013. **159**(Pt 12): p. 2456-66.
119. Liu, Y., et al., *Transcriptome dynamics of Deinococcus radiodurans recovering from ionizing radiation.* Proc Natl Acad Sci U S A, 2003. **100**.
120. Xu, Z., et al., *Identification and functional analysis of a phytoene desaturase gene from the extremely radioresistant bacterium Deinococcus radiodurans.* Microbiology, 2007. **153**(Pt 5): p. 1642-52.
121. Makarova, K.S., et al., *Deinococcus geothermalis: The Pool of Extreme Radiation Resistance Genes Shrinks.* PLOS ONE, 2007. **2**(9): p. e955.
122. Shimizu, K., *Regulation Systems of Bacteria such as Escherichia coli in Response to Nutrient Limitation and Environmental Stresses.* Metabolites, 2013. **4**(1): p. 1-35.
123. Green, J., et al., *Cyclic-AMP and bacterial cyclic-AMP receptor proteins revisited: adaptation for different ecological niches().* Current Opinion in Microbiology, 2014. **18**(100): p. 1-7.
124. Soberon-Chavez, G., et al., *The Transcriptional Regulators of the CRP Family Regulate Different Essential Bacterial Functions and Can Be Inherited Vertically and Horizontally.* Front Microbiol, 2017. **8**: p. 959.
125. Yang, S., et al., *Cyclic AMP Receptor Protein Acts as a Transcription Regulator in Response to Stresses in Deinococcus radiodurans.* PLoS One, 2016. **11**(5): p. e0155010.
126. Wang, Y., et al., *Protease Activity of PprI Facilitates DNA Damage Response: Mn(2+)-Dependence and Substrate Sequence-Specificity of the Proteolytic Reaction.* PLOS ONE, 2015. **10**(3): p. e0122071.
127. Murray, R.G.E., *The Family Deinococcaceae*, in *The Prokaryotes: A Handbook on the Biology of Bacteria: Ecophysiology, Isolation, Identification, Applications*, A. Balows, et al., Editors. 1992, Springer New York: New York, NY. p. 3732-3744.
128. He, Y., *High cell density production of Deinococcus radiodurans under optimized conditions.* J Ind Microbiol Biotechnol, 2009. **36**(4): p. 539-46.
129. Garsin, D.A., *Ethanolamine utilization in bacterial pathogens: roles and regulation.* Nat Rev Micro, 2010. **8**(4): p. 290-295.
130. Meadows, J.A. and M.J. Wargo, *Carnitine in bacterial physiology and metabolism.* Microbiology, 2015. **161**(6): p. 1161-74.
131. Zhang, X., X. Fang, and C. Liu, *Genomic and Proteomic Analysis of Escherichia coli After Spaceflight Reveals Changes Involving Metabolic Pathways.* Archives of Medical Research, 2015. **46**(3): p. 181-185.

132. Li, T., et al., *Impact of a short-term exposure to spaceflight on the phenotype, genome, transcriptome and proteome of Escherichia coli.* International Journal of Astrobiology, 2015. **14**(3): p. 435-444.
133. Wilson, J.W., et al., *Microarray analysis identifies Salmonella genes belonging to the low-shear modeled microgravity regulon.* Proceedings of the National Academy of Sciences, 2002. **99**(21): p. 13807-13812.
134. Frosler, J., et al., *Survival of Deinococcus geothermalis in Biofilms under Desiccation and Simulated Space and Martian Conditions.* Astrobiology, 2017. **17**(5): p. 431-447.
135. Allwood, A.C., et al., *Stromatolite reef from the Early Archaean era of Australia.* Nature, 2006. **441**(7094): p. 714-718.
136. Li, J., et al., *The link between biomineralization and fossilization of bacteria: Insights from field and experimental studies.* Chemical Geology, 2013. **359**: p. 49-69.
137. Westall, F., et al., *Implications of in situ calcification for photosynthesis in a similar to 3.3 Ga-old microbial biofilm from the Barberton greenstone belt, South Africa.* Earth and Planetary Science Letters, 2011. **310**(3-4): p. 468-479.
138. Oehler, J.H. and J.W. Schopf, *Artificial microfossils: experimental studies of permineralization of blue-green algae in silica.* Science, 1971. **174**(4015): p. 1229-31.
139. Orange, F., et al., *Experimental silicification of the extremophilic Archaea Pyrococcus abyssi and Methanocaldococcus jannaschii: applications in the search for evidence of life in early Earth and extraterrestrial rocks.* Geobiology, 2009. **7**(4): p. 403-18.
140. Kish, A., et al., *Preservation of Archaeal Surface Layer Structure During Mineralization.* Scientific Reports, 2016. **6**.
141. Miot, J., et al., *Experimental maturation of Archaea encrusted by Fe-phosphates.* Scientific Reports, 2017. **7**.
142. Auernik, K.S. and R.M. Kelly, *Identification of components of electron transport chains in the extremely thermoacidophilic crenarchaeon Metallosphaera sedula through iron and sulfur compound oxidation transcriptomes.* Appl Environ Microbiol, 2008. **74**(24): p. 7723-32.
143. Kölbl, D., et al., *Exploring Fingerprints of the Extreme Thermoacidophile Metallosphaera sedula Grown on Synthetic Martian Regolith Materials as the Sole Energy Sources.* Frontiers in Microbiology, 2017. **8**: p. 1918.
144. Russell, S.S., et al., *The Meteoritical Bulletin, No. 86, 2002 July.* Meteoritics & Planetary Science, 2002. **37**(7): p. A157-A184.
145. Kim, S.S., et al., *Searching for biosignatures using electron paramagnetic resonance (EPR) analysis of manganese oxides.* Astrobiology, 2011. **11**(8): p. 775-86.
146. Ivarsson, M., et al., *Biogenic Mn-Oxides in Subseafloor Basalts.* PLoS One, 2015. **10**(6): p. e0128863.

LIST OF FIGURES

Fig. 1: Manganese and iron cycle induced upon irradiation. [19] 3
Fig. 2: Mechanisms of microbial metal resistance [21]..... 5
Fig. 3: Transmission Electron Micrograph of *M. sedula* cells [7]. 6
Fig. 4A: Transmission electron section of *D. radiodurans* tetrads. [43, 19]..... 9
Fig. 4B: Overlaid transmission electron-, light microscopy and X-ray fluorescence picture of *D. radiodurans* diplococci……9
Fig. 5: Aluminium wells with dried *Deinococci* cells (red) inside. ……11
Fig. 6: Logarithmic growth curve of *M. sedula* cultivated in Sulfolobales medium for 12 days, supplemented with 5g/L meteorite material NWA 1172……63
Fig. 7: Electron Paramagnetic Resonance (EPR) measurement of freeze-dried *M. sedula* NWA 1172 culture ……64
Fig. 8: Tranmission Electron Microscopy (TEM) images of *M. sedula* grown on the stony meteorite NWA 1172**.** ……66